INTEGRATED PLANT MODELING AND OPTIMIZATION UNDER UNCERTAINTY

INTEGRATED PLANT MODELING AND OPTIMIZATION UNDER UNCERTAINTY

by

David Gerardi, B.Sc (Eng)

A Thesis
Submitted to the School of Graduate Studies
in Partial Fulfillment of the Requirements
for the Degree
Master of Engineering

McMaster University

MASTER OF ENGINEERING (2010) McMaster University

(Chemical Engineering) Hamilton, Ontario, Canada

TITLE: Integrated Plant Modeling and Optimization Under Uncertainty

AUTHOR: David Gerardi, B.Sc(Eng)

(McMaster University, Canada)

SUPERVISOR: Dr. Tom E. Marlin and Dr. Christopher L.E. Swartz

NUMBER OF PAGES: xv, 177

ABSTRACT

A centralized optimization strategy is proposed to determine optimal raw material purchasing and plant operation practices as applied to the steel processing industry. Primary steelmaking can be separated into three sub-areas: cokemaking, ironmaking, and steelmaking. Raw materials are purchased on the open market for each area and include coal, iron ore pellets, and scrap steel. Many raw material vendors exist, providing products varying in quality and price. Additionally, the processing of raw materials within each area has an impact on its neighbours and, therefore, it is desired to determine the least costly method of both purchasing and processing the raw materials to make steel of acceptable quality.

This work studies the modeling of primary steelmaking using a combination of mass balances and empirical relationships. The model, in addition to process constraints, is combined with a cost objective function and solved using a mixed-integer nonlinear programming (MINLP) solver. Various case studies are shown that illustrate the strong connection between the cokemaking and ironmaking as the carbon, volatile matter, and phosphorous contents of the coals and pellets have a large impact raw material selection. The centralized optimization results are then compared to the classic decentralized approach showing a clear reduction in cost.

Raw material uncertainty is incorporated using two-stage stochastic programming. The formulation considers numerous raw material quality scenarios and the optimizer is required to make purchasing decisions based on the probability of each scenario occurring. The results indicate that by making a slightly more expensive raw material purchase, the frequency of constraint violation during processing can be significantly reduced.

Multi-period optimization is also studied to determine how multi-tiered raw material pricing affects purchasing decisions. Steel demand forecasting is combined with the multi-period formulation to make planning decisions over an entire year. Case studies are provided that illustrate how multi-tiered pricing can significantly change the slate of raw materials purchased. A rolling horizon optimization approach is then incorporated to determine how decisions change throughout the year in the face of errors in demand forecasting.

ACKNOWLEDGEMENTS

I would like to thank my supervisors Dr. Christopher Swartz and Dr. Tom Marlin for their guidance throughout my studies. I am extremely grateful for their input and direction over the past two years as this thesis could not have been completed without their support.

I wish to acknowledge the McMaster Advanced Control Consortium and Department of Chemical Engineering at McMaster University for financial support. In addition, thank you to Vit Vaculik, Laura Ronholm, Harry Gou, and ArcelorMittal Dofasco for dedicating their time and resources in the completion of this work.

This thesis is dedicated to my parents who have always taken an interest in my education. Together, they formed the support system that has allowed me to succeed throughout my academic career and I cannot thank them enough for all they have done.

Table of Contents

1 Introduction **1**

1.1 Objective 1

1.2 Main Contributions 2

1.3 Thesis overview 3

2 Literature Review **4**

2.1 Steel Production 4

2.1.1 Unit Modeling and Optimization 5

2.1.2 Integrated Planning 12

2.2 Optimization Under Uncertainty 14

2.3 Multi-period Planning 18

3 Problem Formulation **22**

3.1 Introduction 22

3.2 Cokemaking 24

3.2.1 Equality Constraints 29
3.2.2 Inequality Constraints 34
3.2.3 Cokemaking Summary 52
3.3 Ironmaking 53
3.3.1 Equality Constraints 57
3.3.2 Inequality Constraints 67
3.3.3 Ironmaking Summary 69
3.4 Steelmaking 70
3.4.1 Equality Constraints 73
3.4.2 Inequality Constraints 78
3.4.3 Steelmaking Summary 79
3.5 Objective Function Development 79
3.6 Integrated Formulation and Problem Size 82
3.7 Problem Structure and Solution Method 85
3.8 Chapter Summary 86

4 Centralized Optimization **88**

4.1 Cost Parameters and Assumptions 88
4.2 Optimization With No Uncertainty 91
4.2.1 Problem 1a Results 91

4.2.2 Problem 1b Results - New Coal Availability: Coal E 98

4.2.3 Problem 1c Results - New Coal Availability: Coal F and Coal G . . 100

4.2.4 Summary 104

4.3 Optimization Under Uncertainty 105

4.3.1 Two-Stage Stochastic Programming 105

4.3.2 Two-Stage Stochastic Optimization Case Study 115

4.3.3 Two-Stage Scenario Size Study 122

4.3.4 Goal Programming Constraint Violation Penalty Study 123

4.3.5 Summary 126

4.4 Centralized vs. Decentralized Optimization 128

4.4.1 Problem 3a: Centralized vs. Decentralized Optimization No Uncertainty 132

4.4.2 Problem 3b - Centralized vs. Decentralized Optimization With Uncertainty 136

4.4.3 Summary 138

4.5 Chapter Summary 139

5 Multi-period Planning **141**

5.1 Formulation 141

5.2 Planning vs. No Planning Case Study 151

5.3 End Point Inventory Condition 157

5.4 Rolling Horizon Case Study 162

5.5 Chapter Summary 167

6 Conclusions and Recommendations **169**

6.1 Conclusions 169

6.2 Recommendations for Further Work 171

References **173**

A Raw Material Compositions and Variable Definitions 178

B Case Study Results **187**

List of Figures

2.1 Steel production flow diagram. 4

2.2 General supply chain framework diagram. 19

2.3 Bemporad and Morari formulation as applied to primary steelmaking. . . . 21

3.1 An overview of the primary steelmaking process. 23

3.2 Integration of three BOF models to primary steelmaking process. 24

3.3 Overview of the cokemaking process. 25

3.4 Cokemaking variable definition diagram. 28

3.5 Regression fit for sulphur loss during coking. 32

3.6 Regression fit for volatile matter loss during coking. 32

3.7 Observed vs. predicted results for CSR model. 42

3.8 VIP plot for CSR model. 42

3.9 Mean centered prediction results for coke stability model. 43

3.10 VIP plot for coke stability model. 44

3.11 Mean centered prediction results for initial coke oven wall pressure model. . 45

3.12 Wall pressure latent variable score plot for the first component. 46

3.13 Mean centered prediction results for wall pressure model. 47

3.14 VIP plot for modified wall pressure model. 47

3.15 Overview of ironmaking process. 53

3.16 Variable definition diagram for ironmaking. 56

3.17 Observed vs. predicted results for coke rate addition model. 64

3.18 Observed vs. predicted results for blast air addition model. 65

3.19 Overview of steelmaking process. 70

3.20 Variable definition diagram for steelmaking. 73

3.21 Observed vs. predicted results for BOF hot metal addition model. 76

3.22 Observed vs. predicted results for BOF scrap addition model. 76

4.1 CSR model input SPE-X contributions. 95

4.2 Cost breakdown of production and purchasing for primary steelmaking. . . 97

4.3 Problem 1a and 1b raw material selection comparison. 98

4.4 Problem 1c and 1b raw material selection comparison. 102

4.5 Time line of two-stage stochastic programming. 106

4.6 Two-stage stochastic separation of variables. 106

4.7 Uncertainty method comparison approach for nominal and two-stage operation. 119

4.8 Decentralized optimization solution sequence. 128

4.9 Decentralized optimization solution cost distribution for simulation study. . 137

5.1 Two-tiered vendor raw material pricing for coal c. 142

5.2 Inventory and purchasing result comparison for Problem 4a. 154

5.3 Resulting final inventory levels for varying working capital values. 160

5.4 Initial purchasing and final inventory level results for varying Coal F working capital values. 161

5.5 Purchasing and coke production results for rolling horizon approach in Problem 4a. 163

5.6 Forecast and demand profiles for all three grades of steel. 165

5.7 Purchasing and inventory solution for rolling horizon demand discrepancy case study. 166

List of Tables

3.1 Coal composition analysis on a dry basis. 25

3.2 Approximate coke oven gas composition on a dry basis. 27

3.3 Classification of coke property PLS model inputs. 40

3.4 Coke PLS model summary statistics. 41

3.5 Resulting number of inputs and principle components in coke prediction models. 50

3.6 Approximate composition of an iron ore pellet. 53

3.7 Approximate mass percent composition of blast furnace exit streams. 55

3.8 Classification of blast furnace "black box" model manipulated inputs. . . . 62

3.9 Classification of blast furnace "black box" model constant inputs. 62

3.10 List of blast furnace"black box" model outputs. 63

3.11 Steel grade product classification with respect to grade G_A. 71

3.12 Approximate final steel composition. 72

3.13 BOF "black box" model inputs and outputs. 74

3.14 Model results for BOF prediction models. 77

3.15 Primary steelmaking scaled production costs. 80

3.16 Variable and equation size of final formulation. 84

4.1 Primary steelmaking raw material scaled cost values. 89

4.2 Cokemaking results for Problem 1a. 91

4.3 Ironmaking results for Problem 1a. 92

4.4 Steelmaking results for Problem 1a. 93

4.5 Important active inequality constraints for Problem 1a. 94

4.6 Coal blend properties for CSR model in Problem 1a. 95

4.7 Comparison of Problem 1b and Problem 1a results. 99

4.8 Important active constraints and marginal costs per tonne for Problem 1b. 100

4.9 Comparison of Problem 1c and Problem 1b results. 103

4.10 Important active constraints and marginal costs per tonne for Problem 1c. . 104

4.11 Standard deviation of uncertain components in coals and pellets. 116

4.12 First stage purchasing comparison of stochastic and nominal solutions. . . . 117

4.13 Nominal and two-stage production comparison if no uncertainty were present. 118

4.14 Constraint violation for plant simulations of nominal and two-stage solutions. 121

4.15 Varying scenario size results for simulated two-stage solutions. 122

4.16 Approximate cost value of constraint violations in objective function. 124

4.17 Increased constraint penalty simulation results for two-stage solutions. . . . 125

4.18 Decentralized coke and hot metal stream quality assumptions. 132

4.19 Decentralized blast furnace hot metal upper limit deviation from centralized value x_i^{max}. 133

4.20 Centralized vs. decentralized solution comparison. 134

4.21 Decentralized standard deviations for assumptions and upper limits on quality streams. 136

4.22 Scaled cost results for Problems 1c and 3b. 137

5.1 Minimum inventory requirements and initial inventory and coke quality conditions. 152

5.2 Tiered purchasing breakpoints and cost for coal and scrap. 152

5.3 Summary of scaled costs for multi-period optimization methods. 153

5.4 Comparison of raw material purchasing quantities for Forecast and Short sight methods. 155

5.5 Comparison of coal blending decisions for Forecast and Short sight methods. 156

5.6 Initial working capital values for raw materials offered with tiered pricing. . 159

A.1 Coal cost and composition parameters. 178

A.2 Pellet cost and composition parameters. 179

A.3 Dependent variable listing and definition. 180

A.4 Dependent variable listing and definitions continued. 181

A.5 Independent decision variable and definition listing. 182

A.6 Constant parameter definition listing. 183

A.7 Constant parameter definition listing part II. 184

A.8 Constant parameter definition listing part III. 185

A.9 Formulation sets and definitions. 186

B.1 Optimization results for various case studies. 188

B.2 Continued optimization results for various case studies. 189

B.3 Inequality constraint status for Problem 1a. 190

B.4 Inequality constraint status for Problem 1b. 191

B.5 Inequality constraint status for Problem 1c. 192

B.6 Inequality constraint status for Problem 3a. 193

Chapter 1

Introduction

1.1 Objective

Raw material purchasing is a very important aspect of steel production as it comprises the vast majority of overall operational costs. Decisions must be made for various sub-areas of the plant with regard to both what types of material should be purchased, as well as how to subsequently operate the plant. Due to the impact each sub-area has on its neighbours, cost effective decisions are very difficult to make. This is compounded by the fact there are often numerous raw material suppliers offering products of varying price and quality.

In this thesis, optimization of raw material purchasing and plant operation is studied, based on application to the steel processing industry. The flow sheet is broken down into three sub-areas, each with an individual raw material to purchase being that of coal, iron ore pellets, and scrap steel. It is proposed to first model each area individually, including mass and energy relationships, in addition to physical and quality constraints based on an actual steel plant. A cost objective function is developed and combined with the models in a centralized optimization formulation which is solved using a mixed-integer nonlinear programming (MINLP) solver. The goal is to determine the minimum purchasing and operation cost in order to produce a specified quantity of steel in a single time period.

Uncertainty with respect to raw material quality further complicates the decision process as variation in composition can have detrimental affects on optimization feasibility and subsequent production costs. A method by which to incorporate uncertainty is developed in order for the optimizer to include composition variance knowledge into its decision.

Finally, the centralized optimization formulation is extended to multiple periods. Raw material suppliers offer product at tiered discounts in order to encourage bulk purchases. The formulation is used to study the potential benefits of forecasting demand and making bulk purchases to take advantage of these discounts.

1.2 Main Contributions

1. **Primary steelmaking model.** An integrated model for primary steelmaking is developed accounting for operation in cokemaking, ironmaking, and steelmaking. The model includes both mass and energy balances, as well as relationships relating to coke strength quality.

2. **Benefits of centralized optimization.** The cost saving opportunities for using one centralized decision maker are determined in this thesis. These benefits are reported in contrast to the traditional decentralized approach in which each sub-area, within primary steelmaking, makes purchasing decisions independently.

3. **Formulation incorporating raw material uncertainty.** Two-stage stochastic programming is applied to the steel plant formulation in order to account for raw material uncertainty. The results provide insight into how purchasing can be changed to minimize the possible future violation of inequality constraints.

4. **Multi-period planning formulation.** A model is developed to include multiple time periods in the optimization decision. This introduces inventory management into the problem and explores the benefits accrued by making intermittent bulk purchases in anticipation of future demand.

1.3 Thesis overview

Chapter 2 – Literature Review

An overview is given with respect to prior research in the areas of steel modeling, optimization under uncertainty, and multi-period planning.

Chapter 3 – Problem Formulation

This chapter gives a detailed description of each major area within primary steelmaking. Models for cokemaking, ironmaking, and steelmaking are developed in addition to a cost objective function for the process. The problem structure is then discussed including issues such as overall size and convexity.

Chapter 4 – Centralized Optimization

The scaled cost parameters for purchasing and production are provided in this chapter. Various case studies are then solved to demonstrate how the optimizer makes decisions to minimize steelmaking costs. A formulation is developed to handle raw material uncertainty and examples are provided to explain the trade-offs that exist between minimizing cost and satisfying inequality constraints. Decentralized optimization is then applied to the process in order to determine the cost of using multiple decision makers and compare the result to the centralized optimizer.

Chapter 5 – Multi-period Planning

The centralized formulation is extended to include multiple time periods. The benefits of optimizing with respect to forecast demand are studied in this chapter.

Chapter 6 – Conclusions and Recommendations

The important findings of the thesis are summarized and recommendations provided for future research opportunities.

Chapter 2

Literature Review

The intent of this chapter is to provide a review of the important concepts involved in this research. Three areas are explored: steel production, optimization under uncertainty, and multi-period optimization. In each case the reader will be provided with a background of each topic and an overview of previously completed research.

2.1 Steel Production

An outline of steel slab production is given in Figure 2.1.

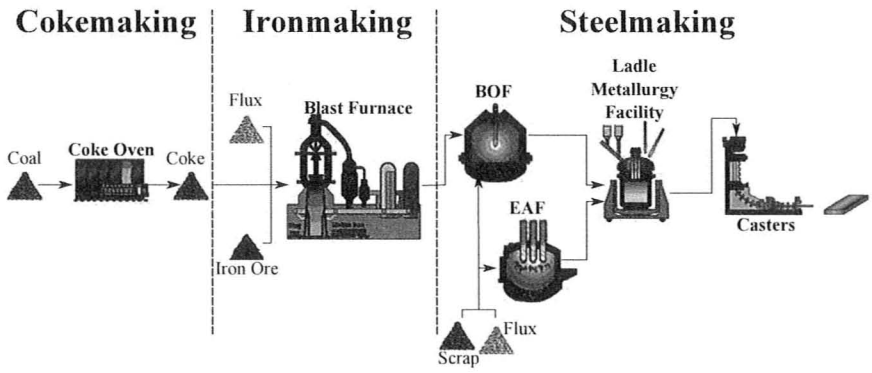

Figure 2.1: Steel production flow diagram.

The first process step involves production of coke for the blast furnace, where iron ore is reduced, to produce liquid hot metal. From the blast furnace outlet, the hot metal is transported to a Basic Oxygen Furnace (BOF) where oxygen is blown through the vessel to oxidize non-ferrous impurities. The Electric Arc Furnace (EAF) operates in parallel to the BOF and produces liquid steel from scrap metal alone. The BOF and EAF batches are then taken to the Ladle Metallurgy Facility (LMF) where product specific alloys are added depending on customer orders. Finally, this hot steel is processed in the casters where it is cooled and drawn into long slabs of finished steel.

Previous research has studied each area, as outlined in Figure 2.1, individually, as well as in an integrated manner. The following two sections explain work that has been done on the individual units in addition to that of the entire steel plant.

2.1.1 Unit Modeling and Optimization

Cokemaking

The production of coke is extremely important for the operation of the blast furnace. Bertling [6] summarizes the duty of this material in three roles:

1. **Physical Role**. The iron ore pellets begin to melt and fall downwards in the furnace. At this point, coke remains solid and is required to provide a permeable network in which iron and gases can pass.

2. **Thermal Role**. Carbon content of coke provides a majority of the energy input to the blast furnace.

3. **Chemical Role**. Supplies carbon which reacts and produces reducing gases required in the reduction of iron oxides.

Diez et al. [11] cite the physical strength of coke to be the most important factor in production. This is because energy and reducing gases can be introduced by other means;

however, there is no material that can provide a permeable matrix under the temperature and pressure inside the furnace. In this review paper, the authors identify good coke strength by testing for Coke Strength after Reaction (CSR), and discuss models that have been developed to predict this characteristic. The models referenced look at the impact of coal petrographical, rheological, and chemical parameters on the final coke strength. Petrographical properties are those which are studied on a microscopic level and include the coal reflectance and mineral content. Rheological properties are related to the fluidity of coal such as the dilation, contraction, and the temperature at which it begins to soften. Chemical properties are those of the coal composition such as carbon and other compounds.

Diez et al. show a model from Kobe Steel in Japan where CSR is predicted from reflectance, maximum fluidity, and the basicity of coal chemical impurities. Zhang et al. [49] develop a CSR model based on Chinese coals and include maximum fluidity, volatile matter content, inert content, and mineral catalysis index as predictor variables. The model was tested and predictions were found to deviate 0.82% absolute from measured values. Finally, Todoschuk et al. [44] include the conditions of the coking process in the creation of a linear CSR model. These include factors such as the bulk density of the coke oven after the coals are charged and the final oven temperature. The model R^2 value was 0.84 with the operating variable of bulk density explaining most of the variance in CSR.

Pearson [35] reviews several CSR models, including one from Nippon Steel Corp. in which the petrographical properties of inertinite content and vitrinite reflectance are used to predict CSR. A relationship is identified which explains as vitrinite reflectance increases so does CSR, but only to a point before the CSR value lowers. The optimal inertinite value ranges between 15% and 25%. The author acknowledges that while the model may provide accurate results for Japanese coals, using other geographically located coals generally results in CSR predictions that are consistently higher than that measured in experimentation. Since there is a lower limit on coke strength imposed by the blast furnace, using this model in actual production could be dangerous. In fact, the author identifies that despite effort in the cokemaking community, there is no universally accepted model.

Todoschuk et al. [44] provide models for two additional coke parameters not given much attention in the literature. The first is that of coke stability which is similar to CSR but seeks to measure strength under far lower temperatures. The second is coke oven wall pressure which measures the exertion of forces by the coal mass on the oven walls as it transforms into coke. These two models involve only petrographical coal properties and oven operating conditions as predictor variables. The stability prediction yields an R^2 value of 0.845 with the wall pressure model being 0.746. The relationship between model inputs and wall pressure was determined to be logarithmic in order to maximize its R^2 value.

Modeling attempts, with respect to cokemaking, are focused in the prediction of CSR while other coke properties such as stability and oven wall pressure have not been developed in great detail. Even with the numerous CSR models cited in the literature, there still remains great debate over what coal variables accurately predict CSR. Todoschuk et al. [44] have provided the most comprehensive analysis of coke model building, as they consider both coal properties and oven operating condition variables in their models. All modeling efforts described in this section were developed using stepwise linear regression. Therefore, there exists an opportunity to use a combination of coal properties and oven conditions, in a multivariate model, in order to improve the model prediction capabilities.

Ironmaking

Research specifically focused on ironmaking, from a modeling standpoint, is not common in the literature and is most likely due to the complexity of blast furnace operation. Ertem et al. [14] collected data from a single blast furnace over an entire month in order to develop complete mass and energy balances. This included measurements of blast air intake, moisture contents, temperatures, and chemical analysis of exit hot metal. The objective was to hold production as close to steady state as possible to investigate possible energy recovery from operation. The results showed that reduction of iron consumes the majority of energy input at approximately 36%. Also, sensible heat from the exit blast furnace gas

and slag could be recycled elsewhere in the plant. The authors propose to use this wasted energy in order to dry the wet combustion air input to the furnace, saving 2% in energy consumption.

Jindal et al. [23] developed a dynamic ironmaking model that comprises all reactions and components involved inside the blast furnace. Due to complexities involved in modeling the various zones within the furnace, the authors assume the furnace can be divided up into two areas: raceway, and shaft. The shaft represents the furnace from where raw material is charged at the top, until it is liquefied near the bottom. The raceway is located at the bottom and involves the zone where blast air is blown into the furnace and ascends upwards through the falling mass charge. The authors model the shaft at steady state and the raceway dynamically, reducing the total number of required differential equations. The two models are then combined and blast furnace plant data is used to estimate parameters such as heat transfer coefficients. No results are explicitly given as to the quality of predictions the final model provides.

A simplified blast furnace model is presented by Davenport and Peacey [34] where steady state mass and energy balances are completed. The model was validated using data from blast furnaces operating at several geographic locations. Making assumptions about coke, exit hot metal composition, and inlet air temperature, the model becomes linear and can be included in a linear optimization program. The authors then include physical constraints such as maximum air flow and oil consumption to show how optimization can effectively reduce the overall operation cost of production.

The dynamic model created Jindal et al. [23] is useful to study the resulting temperature profiles inside the blast furnace for various operating scenarios; however, it is highly non-linear and not suitable for making general planning decisions. The steady state model developed by Davenport and Peacey is very simplistic and only involves a small subset of components involved in actual practice. Not present in the literature is a model that is simple enough to include in an optimization formulation, yet also includes enough detail to make the results representative of actual blast furnace operation.

Steelmaking

The steelmaking process centers around BOF and EAF operation. Johansson et al. [24] provide a model to estimate the decarburization rate inside the BOF. The goal of this process is to achieve a specific carbon content after blowing oxygen through the furnace. The proposed model is tested in open-loop yielding suboptimal performance. An analysis of the BOF off-gas is then used to provide feedback and is incorporated using a nonlinear observer. The observer gain is adjusted and results show the final carbon content prediction error is in the order of 0.003% absolute. The drawback of the model is that only the components carbon and silicon are included in the model.

A comprehensive dynamic EAF model is reported by MacRosty and Swartz [28] where four zones are used to represent the different mass phases inside the furnace. The final model contains 13 adjustable parameters ranging from mass transfer coefficients to the initial boundary conditions. A sensitivity analysis was completed to identify a subset of insignificant parameters that could be kept constant and thus eliminated from the parameter estimation. Rigorous parameter estimation was completed on the six significant parameters using plant data. A subsequent paper was published using the final model in a dynamic optimization framework [27]. The objective function used minimizes the electrical energy input, scrap and flux usage, high purity oxygen input, and natural gas consumption. Case studies included demonstrate the benefits of such a model in that the optimal operating cost can be determined for scenarios such as preheating of the furnace before electricity is used and market fluctuations in electricity pricing.

Sandberg et al. [40] developed an EAF model based on operation data from four Swedish steel facilities. Partial Least Squares (PLS) regression was used to create three models predicting the final chemical analysis, energy consumption, and mass yield of the batch. The explained variance of the models is poor, however, as industrial raw data often contains a great amount of noise and therefore explains some of the model prediction errors. The authors also demonstrate how the resulting models can be used to back-calculate and estimate properties of the individual scraps added to the furnace.

This concept of modeling the EAF from a database of production batches was also done by Miletic et al. [31]. Two linear PLS models were developed to predict final hot steel chemistry and electrical energy consumption. These empirical models were built using historical batch data from EAF plant operation. For each batch run, the steel composition, electricity usage, input material quantities, and operating conditions were all catalogued. Equation 2.1 shows the basic model structure.

$$\begin{bmatrix} y^{elec.} \\ y^{comp.} \end{bmatrix} = f\,(\text{Scrap grades used, Flux addition, Temperature settings}) \tag{2.1}$$

Modeling of the scrap purchasing practice was also completed in order to capture the various scrap grades available for production. These models were then cast into an optimization framework with the objective of minimizing the overall cost and electricity usage. The optimization inputs are the steel demand, internal scrap inventory quantities, and vendor scrap pricing for a single time period. Upon solving, a solution is provided that determines the exact sources from which scrap should be ordered, and the total quantity that is purchased. The paper does not provide the accuracy of the PLS prediction models but does note the optimization tool is used on a consistent basis and has provided significant economic savings with regard to scrap purchasing.

Optimization of scrap usage was also studied by Bernatzki et al. [5] based on BOF operation. Here, a simplified BOF model is based on rules of thumb for scrap to hot metal addition to the furnace. For example, iron ore pellets are sometimes added to the BOF, instead of scrap, in order to cool down the hot metal fed from the blast furnace. However, to reduce this iron ore, slightly more hot metal needs to be added. The authors use a rule of thumb that says 4 units of scrap can be replaced by 1.1 units of iron ore plus 3.3 units of additional hot metal. This paper does not place great importance on furnace modeling but rather focuses on the problems imposed by the manner in which scrap is transported to the BOF. The scraps are stored based on grade and sorted into categories of train tracks and individual rail cars. The authors worked with an industrial sponsor who used heuristics to determine the optimal scraps to use in production of certain steel grades. However, due to the numerous constraints governing rules by which cranes can remove and sort the scrap

rail cars, the heuristics were often abandoned in favour of more costly scrap choices. A mixed-integer linear program was formulated with the objective of minimizing the cost of scrap used in BOF production. The optimization results show 5% average cost improvement in comparison to the industrial sponsor's previous practice.

Production downstream of the BOF and EAF involves solidifying the liquid steel by cooling in units called casters. Depending on the desired steel grade to be produced, the temperature of hot steel exiting the furnaces differs. Therefore, the speed at which different products are cast changes and places importance on synchronizing BOF and EAF batch completion with caster operation. Tang et al. [43] provide an extensive review of research in this area extending all the way to processes after casting which include the reheating and rolling of cooled steel slabs.

Modeling of these steel scheduling problems requires introducing binary variables to enforce sequencing of product batches through the connected units. Industrial sized problems were studied by Harjunkoski and Grossmann [20] in which a decomposition approach was provided in order for the problem to be computationally tractable. Scheduling is broken down by categorizing customer orders into families and subgroups. Three MILP's and one LP are solved sequentially providing a framework in which a problem of 33,000 discrete variables and 74,000 equations can be solved within 5% optimality in a matter of 3 hours.

The work of Davenport et al. [10] at IBM provides a solution for industrial sized steel scheduling problems based on a small desired time granularity. In this study, the caster schedule is optimized based on a discretization of 15-30 minutes and solved using a standard MILP solver. The solution is then input to a formulation of the upstream caster processes which is based on a 30 second time granularity. This is then solved using constraint programming providing 2 day schedules in a matter of 10 minutes which increase the steel produced by 10%.

It is evident that the amount of research focused on the individual areas of steel production is extensive and provides an insight into the complexities involved in both modeling and optimization.

2.1.2 Integrated Planning

The operation of a steel plant involves numerous units with many degrees of freedom by which to optimally manipulate the performance of the entire network. Optimization at any period in time must therefore consider several important points such as purchasing of raw materials and the individual throughput rates of multiple units. In order for this to be successful, there must exist constant communication between each facility. Grossmann [19] stresses the importance of integrated decision making across a company's business units in order to operate efficiently.

A review of work in this area related to the steel industry was completed by Dutta and Fourer [12]. The areas of raw material blending, planning, scheduling, and inventory management are outlined and key researchers are identified. The authors note that pioneering work related to steel plant integration was done by Fabian [15]. In this paper, modeling was done for the blast furnace, basic oxygen furnace, and rolling mills downstream of the casters. Mass balances for oxygen and silicon are neglected as well as energy related to reduction of impurities such as silicon, manganese, and phosphorous. Despite these drawbacks, the attempt at modeling multiple units was novel and encouraged others to contribute research in this area. Fabian [16] improved upon his previously simplistic steel model and included balances on silicon, oxygen, and a more comprehensive energy balance. The model is cast as an LP with the total cost of raw materials minimized.

The work of Fabian encouraged Lawrence and Flowerdew [26] to develop a model that integrated the blast furnace and BOF. The authors note that complete mass and energy balances are not included and several rules of thumb are used to express missing relationships. An example of this involves assuming the required blast furnace coke rate is a linear function of the iron pellet input and slag output. Optimization is completed using the model in order to minimize raw material and operating costs. The results provide the burden mix charged to the blast furnace, as well as the proportions of hot metal and scrap to the BOF. The authors stress the need to expand their approach to more units and also refine the models currently used.

A later study done by Bandyopadhyay [3] looked at a BOF and open-hearth furnace operating in parallel to produce steel. An open-hearth furnace produces steel in a different manner than a BOF in that air is used instead of high purity oxygen to oxidize the impurities. The blast furnace delivers hot metal to both steelmaking furnaces and the objective is to determine how to optimally allocate the input feed between the two units. Steady state mass and energy balances are written for both furnaces creating two linear models. Optimization is completed minimizing utility, raw material, and labour costs. However, the results in this study are limited to steelmaking only and do not consider any costs with regard to cokemaking or the blast furnace.

Gao and Tang [17] modeled an integrated steel plant by using simple rules of thumb. For example, in the blast furnace it is assumed that one unit of liquid iron requires two units or iron ore, one unit of coal, and half a unit of limestone. The objective of this study was not to accurately model the actual process, but rather investigate raw material vendor selection based on factors of quality, price, and delivery time. These three parameters were provided for seven vendors, based on data from a real steel plant, and a linear program was formulated using a weighted objective function. The results demonstrate how goal programming can be used in steel production, but do not provide realistic answers since the level of model detail was poor.

Chen and Wang [9] enlarged the scope of the integrated plant to include transportation of raw materials delivered on-site and to the distribution of product to customers. Similar to Gao and Tang, rules of thumb were used to represent production in the plant as no component or energy balances were completed. The supply chain was modeled as an LP with the objective of maximizing profit based on steel demand from various geographical locations supplied by the steel facility. While the results cover a larger set of decisions regarding steel production, the model detail was simplistic and therefore may not provide optimal profit upon implementation.

Steel inventory was studied by Zanoni and Zavanella [48] where focus was placed on the integration of EAF steelmaking and the continuous casters. The authors cite customer

orders from a real steel plant and show the wide distribution of grades desired. They indicate that due to inventory space and EAF throughput limitations, determining the sequencing of product batches is difficult to schedule. A MILP formulation was developed in order to minimize holding, production, and back order costs over a planning period of one month. The inventory warehouse size was then manipulated to explore the breakpoints where increasing storage space dramatically increased profit. The formulation is important for optimizing the connection between steelmaking and casting, however, it does not include any information about costs or impact from ironmaking or cokemaking.

The literature gives ample evidence of research in the area of integrated steelmaking. Very few papers, however, take a look at the entirety of steel production and instead focus on the connection between two units. In the cases where more than two units are included in the formulation, generic rules of thumb are used to represent production. This coarse modeling approach leads to impractical and thus suboptimal solutions. Therefore, great opportunity exists in creating an optimization problem that models steel production on a finer level and looks at multiple units simultaneously.

2.2 Optimization Under Uncertainty

Integrated modeling and optimization of steelmaking has been researched in the literature; however, it is important to note that past work in this area has not considered the uncertainty involved. This could be related to raw material quality, modeling errors, and demand forecasting inaccuracies.

With regard to steel production, Anandalingam [1] modeled seven integrated units using linear empirical relationships developed from industrial data. The cost parameters were then considered to be uncertain, with known probability distributions, and an investigation was completed to determine how implementing different energy technologies can minimize the impact of cost fluctuations. Scenarios were generated using Latin hypercube sampling, from the cost probability distributions, and the model solved for each scenario. The overall

purchasing and production costs were recorded for each scenario solution and it was determined that no matter the technology used, the variance in cost was significant indicating the necessity of incorporating parameter uncertainty in the model.

While there are many approaches that can be taken to incorporate uncertainty, three methods will be explained in this section: fuzzy programming, chance constraints, and stochastic programming.

Fuzzy programming identifies all uncertain parameters to be fuzzy numbers. Normally, an uncertain number belongs to a probability distribution based on the degree of uncertainty. Rather than using a probability function, fuzzy programming uses a membership function to represent the extent to which a parameter is associated with a particular value. Different types of functions exist along with methods to transform probability distributions into these fuzzy membership functions.

Rong and Lahdelma [38] use fuzzy programming to incorporate scrap steel uncertainty into an optimization framework. EAF production uses only scrap steel as an input and since there exist strict upper limits with regard to final impurity concentrations, careful consideration must be given to the scrap mix charged. Additionally, the actual concentration of these impurities is often not accurately known since scrap is recycled from various sources. The authors consider scrap impurity concentrations to be fuzzy numbers and use component balances to create linear fuzzy quality constraints which can be violated to a specified tolerance level. Optimization is completed for various constraint tolerances and the solution simulated for randomly generated scrap qualities. The constraint failure rate and subsequent scrap cost are listed in order to show the trade off between quality and purchasing cost.

Chance constrained programming is similar to fuzzy programming in that inequality constraints are manipulated to allow for violations up to a certain tolerance level, α, based on a probability distribution. The left hand side of the inequality constraint is a function of the variable x and parameter β. Based on uncertainty in β, it is desired to remain within

feasibility of the upper limit γ. This is expressed in Equation 2.2

$$\Pr\left(f\left(x,\beta\right)\leq\gamma\right)\geq\alpha \tag{2.2}$$

If the distribution of uncertainty is not known, an assumption must be made in order to transform the inequality into a chance constraint. Assuming a normal probability distribution function Φ, the constraint can be written as in Equation 2.3.

$$E\left(f\left(x,\beta\right)\right)+\Phi^{-1}\left(\alpha\right)\cdot\sigma_{f}\left(x,\beta\right)\leq\gamma \tag{2.3}$$

$E\left(\cdot\right)$ represents the expected value of the bracket term, and $\Phi^{-1}\left(\alpha\right)$ is the value of the inverse probability distribution at α. The variable $\sigma_{f}\left(x,\beta\right)$ represents the standard deviation of f, which is a function of x and β, and can be calculated by propagating the variance in β through f. If f is linear, then so is $\sigma_{f}\left(x,\beta\right)$ and vice versa.

Shih and Frey [42] employ chance constraints in a coal blending problem. Here, uncertainty exists with regard to coal quality, namely in the concentrations of sulphur and ash. There are strict upper limits for these two components and thus chance constraints are written to limit the sulphur and ash violation probabilities to 5% and 10% respectively. The overall blend cost is a function of coal quality and the authors seek to minimize both the expected value and variance of cost in the objective function. Objective function weights are used to place priority on the sulphur and ash cost factors.

Miletic et al. [31] also use chance constraints in a problem similar to that of Rong and Lahdelma [38]. Impurities in scrap, used as a feed to the EAF, are assumed to be uncertain and follow standard normal distributions. Chance constraints are then included, limiting the violation of impurity constraints to a certain tolerance level. These are then embedded in an optimization formulation which selects the least costly EAF scrap blend that satisfies the chance constraints.

In all cases of chance constraints, the violation tolerance is considered an optimization tuning parameter. When multiple constraints are written, several parameters are introduced and change the implication that this tuning has on the actual constraint violation. Zhang et al.

[50] cite the difference between individual and joint chance constraints. An example is given where if 10 chance constraints are desired to be satisfied individually at a probability level of 95%, the worst case scenario shows that all 10 constraints will be satisfied simultaneously at a probability of only 60%. The authors then developed an algorithm which tunes the chance constraints to a joint tolerance level. The disadvantage to the method is that for a few chance constraints, the computation solving time is large.

Stochastic programming is an alternate method that uses scenarios to represent each uncertainty occurrence. The goal is to obtain a solution that is optimal based on all possible scenarios, and is weighted by the probability of each scenario arising. Two-stage stochastic programming, as described by Sen and Higle [41], divides variables into first stage, x_1, and second stage, x_{2s}, decisions. The second stage variables are also indexed by scenario using the variable s which is contained within the set S.

$$min \quad c_1 x_1 + \sum_{s \in S} p_s c_{2s} x_{2s} \tag{2.4}$$

Subject to :

$$h(x_1) \leq 0$$

$$h_s(x_1, x_{2s}) \leq 0 \quad \forall\, s$$

$$g(x_1) = 0$$

$$g_s(x_1, x_{2s}) = 0 \quad \forall\, s$$

First stage variables are those that are decided prior to uncertainty realization. Second stage variables represent recourse decisions that can be made once the uncertainty impacts the process. By incorporating these recourse decisions, the formulation achieves a lower cost than if all variables were decided in the first stage. Also, the recourse flexibility models actual operation quite accurately as, in practice, the steel plant operation can be altered depending on fluctuations in uncertainty. The requirements in developing this two-stage formulation are deciding which variables are first and second stage, and assigning a probability to each scenario. While this is simple to implement, there are disadvantages to

the stochastic approach. Uncertainty is often present in a continuous form which requires infinite scenarios. A subset must therefore be selected which simultaneously represents the overall uncertainty to a degree, and keeps the problem of a size that is computationally tractable.

In this thesis, the method of two-stage stochastic programming is used to account for raw material quality uncertainty. In comparison to the fuzzy and chance constrained approaches, it is more computationally intensive as the problem size grows. However, the implementation and flexibility of the formulation far better suits the primary steelmaking process. Chance constraints assume the worst case scenario of variance occurs at all times and bases its solution on essentially a single scenario outcome. While the probability of constraint violation is guaranteed to be equal to the constraint tolerance level, no consideration is given to the instance where the constraint is violated. In contrast, the two-stage method bases its solution on both common and uncommon uncertainty outcomes and provides a set of decisions for all scenarios. By including these scenarios in the objective function, the optimizer makes decisions that are optimal for more than just extreme conditions. This is similar to how decisions would be made and implemented in the plant. The purchasing planners would consider the variance of raw material quality on the process, and make a purchasing decision. Once the materials are delivered and measured, operators would then adjust the plant to accommodate the realized uncertainty.

2.3 Multi-period Planning

Within the integrated planning literature citations, none have studied modeling and optimization over multiple time periods. This area involves incorporating inventory management and demand forecasting into the integrated planning problem. This thesis investigates the opportunities available by optimizing bi-monthly production periods over an entire year. It is motivated by the work of Miletic et al. [31] in which it is mentioned that multi-tiered purchasing discounts are offered by steelmaking raw material suppliers. In other words, discounts are offered if purchasing orders exceed certain threshold levels. Miletic et al. model

these purchasing rules into a scrap purchasing model, but only ever optimize over a single time period. Therefore, the possibility exists to accrue greater savings if steel demand in future time periods is considered.

The multi-period model developed in this thesis is based on that of Perea-Lopez et al. [36] and Mestan et al. [30]. These two articles develop mixed-integer linear programs (MILP's) for multi-product supply chains. Traditional supply chains are comprised of various connected nodes that include suppliers, the production facility, warehouses, distribution centers, and customer retail locations as shown in Figure 2.2.

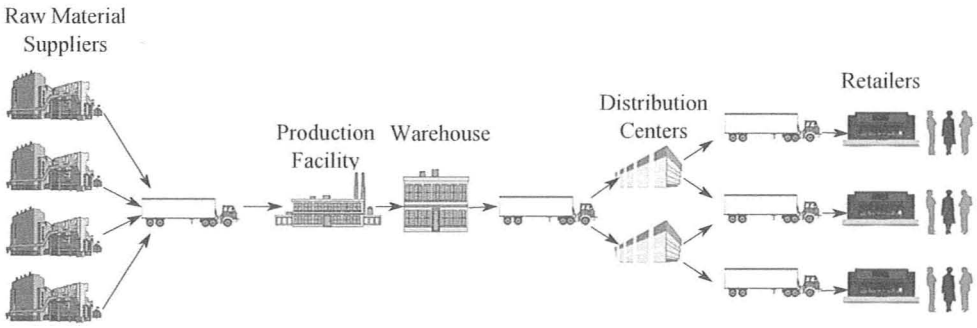

Figure 2.2: General supply chain framework diagram.

The authors complete overall mass balances on each node, and since the multi-period formulation considers changing node inventory levels, the model is dynamic. Binary decisions are required to decide if production should be started during a particular time period, as inventory levels may dictate that customer demand can be satisfied without making new product. The optimization goal is to maximize revenues and minimize inventory, production, distribution, and customer satisfaction costs.

The multi-period MILP optimization problem is considered to operate as a Model Predictive Controller. The demand forecast is fed to the controller, optimization completed over a time horizon, and the first time period decision implemented on the supply chain. Depending on disturbances with respect to production, distribution, and actual demand, re-optimization is required at the next time step, similar to how a Model Predictive Control (MPC) would monitor a process. The controller makes logical ($p(t)$) and continuous ($u(t)$) decisions

based on a dynamic model of states ($x(t)$) and output ($y(t)$) variables. This resulting MPC formulation was first presented by Bemporad and Morari [4].

$$\min_{u} \quad \sum_{t} J\left(y, x, u, t\right)$$

Subject to,

Dynamic Model

$$x(t+1) = Ax(t) + B_1 u(t) + B_2 p(t)$$

$$y(t) = Cx(t) + D_1 u(t) + D_2 p(t)$$

Problem Constraints

$$\phi = Ex(t) + F_1 u(t) + F_2 p(t)$$

$$\psi \leq Gx(t) + H_1 u(t) + H_2 p(t)$$

$$y_{min} \leq y(t) \leq y_{max}$$

$$x_{min} \leq x(t) \leq x_{max}$$

$$u_{min} \leq u(t) \leq u_{max}$$

$$p(t) \in [0,1],\ x(0) = x_0$$

The supply chain inventory nodes are represented by $x(t)$ and the final product output by $y(t)$. These variables are dependent upon the purchasing and transportation decisions represented by $u(t)$. Additionally, the binary variable $p(t)$ decides whether or not the production facility in Figure 2.2 makes product during time period t.

The units involved in primary steelmaking can be applied to the works of Perea-Lopez et al. [36] and Mestan et al. [30]. Steel production in this thesis is not technically a supply chain since it does not involve transportation intricacies or product distribution. However, the three nodes of cokemaking, ironmaking, and steelmaking can be considered a local supply chain as they involve inventory management and are dependent on one another. Detailed models for these three production areas can be used in a multi period formulation in which a

steel demand forecast is provided. Based on the raw material inventories, optimization can be executed in the same rolling horizon MPC approach. The transformation of variables into this MPC formulation is shown in Figure 2.3.

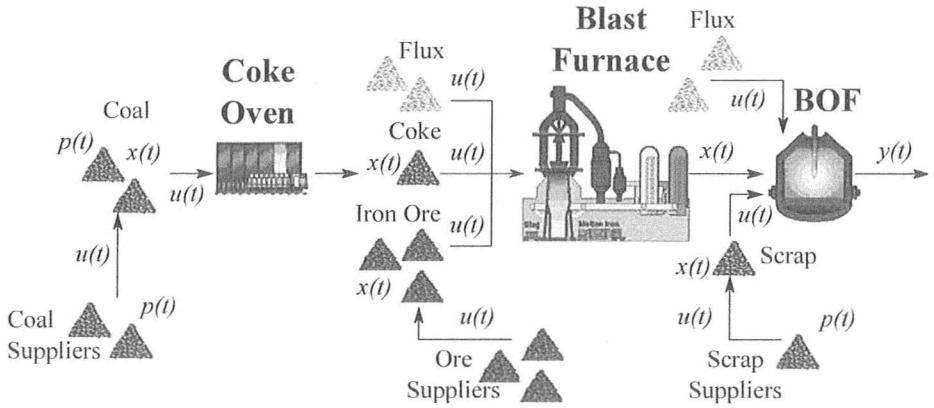

Figure 2.3: Bemporad and Morari formulation as applied to primary steelmaking.

The classification of variables with respect to primary steelmaking are as follows:

- $p(t) \rightarrow$ tiered pricing and coal blending binary decision variables
- $u(t) \rightarrow$ purchasing quantities and internal mass flows
- $x(t) \rightarrow$ inventory levels, component mass flows
- $y(t) \rightarrow$ steel production quantities

Chapter 3

Problem Formulation

This chapter introduces the various units which comprise primary steelmaking . Modeling of each area is performed using a combination of rigorous mass balances and empirical regression models. These models are combined with equations expressing the physical process constraints in a mixed-integer nonlinear programming formulation.

3.1 Introduction

Optimization of this process can be accomplished by first modeling the three main production areas. This involves mass and energy balances on each unit as well as empirical models to express relationships that cannot be developed from first principles. The project objective is to minimize the overall cost per ton of steel produced in primary steelmaking. The process considered in this study is shown in Figure 3.1 encapsulated by a box.

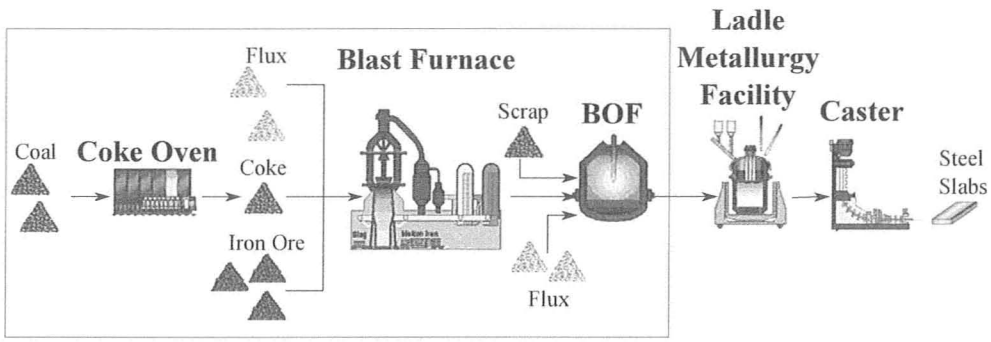

Figure 3.1: An overview of the primary steelmaking process.

This process can be broken down into three main areas: cokemaking, ironmaking, and steelmaking. In cokemaking, coals are transformed into coke, an important energy input to the blast furnace. This coke is then used in ironmaking, along with iron ore pellets, to produce liquid iron saturated with carbon. Fluxing agents are also added at this stage in order to remove impurities entering through coke and iron pellets. Steelmaking removes most carbon and reduces other impurities in a Basic Oxygen Furnace (BOF) producing hot liquid steel. At this point, as shown in Figure 3.1, the output of primary steelmaking is sent to the Ladle Metallurgy Facility (LMF) where product-specific alloys are added before the steel is cast into solidified slabs.

The models will be used in optimizing the iron, coal, and scrap purchases, as well as selected process operating conditions to match the optimized purchases. In this chapter, models are developed for a one-week period, assuming that the purchases are fully consumed during the week. On this basis, the models can be developed for a steady-state process manufacturing the desired product steels within the one-week period. We note that the detailed schedule, allocating materials and operations to equipment at specific times, is not modeled because purchase decisions and the operating conditions for each steel type are adjusted infrequently.

Since ironmaking is a continuous process, the balances are developed for the entire one-week operating period. By contrast, cokemaking is a batch process and the balances are developed for a single batch; the weekly model is determined by multiplying the single-batch results by the number of batches.

Steelmaking is also a batch process; however, not all batches are operated similarly. Depending on the type of steel made, operation changes accordingly, and therefore, separate batch models are developed for each steel grade. In this sense, cokemaking produces one type of coke during the optimization period. Ironmaking uses the coke in production of one type of hot metal. The same hot metal is then distributed to all three BOF batch models, as shown schematically in Figure 3.2.

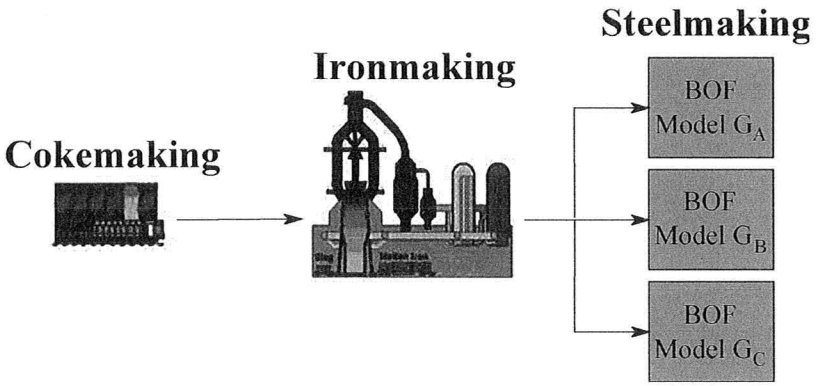

Figure 3.2: Integration of three BOF models to primary steelmaking process.

The net result is a set of equations that represent the overall weekly manufacturing material and energy flows. These models can be solved for each process individually or in an integrated manner. Both modeling approaches will be employed when comparing decentralized with centralized optimization in Chapter 4.

3.2 Cokemaking

Coke is the most important fuel feed to the blast furnace as its combustion provides more than half the required energy input [34]. An overview of this process is shown in Figure 3.3 including all components considered in this formulation.

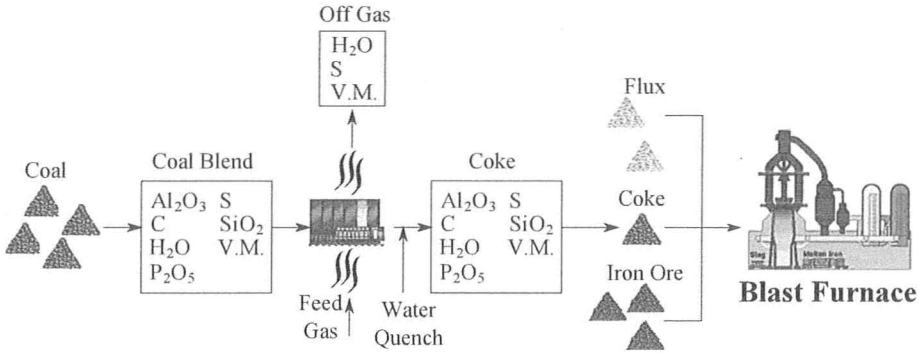

Figure 3.3: Overview of the cokemaking process.

Coke is produced from subjecting raw coals to high temperatures in a coking oven. First, different coal types are blended and charged into the oven. Coke composition significantly impacts blast furnace operation and is dependent upon the composition of the charged coal blend. Coal composition can be broken down into three areas: ash, fixed carbon, and volatile matter (V.M.).

Table 3.1: Coal composition analysis on a dry basis.

	Approx. Mass Percent	Components [8],[34]
Ash	5%-10%	Al_2O_3 P_2O_5 S SiO_2
Fixed Carbon	60%-70%	C
Volatile Matter	15%-30%	CH_4 Aromatic compounds Other hydrocarbons

The fixed carbon value is perhaps the most important component of a coal. High coal carbon content yields a coke with high carbon content and provides a higher heat of combustion per mass of coke.

Ash is an undesirable coal component as it represents impurities that must be removed at an additional cost in the blast furnace and BOF. Sulphur (S) and phosphorous oxide (P_2O_5) are two ash components that are monitored closely because finished steel has strict upper limits regarding their final concentrations. Alumina (Al_2O_3) and silica (SiO_2) can be easily removed in both the blast furnace and BOF using fluxing agents. Flux, however, consumes a great amount of energy, and thus, the amount added should be as low as possible.

After the coals have been charged to the coke oven, they are heated using a combination of hot recycled gases and burned natural gas. As the temperature reaches 400°C, this reducing environment, void of air, causes volatile matter in the coals to be released into the off-gas. The coals begin to decompose and form plastic-like layers at the coke oven wall. As the temperature inside the oven rises, these layers begin to grow towards the middle of the charge until all the coals have transformed and stabilized into coke. At this point, the temperature is over 1000°C, and the newly formed coke contracts enough for it to be discharged from the oven. Upon completion, most of the coal ash and fixed carbon remain with only trace amounts of the initial volatile matter.

The gas released during coking is considered to be a revenue stream. Aromatic compounds such as benzene, toluene, and xylene are present in small amounts and can be recovered and sold for profit. The remaining volatiles produce gas with a high calorific value that can be reused in other areas of the plant, including the production of more coke. The approximate composition of this gas is given in Table 3.2.

Table 3.2: Approximate coke oven gas composition on a dry basis.

Component	Volume Percent [22] [8]	Combustible?
CH_4	30%	Yes
CO	8%	Yes
CO_2	3%	No
H_2	51%	Yes
N_2	5%	No
Aromatics	0.1%	Yes

As previously mentioned, the actual coke is used as the major fuel source inside the blast furnace. It is charged into the top of the furnace, along with iron ore pellets and fluxing agents, and descends slowly into the hotter heating zones in the middle of the blast furnace. At all times, it is imperative for air flow to be uniform across the cross sectional area of the furnace. If the inlet charge crumbles and clumps together as it descends, air will not flow properly and an uneven furnace heat profile will result. Coke is the only material that can provide this required packed bed support structure [11]. It is vital that the coke remain strong enough to withstand the immense pressure inside the furnace and not break apart.

Coke strength is measured by two variables: coke strength after reaction (CSR), and stability. CSR is a measure of the coke's ability to hold up at temperatures similar to those experienced in the lower half of the furnace. Stability is measured at room temperature which simulates the environment at the very top of the furnace where the iron pellets and fluxes are added.

Coke oven wall pressure is another important part of coke production. The plastic layers of coke that first develop against the oven walls immediately begin to exert pressure outward. Over time, this pressure build-up can cause serious damage to the oven lining and may require repair. It is therefore important to maintain this variable below an upper limit. Good quality coke can therefore be evaluated by five factors:

1. High carbon content → Highly reactive coke will provide a greater energy output upon combustion in blast furnace
2. Low ash content → Ash must be removed and therefore consumes unnecessary energy
3. High CSR value → Coke must remain intact when subjected to high temperatures existing at the bottom of the blast furnace
4. High stability value → Coke should not break upon initial charge at the mouth of the furnace
5. Low wall pressure → High pressure exertion damages oven walls over time requiring repair

The following sections describe the modeling of cokemaking through both equality and inequality constraints and explain how these variables can be related to the types of coal used in cokemaking. System boundaries and variables used in modeling are defined in Figure 3.4 and help in the understanding of equations describing the coking process.

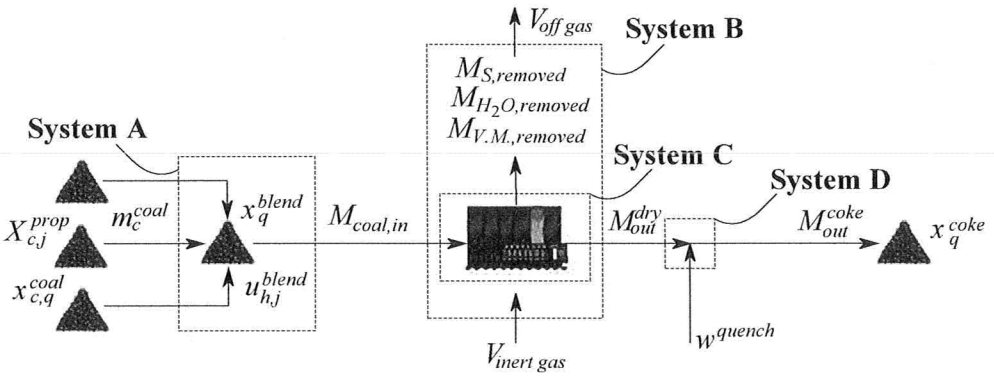

Figure 3.4: Cokemaking variable definition diagram.

3.2.1 Equality Constraints

The cokemaking process begins with the charging of various coal types to the oven. This blending procedure is represented by System A in Figure 3.4 and the mass balance shown in Equation 3.1.

$$M_{coal,in} = \sum_{c} m_c^{coal} \tag{3.1}$$

where,

$$c = \{\text{Coal A, Coal B, Coal C, Coal D, Coal E, Coal F, Coal G}\}$$

The sum of these coal masses comprises the entirety of the coke oven capacity, $M_{coal,in}$, which is a constant parameter. Here, the variable m_c^{coal} is the mass of coal type c added to the coke oven.

An overall mass balance for a single coke batch is written in Equation 3.2 and represented in Figure 3.4 by System B.

$$M_{coal,in} + \rho_{feed\ gas} V_{inert\ gas} = M_{out}^{dry} + \rho_{off\ gas} V_{off\ gas} \tag{3.2}$$

The inputs are charged coal mass $M_{coal,in}$, and hot feed gas volume $V_{inert\ gas}$. Outputs are represented by the solid discharged coke M_{out}^{dry} and released off gas $V_{off\ gas}$.

Equation 3.2 is not included in the model for optimization but serves as a starting point from which to describe the process. The inert feed gas stream conditions with respect to flow and temperature are constant for every batch and are not changed in total mass or composition while in the coke oven. Additionally, the off-gas flow is simply equal to the inlet inert gas plus matter released from the coals during coking. The mass of coal charged is equal to the net mass of coke pushed from the oven, plus coal components removed during coking. There exist three such components being water $M_{H_2O,removed}$, sulphur $M_{S,removed}$, and volatile matter $M_{V.M.,removed}$. Therefore, a mass balance on System C, with the inert gas in and out canceled, is more useful with regard to the formulation.

$$M_{coal,in} = M_{H_2O,removed} + M_{S,removed} + M_{V.M.,removed} + M_{out}^{dry} \tag{3.3}$$

This dry coke mass is then quenched with cooling water, resulting in a final wet coke mass represented by M_{out}^{coke}. A balance on System D is written in Equation 3.4 to express this water addition.

$$M_{out}^{dry} + w^{quench} = M_{out}^{coke} \tag{3.4}$$

A rule of thumb used in industry is to assume after quenching, the coke water content is 6% [18].

$$w^{quench} = 0.06 \cdot M_{out}^{coke} \tag{3.5}$$

The water quench relationship can be inserted into Equation 3.4, and rearranged to isolate M_{out}^{dry}. This can then be included into Equation 3.3 to solve for the final coke mass. Following these steps yields:

$$M_{out}^{coke} = (M_{coal,in} - M_{H_2O,removed} - M_{S,removed} - M_{V.M.,removed}) \cdot \frac{1}{0.94} \tag{3.6}$$

It is assumed that all water initially present in the coal is driven off during coking; however, not all volatile matter and sulphur are removed. In practice, the operating conditions of each coke batch remain constant meaning that the heating rate and final temperature do not change from batch to batch. Also, the temperature of the inlet gas stream $V_{inert\ gas}$ and composition remain fairly constant. If these assumptions are true, the percentage of sulphur and volatile matter released during each batch should change very little. When held at a temperature of over 1000°C, it is unlikely that the heating rate and exact final temperature impact the amount of sulphur and volatile matter remaining in the coals. Therefore, the variables $M_{S,removed}$ and $M_{V.M.,removed}$ can be calculated by assuming they are equal to a constant fraction of their initial coal mass quantities.

Experimental data from 450 coke batches were used to determine the appropriate mass lost for these two components during coking. The experimental database contained measurements of the initial coal sulphur, ash, carbon, and volatile matter contents. Also included were end batch coke composition measurements for sulphur and volatile matter. Water was assumed to be removed, and carbon and ash masses are not changed during coking. A

nonlinear regression was completed in order to minimize the error between the experimental and predicted values.

$$\underset{\beta_S,\,\beta_{V.M.}}{min} \quad \sum_{i=1}^{450} \left(y_i^S - \hat{y}_i^S\right)^2 + \left(y_i^{V.M.} - \hat{y}_i^{V.M.}\right)^2$$

Subject to,

$$\hat{y}_i^S = \frac{\text{Coke sulphur mass}}{\text{Coke mass produced}} = \frac{(1-\beta_S)\cdot S_i^{in}}{A_i^{in} + (1-\beta_S)\cdot S_i^{in} + C_i^{in} + (1-\beta_{V.M.})\, V_i^{in}}$$

$$\hat{y}_i^{V.M.} = \frac{\text{Coke V.M. mass}}{\text{Coke mass produced}} = \frac{(1-\beta_{V.M.})\cdot V_i^{in}}{A_i^{in} + (1-\beta_S)\cdot S_i^{in} + C_i^{in} + (1-\beta_{V.M.})\, V_i^{in}}$$

where,

A_i^{in} = Mass of ash in coal blend charged in experiment i

C_i^{in} = Mass of carbon in coal blend charged in experiment i

S_i^{in} = Mass of sulphur in coal blend charged in experiment i

V_i^{in} = Mass of volatile matter in coal blend charged in experiment i

y_i^S = Coke mass fraction of sulphur measured in experiment i

$y_i^{V.M.}$ = Coke mass fraction of volatile matter measured in experiment i

$\hat{y}_i^S$ = Predicted coke sulphur mass fraction for experiment i

$\hat{y}_i^{V.M.}$ = Predicted volatile matter mass fraction for experiment i

β_S = Fraction of inlet sulphur removed during coking

$\beta_{V.M.}$ = Fraction of inlet volatile matter removed during coking

The solution, which minimizes the total squared prediction error, yields the following parameter values:

$$\beta_S = 0.2585$$

$$\beta_{V.M.} = 0.9833$$

Prediction results are shown in Figures 3.5 and 3.6.

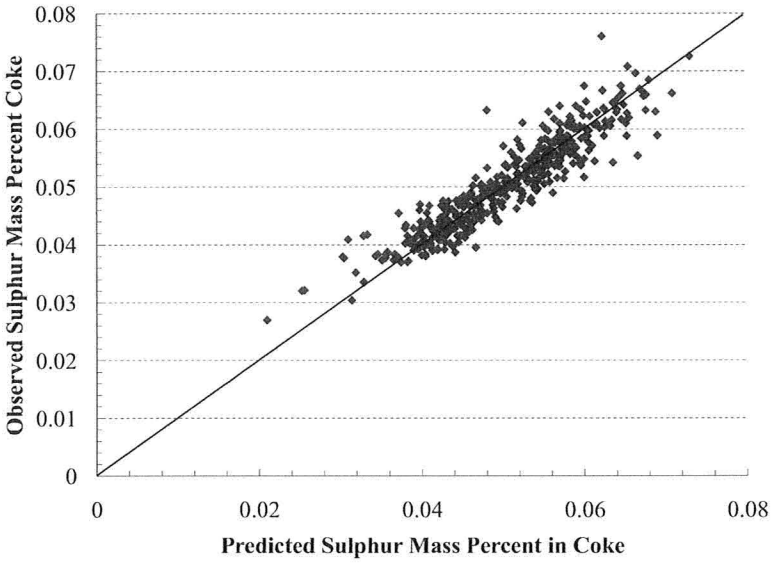

Figure 3.5: Regression fit for sulphur loss during coking.

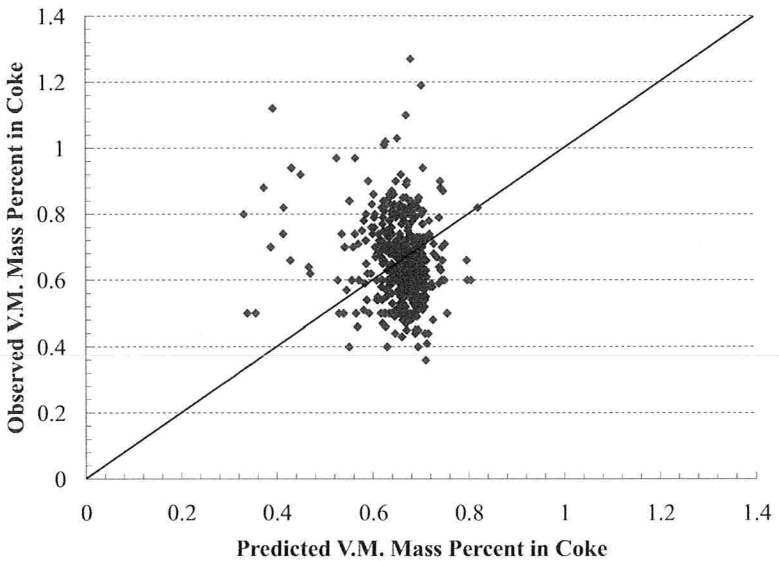

Figure 3.6: Regression fit for volatile matter loss during coking.

The fit of volatile matter data is quite poor, as seen by the deviation between experimental and predicted results in Figure 3.6. However, considering the result of 98.33% loss is in accordance to what is assumed in industry [39], the result is used in this study.

The model fit for sulphur content is far better as can be seen in Figure 3.5. The raw data

for sulphur contained four significant digits indicating far more precise measurements. This percent loss value of 25.85% is also very similar to that assumed in industry [39].

From the outlined regression results, and the assumption that all other coke components are not removed, the following variables can be defined.

$$M_{H_2O,removed} = x_{H_2O}^{blend} \cdot M_{coal,in} \tag{3.7}$$

$$M_{S,removed} = \frac{25.85\%}{100\%} \cdot x_{S}^{blend} \cdot M_{coal,in} \tag{3.8}$$

$$M_{V.M.,removed} = \frac{98.33\%}{100\%} \cdot x_{V.M.}^{blend} \cdot M_{coal,in} \tag{3.9}$$

$$M_{P_2O_5,removed} = M_{C,removed} = M_{SiO_2,removed} = M_{Al_2O_3,removed} = 0 \tag{3.10}$$

The variables $x_{H_2O}^{blend}$ and x_{q}^{blend} are the resulting component mass fractions of the coal blend as shown in Figure 3.4. The set q represents all components in the coals that are not water. Using the mass fractions of these components for each individual coal type c, and assuming the compositions blend linearly, the resulting blend compositions can be calculated.

$$x_{H_2O}^{blend} = \frac{\sum_c \left(x_{c,H_2O}^{coal} \cdot m_c^{coal} \right)}{M_{coal,in}} \tag{3.11}$$

$$x_{q}^{blend} = \frac{\sum_c \left(x_{c,q}^{coal} \cdot m_c^{coal} \right)}{M_{coal,in}} \quad \forall q \tag{3.12}$$

where,

$$q = \{\mathrm{Al_2O_3},\ \mathrm{C},\ \mathrm{P_2O_5},\ \mathrm{S},\ \mathrm{SiO_2},\ \text{Volatile Matter}\}$$

After water, sulphur, and volatile matter are removed, and subsequent water quenching completed, the coke composition can be calculated on a wet basis.

$$x_{q}^{coke} = \frac{\left(x_{q}^{blend} \cdot M_{coal,in} \right) - M_{q,removed}}{M_{out}^{coke}} \quad \forall q \tag{3.13}$$

$$x_{H_2O}^{coke} = 0.06 \tag{3.14}$$

An energy balance for the cokemaking process is not modeled. Each coke batch is operated under constant operating conditions, and therefore, no degrees of freedom exist with regard to the optimization formulation.

3.2.2 Inequality Constraints

The amount of each coal type c added can be zero or between minimum and maximum limits represented by the parameters m_{min}^{coal} and m_{max}^{coal}. Adding this constraint ensures that the solution does not call for an addition of an impractically small amount. The binary variable, δ_c^{use}, is used to enforce this constraint.

$$\delta_c^{use} \cdot m_{min}^{coal} \leq m_c^{coal} \leq \delta_c^{use} \cdot m_{max}^{coal} \quad \forall c \tag{3.15}$$

The interpretation of δ_c^{use} is explained as:

$$\delta_c^{use} \begin{cases} 0 & \text{if coal } c \text{ is not used in the coal blend} \\ 1 & \text{if coal } c \text{ is used in the coal blend} \end{cases}$$

In this formulation, it is assumed that no initial coke inventory exists and that any coke used must also be made during the same period in question. Therefore, the total coke used during the optimization period, T_{length}, cannot exceed the total coke production mass. The mass of coke used is defined as the coke addition rate to the continuously operated blast furnace, $\dot{M}^{coke}$. The coke mass produced can be calculated from the size of one coke batch, M_{out}^{coke}, and the total number of batches made, A^{coke}.

$$\dot{M}^{coke} \cdot T_{length} \leq M_{out}^{coke} \cdot A^{coke} \tag{3.16}$$

In reality, the variable A^{coke} is an integer. However, if the optimization period, T_{length}, is sufficiently long, the number of required coke batches to be made will be a large number. Case studies shown in this thesis involve production of 180 to 200 batches on a weekly basis. At this production level, the error involved in not representing A^{coke} as integer is negligible and is certainly smaller than the accuracy of the coke mass per batch in the plant.

Based on the total number of coke batches made, the total mass of coal type c used during the time period must be less than mass purchased represented by B_c^{coal}.

$$m_c^{coal} \cdot A^{coke} \leq B_c^{coal} \quad \forall c \tag{3.17}$$

Upon delivery, different coal types are organized by separating them into individual inventory piles. There is only enough room on site for up to N^{coal} piles.

$$\sum_{c} \delta_c^{use} \leq N^{coal} \tag{3.18}$$

In this study, the value of N^{coal} is set to four and represents that of an actual steel plant [39].

Additional constraints must be written relating to the oven operation and the final coke strength as described in Section 3.2. The final coke strength, y^{CSR}, and stability, $y^{Stab.}$, must meet minimum requirements. Likewise, there exists an upper limit on the pressure exerted on the oven wall during coking which is represented by $y^{W.P.}$.

$$y^{CSR} \geq y_{min}^{CSR} \tag{3.19}$$

$$y^{Stab.} \geq y_{min}^{Stability} \tag{3.20}$$

$$y^{W.P.} \leq y_{max}^{Pressure} \tag{3.21}$$

Developing mechanistic models for these three variables would be very challenging, and therefore, alternative empirical models have been built in order to make predictions.

Model Building

Raw data was obtained from testing completed in a pilot plant coke oven, containing a total of 77 batch runs. During the experiments, 11 coal blend properties and 11 oven operating conditions were recorded, in addition to the final coke CSR, stability, and oven wall pressure. Coal properties include chemical, rheological, and petrographical measurements, whereas, operating conditions are related to such factors as heating rate and coal charge density. Preprocessing was performed by mean centering and scaling the raw data measurements y_e.

$$y_e^{pre} = \frac{y_e - y^{\mu}}{y^{\sigma}} \quad \forall\, e \tag{3.22}$$

where,

y_e^{pre} = Preprocessing raw data value of observation e

y_e = Raw data value of observation e

y^{μ} = Mean of raw data observation values

y^{σ} = Standard deviation of raw data observation values

It is first assumed that wall pressure, stability, and CSR are each a linear function of the coal blend properties and oven operating conditions. The model form is shown in Equation 3.23 where the set h represents the three model prediction variables.

$$y^h = r_h^T \beta_h \tag{3.23}$$

where,

$$r_h = \left[1, u_h^{blend^T}, z_h^{oven^T}\right]^T$$

$$h = \{\text{CSR}, \text{Stability (Stab.)}, \text{Wall Pressure (W.P.)}\}$$

In Equation 3.23, the vector r_h is comprised of a constant term and the vectors u_h^{blend} and z_h^{oven}. Various coal blend properties used for each model h are stored in u_h^{blend}, whereas oven operating conditions are stored in z_h^{oven}.

Partial Least Squares (PLS) regression was used to obtain the β_h coefficients for each model individually. This procedure is called PLS-1, and involves building a separate model for each of the three desired prediction variables. PLS was employed over other methods such as Multiple Linear Regression (MLR) for several reasons. The algorithm used in determining coefficient parameters maximizes the covariance between input and output variables. If no covariance exists, the PLS model is equal to that of MLR which ignores the correlation between variables. Therefore, at worst the PLS model is equivalent to that of MLR. Additionally, missing values in the experimental database are not discarded, as in MLR, and instead the regression develops an estimate of the missing observation.

The basic premise of PLS regression is that raw data points are projected into a lower

dimensional latent space due to correlation between variables. The total number of dimensions is equal to the number of orthogonal directions required to explain the raw data variance in the latent space. Each orthogonal dimension is denoted as a latent variable with the total number being smaller for more correlated data sets.

PLS model performance can be evaluated by looking at it's Q^2 value representing the cross validation model score. A higher Q^2 value indicates better predictive capability. The latent variable explaining the most variance in the latent space is first used to build an initial model. A Q^2 value is computed, the next most important latent variable added, and a new model created. Q^2 is then recomputed and compared to the previous value to see if it increased or decreased. Including more latent variables does not necessarily result in improved predictive capability as the model will pick up on noisy and unimportant variables, thus diminishing Q^2. Therefore, PLS algorithms successively add latent variables until Q^2 is maximized.

Q^2 is computed by dividing the full data set into D sub groups. The procedure begins by removing one group and building a model based on the remaining data. The prediction sum of squares (PRESS) for omitted data is calculated and stored, and the procedure repeated D times, removing each raw data set only once [37]. In this study, the value of D used is 7.

$$PRESS = \sum_{d}^{D} \sum_{m}^{M} (y_{m,d} - \hat{y}_{m,d})^2 \tag{3.24}$$

where,

m = Raw data observation within subgroup

d = Sub group of data set

$y_{m,d}$ = Raw data value of observation m in sub group d

$\hat{y}_{m,d}$ = Predicted value of observation m in sub group d

After adding the individual PRESS statistics for each group d, the calculation of Q^2 is completed.

$$Q^2 = \frac{\sum_e (y_e - \hat{y}_e)^2 - PRESS}{\sum_e (y_e - \hat{y}_e)^2} \tag{3.25}$$

where,

$\hat{y}_e$ = Predicted value of observation e

The predicted value, $\hat{y}_e$, is obtained from the PLS model which uses the full data set and not the individual sub groups. The numerator of Equation 3.25 calculates the difference between the overall model prediction error and that incurred during cross validation. By dividing this difference by the overall error, the result is the fraction of total variance of the y variable that can be predicted by the model [13]. A well performing PLS model, therefore, has a high Q^2 value.

The R^2 value can also be considered a measure of model adequacy and involves subtracting the ratio of prediction sum of squares and residual sum of squares from one. The formula for this calculation is shown in Equation 3.26.

$$R^2 = 1 - \frac{\sum_e (y_e - \hat{y}_e)^2}{\sum_e (y_e - y^\mu)^2} \tag{3.26}$$

This value measures the variance in the data explained by the model. A high R^2 value can sometimes be misleading because this number always increases as more latent variables are included in the regression model. As previously stated, the model predictability can worsen as more latent variables are added, and so, caution must be used when citing R^2 as an explanation for model fit.

Another available evaluation tool is the Variable Importance to Projection (VIP) plot. This measures the influence of each variable in explaining both the x and y data space [46]. The greater the value in the VIP plot, the more important that variable is to the model prediction capability. It is generally considered that variables with a VIP score of 1 or greater are significant to the model; however, this is not always a steadfast rule.

The objective of building empirical models using PLS regression is to maximize the value of Q^2. From the experimental pilot plant data set, it was deemed that not all 22 variables were significant for prediction. These unnecessary variables, as well as outliers, were identified and removed in order to maximize the predictive capability of the models.

The following iterative procedure was used in order to isolate the most important model variables, which we will refer to as pruning.

1. Normalize and mean center raw data
2. Build model based on all 22 coal properties and oven conditions, determining the number of latent variables required to maximize Q^2
3. Remove outliers by investigating residual prediction plots
4. Rebuild model determining the number of latent variables required to maximize Q^2
5. Remove variables with small VIP values
6. Rebuild model
7. Return to step 3 until Q^2 value of model is maximized

Coke Modeling Results

Table 3.3 lists the subset of variables remaining after pruning from the original set of 22 input variables.

Table 3.3: Classification of coke property PLS model inputs.

Model Variable	Description	Units
$u_h^{blend}(FSI)$	Free Swelling Index: a cross-sectional profile measurement of the coal after coking	None
$u_h^{blend}(Ro)$	Measure of the coal reflectance	%
$u_h^{blend}(H_2O)$	Mass percent of water in the coals	%
$u_h^{blend}(V.M.)$	Mass percent of volatile matter in coals	%
$u_h^{blend}(Ash)$	Mass percent of ash in the coals	%
$u_h^{blend}(Inerts)$	Percent of inert material in coals	%
$z_h^{oven}(Grind)$	Measure of coal coarseness	%
$z_h^{oven}(BD)$	Bulk density of coals charge	lb/ft^3
$z_h^{oven}(900)$	Heating rate to $900°C$	in/hr
$z_h^{oven}(Oil)$	Oil added to coal charge	%
$z_h^{oven}(Soak)$	Time after charge reaches 950°C	hr

Prosensus Multivariate 10.02, a commercial software package, was used to build the PLS models. Table 3.4 gives a summary of the final results, including the performance and total number of variables used in each case for predictions. The number of outliers removed and number of latent variables used are also included.

Table 3.4: Coke PLS model summary statistics.

Model (h)	Removed Outliers	Latent Variables	Q^2	R^2	Input Variables in Final Model	
					Coal Property u-variables	Oven Condition z-variables
CSR	0	4	.72	.87	5	3
Stability	3	3	.81	.83	4	5
Wall Press.	2	2	.75	.77	4	4

None of the models used all 11 variables in Table 3.3 and instead are comprised of a fraction of the total. Very few outliers were present in the data set which is important considering that only a total of 77 initial observations existed. Because the data set is relatively small, removing outliers significantly reduces the information available to the regression algorithm. In order to avoid diminishing the data set size, outliers were never removed more than one at a time during model building.

CSR Model Results

The model form for the prediction of CSR is shown in Equation 3.27.

$$y^{CSR} = \Big[1, u^{blend}_{CSR}(Inerts), u^{blend}_{CSR}(Ro), u^{blend}_{CSR}(V.M.), u^{blend}_{CSR}(H_2O), \\ z^{oven}_{CSR}(Oil), z^{oven}_{CSR}(BD), z^{oven}_{CSR}(Grind), z^{oven}_{CSR}(900)\Big]^T \beta_{CSR} \tag{3.27}$$

Four coal properties and oven conditions are used to predict CSR. Figures 3.7 and 3.8 give an indication of the prediction accuracy and importance of input variables. The raw data is centered around a confidential mean value due to the business sensitivity of plant operating values. All other similar model results will be centered in the same manner.

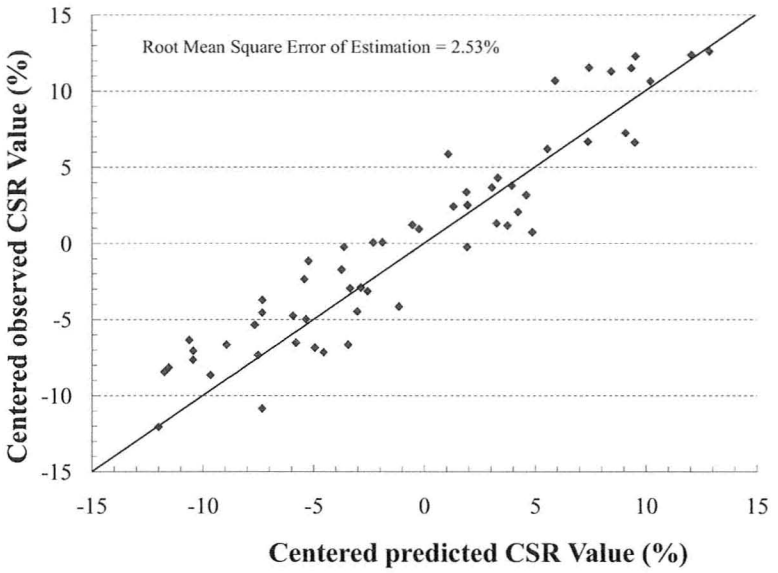

Figure 3.7: Observed vs. predicted results for CSR model.

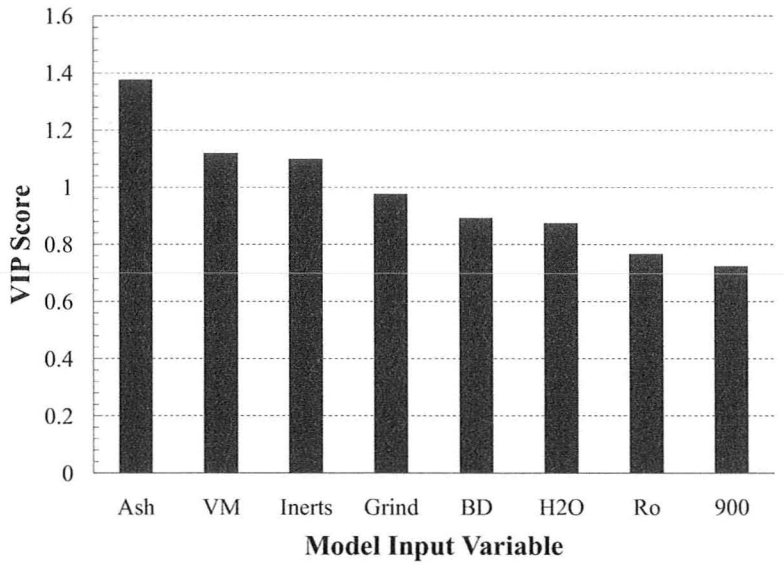

Figure 3.8: VIP plot for CSR model.

The accuracy of the model is fairly good, yielding a Q^2 value of 0.72, meaning the linearity assumption is valid for the prediction of CSR. The VIP plot in Figure 3.8 shows that CSR is highly dependent upon the chemical properties of coal ash, inerts, and volatile matter.

Less importance is placed on the oven operating conditions although the lowest VIP value is still fairly high at a magnitude of 0.73 belonging to the variable z_{900}^{oven}.

The Root Mean Squared Error of Estimation (RMSEE), as indicated in Figure 3.7, is 2.53%. This measures the standard deviation of residuals in the raw data set and gives a sense of prediction reliability.

Stability Model Results

The model form for the prediction of coke stability is shown in Equation 3.28.

$$y^{Stab.} = \Big[1, u_{Stab.}^{blend}(Ash), u_{Stab.}^{blend}(Ro), u_{Stab.}^{blend}(V.M.), u_{Stab.}^{blend}(H_2O), z_{Stab.}^{oven}(Oil), z_{Stab.}^{oven}(BD), z_{Stab.}^{oven}(Grind), z_{Stab.}^{oven}(900), z_{Stab.}^{oven}(Soak)\Big]^T \beta_{Stability} \tag{3.28}$$

In this case, more coke oven operating conditions are present in the final model. Interestingly, seven of the eight variables used to predict CSR also appear in the stability model. The raw data points compared to their predicted values, as well as the VIP plot for the model, are given in Figures 3.9 and 3.10.

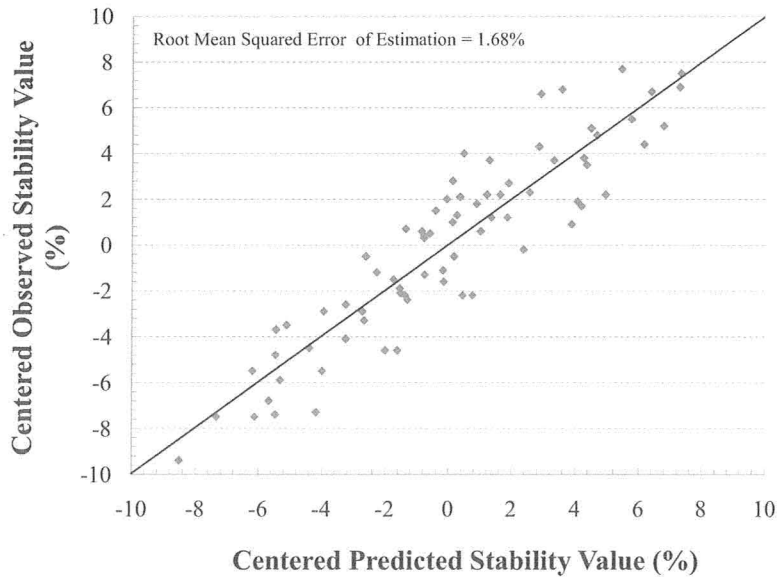

Figure 3.9: Mean centered prediction results for coke stability model.

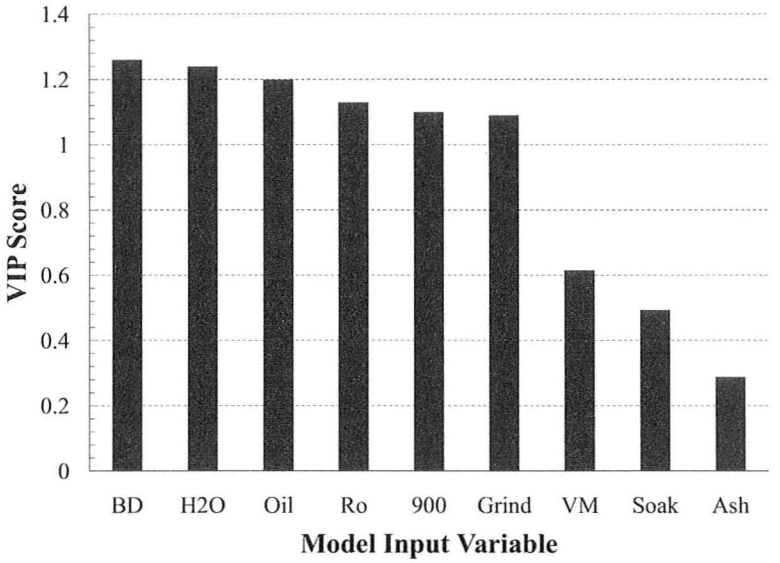

Figure 3.10: VIP plot for coke stability model.

The model performance for the prediction of stability yields a Q^2 value of 0.81 with a RMSEE of 1.68%. These values that indicate the linearity assumption holds for the stability model. Three outliers were removed in the building stages, yielding a model with nine inputs and three principle components. The VIP plot shows that for stability, the oven operating conditions are more important as four of these variables had a score of over one.

While the CSR and stability model inputs are very similar, their respective VIP plots are quite different. For CSR, the coal volatile matter and ash contents are most influential in predictions. For stability, these two variables remain in the model yet possess two of the lowest VIP scores.

Wall Pressure Model Results

An initial PLS model was built yielding a Q^2 value of just 0.50. Figures 3.11 shows the observed versus predicted results for this model.

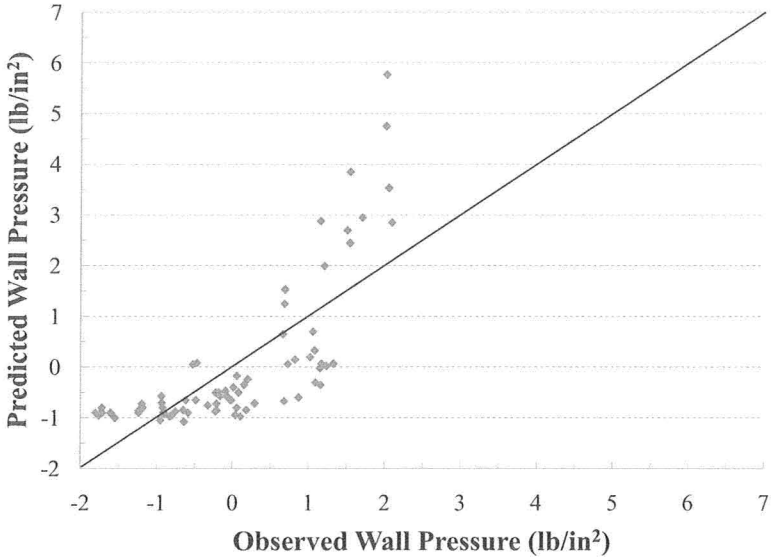

Figure 3.11: Mean centered prediction results for initial coke oven wall pressure model.

Figure 3.11 indicates that the model prediction is very poor; the data points do not fit along the diagonal prediction line and instead the residuals exhibit strong correlation. This most likely indicates that the linearity assumption in predicting wall pressure is incorrect. Validation of this fact can be investigated by looking at the latent variable scores of the data.

When the raw data points are projected into the latent variable space, they are assigned a principle component score. Each x data point is represented by a T-score. For a model using three principle components, the T-score is a 3×1 vector in the latent variable space. Similarly, each y data point is represented by a U-score. Figure 3.12 shows the PLS T and U scores only for the first principle component since it explains an overwhelming majority of the variance.

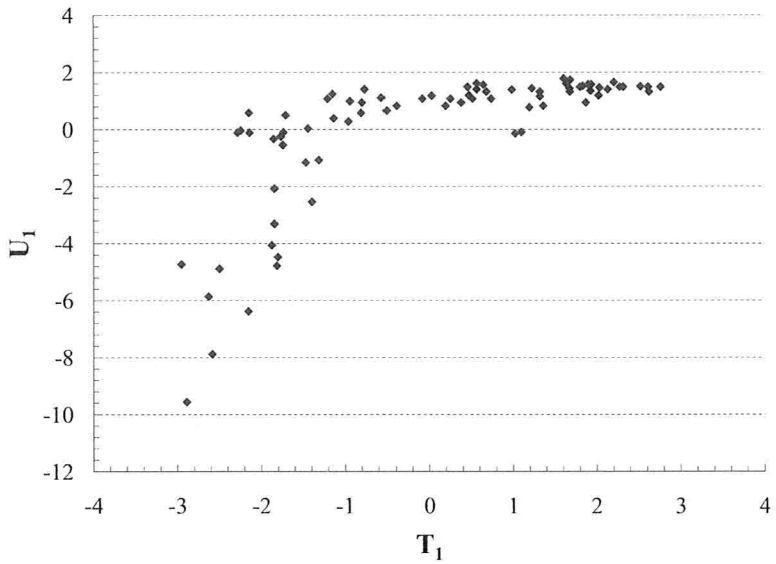

Figure 3.12: Wall pressure latent variable score plot for the first component.

If a linear relationship exists between the wall pressure and model inputs, these scores would also be linearly related in the latent space [2]. Instead, Figure 3.12 shows that the relationship between the x variables and wall pressure is not linear.

Using this information, a variable transformation was completed based on industrial experience that suggested prediction of the natural logarithm of wall pressure yields better results [39]. The model form for the modified prediction of wall pressure is shown in Equation 3.29.

$$\ln\left(y^{W.P.}\right) = \Big[1, u^{blend}_{W.P.}(FSI), u^{blend}_{W.P.}(Ro), u^{blend}_{W.P.}(V.M.),$$
$$u^{blend}_{W.P.}(H_2O), z^{oven}_{W.P.}(Oil), z^{oven}_{W.P.}(BD), z^{oven}_{W.P.}(Grind), z^{oven}_{W.P.}(900)\Big]^T \beta_{W.P.} \tag{3.29}$$

The final model uses an equal number of coal properties and oven operating conditions. Two principle components are used by the model and only two outliers were removed during building. Additionally, the model's Q^2 value is 0.75, with a MSEE of 2.5 lb/in^2, indicating good predictive capability as displayed in Figure 3.13.

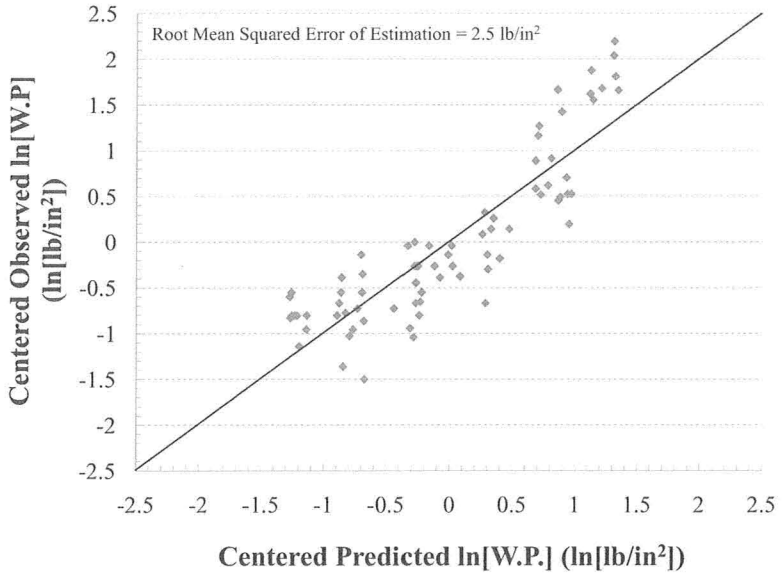

Figure 3.13: Mean centered prediction results for wall pressure model.

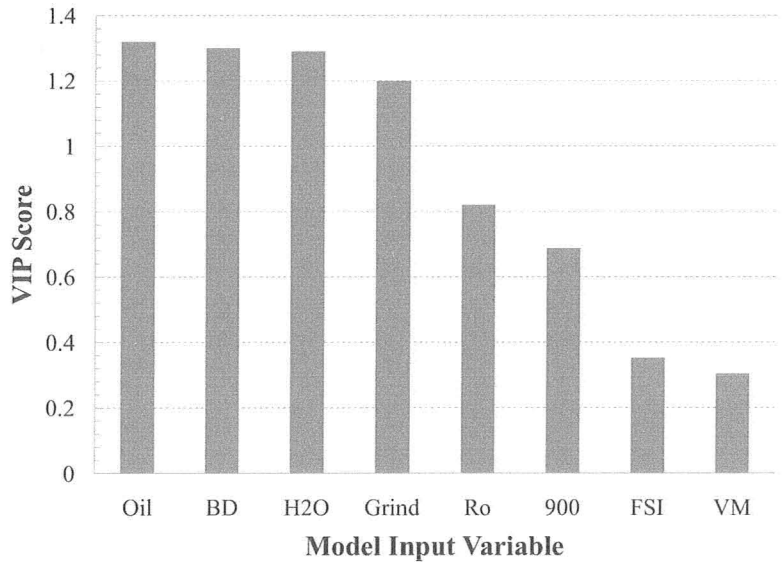

Figure 3.14: VIP plot for modified wall pressure model.

Figure 3.14 shows once more that the most significant model inputs are those of the oven operating conditions. Coal property variables such as volatile matter content and free

swelling index are less important. However, despite their respective low VIP scores, their inclusion in the model is still important; when each variable was removed and the model rebuilt, the Q^2 value decreased significantly.

By using the logarithmic variable transformation, the Q^2 value increased from 0.50 to 0.75. While this adds more non-linearity to the formulation, the model improvement is too large to ignore. Wall pressure is an important consideration in cokemaking, and using a poor quality model would diminish the value of any results.

One of the potential advantages in using PLS regression is that correlation among variables is incorporated in determining the β coefficients. This includes both the x and y variables. Therefore, if two y prediction variables are correlated, they should be developed together in one single model, denoted as PLS-2.

In the case of stability and CSR, these two strength properties are highly correlated. When CSR is high in magnitude, so is stability. A joint PLS-2 model was built, and the maximum Q^2 attainable was 0.69 and not as large as the value for either independent model. Since the objective is to maximize Q^2, it was concluded that the correlation between stability and CSR was not significant enough to include them in the same model.

Defining Fixed Model Inputs vs. Optimization Variable Inputs

The model coefficients have been established. Before including the three PLS models in the formulation, the input variables must be classified as fixed (constant) or variable and adjustable by the optimizer.

Table 3.4 shows that the three models require five oven conditions to be specified. However in industrial practice these values are fixed. Therefore, the model inputs represented by z_h^{oven} are constant and in this study they are set to their respective mean values in the experimental data set.

Properties contained in the vector u_h^{blend} can be determined from vendor supplied coal specifications. Values of these properties are stored in the matrix $X_{c,j}^{prop}$, which is a database where the value of coal property j is stored for each coal type c. This matrix is different from the parameter matrix $x_{c,q}^{coal}$, which stores the mass fraction of component q in coal c, because it also contains coal rheological and petrographical quality information. Some information stored in $x_{c,q}^{coal}$ is therefore duplicated in $X_{c,j}^{prop}$.

Assuming linear blending rules apply, each coal property can be calculated using the variable m_c^{coal} which determines the mass of each coal type c charged to the furnace.

$$u_h^{blend}(j) = \sum_c \left(\frac{m_c^{coal}}{M_{coal,in}} \cdot X_{c,j}^{prop} \right) \quad \forall j, h \tag{3.30}$$

In Equation 3.30, the final blend property value is the weighted average of that property for all the coals used.

Once the values of the oven conditions are fixed in the models, the predictions of y^{CSR}, $y^{Stab.}$, and $y^{W.P.}$ become solely a function of the coal blend properties $u_h^{blend}(j)$. Equation 3.30 demonstrates that these properties are subsequently a function of the decision variables m_c^{coal}; hence, the three prediction models are a function of these variables.

$$y^h = r_h^T \beta_h = f\left(m_c^{coal}\right) \quad \forall\, h$$

The models expressed by Equations 3.27, 3.28, and 3.29 can now be included in the optimization formulation in order to evaluate variables in Equations 3.19, 3.20, and 3.21.

Preventing Extrapolation to Regions Unsupported by Data

Models built from first principles can often be used to make predictions extrapolated, with caution, from the domain of nominal conditions. Since the previously shown coke models were built on empirical correlations, their use in optimization should be limited. The model input vector, r_h, is a function of the decision variable m_c^{coal} which can be manipulated by the optimizer. It is therefore desired that, as a result of changes in m_c^{coal}, the optimizer does

not cause the input r_h to make predictions unsupported by raw data. Constraints can be added in order to limit the amount of model extrapolation executed during the optimization [33].

The input vector r_h contains a total of $K_h + 1$ elements. The value 1 is for the constant term in the linear regression equation and the value K_h is equal to the number of blend properties and oven conditions included in the model h. The set k_h contains each of these blend properties and oven conditions. This information is summarized in Table 3.5 for each model.

Table 3.5: Resulting number of inputs and principle components in coke prediction models.

Model (h)	K_h	Elements in set k_h
CSR	8	k_{CSR} = {Inerts, Ro, V.M., H_2O, Oil, BD, Grind, 900}
Stability	9	$k_{Stab.}$ = {Ash, Ro, V.M., H_2O, Oil, BD, Grind, 900, Soak}
Wall Pressure	8	$k_{W.P.}$ = {FSI, Ro, V.M, H_2O, Oil, BD, Grind, 900}

The first step is to center and scale each model input creating the new vector r_h^* containing K_h elements.

$$r^*_{CSR}(k) = \frac{r_{CSR}(k) - r^{\mu}_{CSR}(k)}{r^{\sigma}_{CSR}(k)} \quad \forall\, k \in k_{CSR} \tag{3.31}$$

$$r^*_{Stab.}(k) = \frac{r_{Stab.}(k) - r^{\mu}_{Stab.}(k)}{r^{\sigma}_{Stab.}(k)} \quad \forall\, k \in k_{Stab.} \tag{3.32}$$

$$r^*_{W.P.}(k) = \frac{r_{W.P.}(k) - r^{\mu}_{W.P.}(k)}{r^{\sigma}_{W.P.}(k)} \quad \forall\, k \in k_{W.P.} \tag{3.33}$$

The parameters r_h^{μ} and r_h^{σ} are the mean and standard deviation vectors for model h. For example, the parameter $r^{\mu}_{CSR}(Ro)$ is the mean of the experimental observations for coal reflectance used to build the CSR model.

In the PLS framework, each data point is first projected onto the model's latent variable space according to the Equation 3.34.

$$T_h^* = (r_h^*)^T \cdot W_h^* \quad \forall\, h \tag{3.34}$$

The parameter matrix W_h^* is of dimension $K_h \times A_h$ and represents loading values of model inputs for each principle component. The number of latent variables used in each PLS model, A_h, is given in column three of Table 3.4.

The T-score, T_h^*, is first used to determine the distance of the new data point from the center of the latent space. This score represents the projection of the r_h^* vector onto the latent space. The Hotelling T^2 value represents the distance from the center of the data set to this projection. It is desired that for any r_h^* vector, this distance be restricted to a maximum user selected distance $T^2_{max,h}$.

$$\sum_{i=1}^{4} \frac{{T^*_{CSR,i}}^2}{s^2_{CSR,i}} \leq T^2_{max,CSR} \tag{3.35}$$

$$\sum_{i=1}^{3} \frac{{T^*_{Stab.,i}}^2}{s^2_{Stab.,i}} \leq T^2_{max,Stab.} \tag{3.36}$$

$$\sum_{i=1}^{2} \frac{{T^*_{W.P.,i}}^2}{s^2_{W.P.,i}} \leq T^2_{max,W.P.} \tag{3.37}$$

In the above equations, $T^*_{h,i}$ is the i^{th} component of vector T_h^*. The parameter $s^2_{h,i}$ is computed from the raw data and is equal to the variance of the latent T-scores used in the building of model h. $T^2_{max,h}$ is a control limit threshold and is set to a 99% level of significance in this study [37].

The new data point's T-score can also be used to determine its orthogonal distance from the model latent space. This score, in combination with loading coefficients for the model, P_h, are used to estimate the value of r_h^*, represented by $\hat{r}_h^*$.

$$(\hat{r}_h^*)^T = T_h^* \cdot P_h^T \quad \forall\, h \tag{3.38}$$

The parameter matrix P_h is of dimension $K_h \times A_h$ and is obtained from the regression model.

The squared difference between the original and estimated point represents the new point's orthogonal distance off the model plane and is called the squared prediction error of x (SPE-X). This distance can be constrained by limiting the result to a user selected upper

control limit of ϵ_h.

$$\sum_{k \in k_{CSR}} \left(r^*_{CSR}(k) - \hat{r}^*_{CSR}(k)\right)^2 \leq \epsilon_{CSR} \tag{3.39}$$

$$\sum_{k \in k_{Stab.}} \left(r^*_{Stab.}(k) - \hat{r}^*_{Stab.}(k)\right)^2 \leq \epsilon_{Stab.} \tag{3.40}$$

$$\sum_{k \in k_{W.P.}} \left(r^*_{W.P.}(k) - \hat{r}^*_{W.P.}(k)\right)^2 \leq \epsilon_{W.P.} \tag{3.41}$$

In this study, a 99% level of significance was used to determine the value of ϵ_h [37].

Equations 3.35 - 3.37, and 3.39 - 3.41 can be added to the formulation in order to ensure the optimization does not obtain a solution which predicts CSR, stability, and wall pressure outside of their respective model regions of validity.

3.2.3 Cokemaking Summary

The preceding sections have given a background of the cokemaking process and the factors involved in production of coke. Modeling of this process has been outlined through mass balance equality constraints and inequality constraints governing the actual production limitations.

3.3 Ironmaking

The blast furnace operation comprises the entirety of ironmaking production. Figure 3.15 gives an overview of this process.

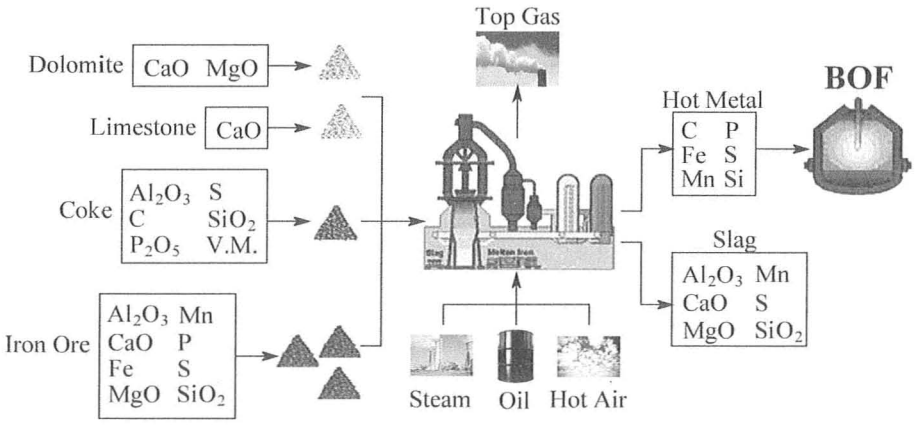

Figure 3.15: Overview of ironmaking process.

The main input stream to the blast furnace is iron ore pellet addition. Iron is usually found in two different forms, magnetite (Fe_3O_4) and hematite (Fe_2O_3). Similar to coal, undesirable ash components are also present. Table 3.6 gives an approximate composition of a pellet.

Table 3.6: Approximate composition of an iron ore pellet.

Component	Mass Percent [34]
Al_2O_3	0.5%
CaO	0.5%-4%
$Fe_2O_3 + Fe_3O_4$	85%-90%
$\hookrightarrow$ Fe	60%-65%
MgO	1%-3%
Mn	0.1%-2%
P	$\approx$ 0.015 %
S	$\approx$ 0.010 %
SiO_2	3%-6%

The ratio of hematite to magnetite is dependent on the geographical source of the ore and therefore when reporting ore composition, the elemental iron content is given. Silica, magnesium oxide, manganese, and calcium oxide are present in significant quantities, all of which are undesirable and must be removed. Trace amounts of phosphorous and sulphur are introduced to the blast furnace via iron pellets as well.

The main objective of the blast furnace is to provide a heating environment that can reduce the hematite and magnetite into elemental iron. Furthermore, it is important to separate this iron from the undesired impurities by creating a slag which floats on top of the hot iron. Slag formation is promoted by controlling the acid to base ratio of impurities. Acidic components consist of alumina and silica entering through the coke and pellets. Basic components are that of magnesium oxide and calcium oxide which are present in the pellets only. In order to control this ratio, fluxing agents are added as inputs to the furnace in the form of lime and dolomite. Lime contains only CaO, while dolomite is comprised of both CaO and MgO.

Depending on the ash contents of the pellets and coke, lime and dolomite are added such that slag can form and separate from the iron at the furnace exit.

The feed components spend a significant amount of time inside the blast furnace before reaching the exit. For efficient operation, it is important that the pellets, coke, and fluxing agents are fed in accurate proportions and mixed well. As these solids descend through the furnace, the coke begins to combust and pellets and flux begin to reduce and liquefy. The reduction must be gradual requiring a specific heating profile from the top to bottom of the furnace. A poor heating profile creates pockets of hot and cold zones inside the furnace, making both slag formation and iron reduction difficult.

Heat is generated from several different sources. These include coke combustion, hot blast air addition, and oil combustion. Blast air is fed from the bottom of the furnace at a temperature of around 1000°C. This air is important to provide oxygen for coke combustion throughout the furnace. As mentioned in Section 3.2, it is necessary that the coke be strong enough to not break apart and clump together in the furnace. In other words, the void

fraction of the descending solid mass of pellets, flux, and coke must be large enough for the air to pass evenly upwards.

If for some reason adjustments need to be made concerning the furnace heat profile, the total coke addition rate can be changed. In some circumstances, however, this may be impractical. Since the solids entering the furnace take over six hours to descend, a change in the coke rate may not be reflected inside the furnace for quite some time. To overcome this delay, oil can be combusted at the bottom of the furnace to provide a quicker heat injection. Additionally, if the coke addition rate is constrained and there is simply not enough supply to meet the blast furnace demand, oil can again be used to make up for the energy input deficit. However, oil is a very costly means of generating heat and is not used on a regular basis.

Alterations to the blast furnace temperature can similarly be made through steam injection. This has the opposite impact of oil combustion in that steam injected into the furnace consumes a great deal of energy. High blast furnace temperatures are undesirable as they can cause the impurity concentration to rise in the exit hot metal. While it is important to reduce the iron oxide compounds, temperatures that are too high also reduce silica to a significant degree. When this happens, the fluxing agents are not able to separate out the SiO_2 resulting in very high Si levels in the exit hot metal.

The blast furnace outputs involve three streams: hot metal, slag, and the top gas. The approximate composition of each stream is given in Table 3.7.

Table 3.7: Approximate mass percent composition of blast furnace exit streams.

Hot Metal [34]		Slag [34]		Top Gas [22]	
C	4%	Al_2O_3	10%	CO	20%
Fe	95%	CaO	40%	CO_2	28%
Mn	0.5%	MgO	15%	H_2	2%
P	<0.1%	Mn	<0.1%	N_2	60 %
S	<0.1%	S	<0.1%		
Si	0.5%	SiO_2	35%		

The blast furnace top gas contains only two combustible components in low quantities and therefore is very low in calorific value. The revenue generated from recycling this gas is very small and considered negligible in this formulation.

Hot metal contains a significant amount of carbon, with the remainder being iron and impurities in liquid form. Table 3.7 lists impurities that are not removed in the slag, and instead exit in the hot metal as well. Silicon, manganese, and sulphur are partially removed in the slag; however, the reducing environment of the furnace does not allow for the phosphorous to oxidize and separate.

The ironmaking process involves several streams comprised of numerous components making modeling of the blast furnace fairly complex. Variables used in modeling are defined in Figure 3.16.

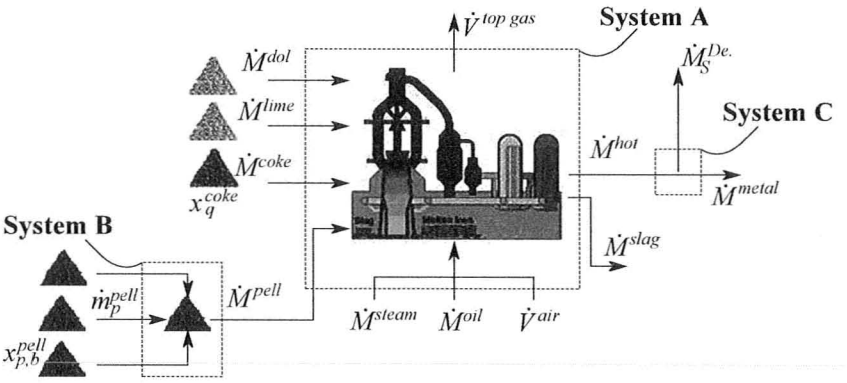

Figure 3.16: Variable definition diagram for ironmaking.

3.3.1 Equality Constraints

The iron blast furnace is a continuous operation, and an overall mass balance is expressed by Equation 3.42, represented by System A in Figure 3.16.

$$\dot{M}^{in} = \dot{M}^{out} \tag{3.42}$$

where,

$$\dot{M}^{in} = \dot{M}^{coke} + \dot{M}^{pell} + \dot{M}^{dol} + \dot{M}^{lime} + \dot{M}^{oil} + \dot{M}^{steam} + \rho_{air}\dot{V}^{air}$$
$$\dot{M}^{out} = \dot{M}^{hot} + \dot{M}^{slag} + \rho_{top\ gas}\dot{V}^{top\ gas}$$

The inputs include coke $\dot{M}^{coke}$, pellets $\dot{M}^{pell}$, dolomite $\dot{M}^{dol}$, limestone $\dot{M}^{lime}$, oil $\dot{M}^{oil}$, steam $\dot{M}^{steam}$, and blast air $\dot{V}^{air}$. Solids exit in the slag $\dot{M}^{slag}$, or hot metal $\dot{m}^{hot}$ streams. Gases resulting from combustion and other reactions leave in the top gas $\dot{V}^{top\ gas}$. All variables are expressed in mass flow units except for the top gas and blast air streams which are volumetric flows.

The pellet addition rate, $\dot{M}^{pell}$, is the major mass input and is equal to the sum of the individual pellet type mass rates, $\dot{m}_p^{pell}$. This represents a balance on System B.

$$\dot{M}^{pell} = \sum_p \dot{m}_p^{pell} \tag{3.43}$$

where,

$$p = \{\text{Pellet A, Pellet B, Pellet C}\}$$

System C, in Figure 3.16, represents sulphur removed by the Desulphurization Facility. The blast furnace can only separate a fraction of the inlet sulphur, and therefore, an additional removal stage is added in order to bring down the sulphur concentration. The mass rate removal is represented by the variable $\dot{M}_S^{De.}$ and the balance shown in Equation 3.44.

$$\dot{M}^{hot} = \dot{M}^{metal} + \dot{M}_S^{De.} \tag{3.44}$$

The variable $\dot{M}^{metal}$ represents the net hot metal, after desulphurization, which is used to provide part of the charge to downstream BOF batches. Mass balances for the three systems in Figure 3.16 have now been written. Component balances must also be specified to complete the model.

Hot metal is made up of six components, represented by the set i, being carbon, iron, manganese, phosphorous, silicon, and sulphur. The summation of these individual masses, $\dot{m}_i^{hot}$, is equal to the total hot metal leaving the blast furnace.

$$\dot{M}^{hot} = \sum_i \dot{m}_i^{hot} \tag{3.45}$$

where,

$$i = \{\text{C, Fe, Mn, P, Si, S}\}$$

Iron enters through pellet addition and is assumed to exit entirely in the hot metal stream represented by $\dot{m}_{Fe}^{hot}$. This iron balance is completed by multiplying the iron mass fraction in pellet p, $x_{p,Fe}^{pell}$, by the mass of that particular pellet added to the furnace.

$$\sum_p \left(x_{p,Fe}^{pell} \cdot \dot{m}_p^{pell} \right) = \dot{m}_{Fe}^{hot} \tag{3.46}$$

Manganese enters through the iron pellets and exits in both the slag, $\dot{m}_{MnO}^{slag}$, and hot metal, $\dot{m}_{Mn}^{hot}$. Since manganese is of the form MnO in slag, the parameter α_{Mn} is used to convert manganese oxide into the mass of manganese only.

$$\sum_p \left(x_{p,Mn}^{pell} \cdot \dot{m}_p^{pell} \right) = \dot{m}_{Mn}^{hot} + \alpha_{Mn} \dot{m}_{MnO}^{slag} \tag{3.47}$$

The exact separation of manganese between the slag and hot metal is determined using an industry rule of thumb represented by the ratio factor r_{Mn}^{slag} [18].

$$\frac{\alpha_{Mn} \cdot \dot{m}_{MnO}^{slag}}{\dot{m}_{Mn}^{hot}} = r_{Mn}^{slag} \tag{3.48}$$

Phosphorous enters the furnace through the coke and pellets and exits in the hot metal represented by $\dot{m}_P^{hot}$.

$$\alpha_P \cdot x_{P_2O_5}^{coke} \cdot \dot{M}^{coke} + \sum_p \left(x_{p,P}^{pell} \cdot \dot{m}_p^{pell} \right) = \dot{m}_P^{hot} \tag{3.49}$$

In coke, phosphorous is in the form of P_2O_5 and is reduced to elemental phosphorous inside the furnace. The parameter α_P converts the phosphorous oxide mass into an elemental phosphorous mass and the variable $x_{P_2O_5}^{coke}$ is the mass fraction of phosphorous oxide in the coke fed to the furnace.

Silica enters the furnace through both the coke and pellets. Some of this silica leaves as part of the slag, $\dot{m}_{SiO_2}^{slag}$, while the remainder is reduced to silicon and exits in the hot metal stream represented by $\dot{m}_{Si}^{hot}$.

$$\alpha_{Si} \cdot x_{SiO_2}^{coke} \cdot \dot{M}^{coke} + \alpha_{Si} \sum_p \left(x_{p,SiO_2}^{pell} \cdot \dot{m}_p^{pell} \right) = \dot{m}_{Si}^{hot} + \alpha_{Si} \cdot \dot{m}_{SiO_2}^{slag} \tag{3.50}$$

In Equation 3.50, the parameter α_{Si} converts the silicon dioxide mass into solely silicon.

Sulphur also enters through both coke and pellets, exiting in the hot metal, $\dot{m}_S^{hot}$, and slag stream, $\dot{m}_S^{slag}$.

$$x_S^{coke} \cdot \dot{M}^{coke} + \sum_p \left(x_{p,S}^{pell} \cdot \dot{m}_p^{pell} \right) = \dot{m}_S^{hot} + \dot{m}_S^{slag} \tag{3.51}$$

Similar to manganese, a rule of thumb exists in order to determine the sulphur ratio, r_S^{slag}, between the exit slag and hot metal.

$$\frac{\dot{m}_S^{slag}}{\dot{m}_S^{hot}} = r_S^{slag} \tag{3.52}$$

Alumina is introduced into the furnace through coke and pellets and exits entirely in the slag stream $\dot{m}_{Al_2O_3}^{slag}$.

$$x_{Al_2O_3}^{coke} \cdot \dot{M}^{coke} + \sum_p \left(x_{p,Al_2O_3}^{pell} \cdot \dot{m}_p^{pell} \right) = \dot{m}_{Al_2O_3}^{slag} \tag{3.53}$$

Calcium oxide enters through the pellets, limestone, and dolomite and leaves in the slag stream $\dot{m}_{CaO}^{slag}$.

$$\sum_{p} \left(x_{p,CaO}^{pell} \cdot \dot{m}_{p}^{pell} \right) + x_{CaO}^{lime} \cdot \dot{M}^{lime} + x_{CaO}^{dol} \cdot \dot{M}^{dol} = \dot{m}_{CaO}^{slag} \tag{3.54}$$

In this equation, x_{CaO}^{lime} and x_{CaO}^{dol} represent the mass fractions of CaO in the limestone and dolomite, respectively.

Magnesium oxide enters through the iron pellets and dolomite, leaving in the stream $\dot{m}_{MgO}^{slag}$.

$$\sum_{p} \left(x_{p,MgO}^{pell} \cdot \dot{m}_{p}^{pell} \right) + x_{MgO}^{dol} \cdot \dot{M}^{dol} = \dot{m}_{MgO}^{slag} \tag{3.55}$$

Slag is comprised of six components represented by the set w. The variable $\dot{m}_{w}^{slag}$ represents the individual mass flows of components reporting to slag, and the summation over the set w defines the total slag flow rate $\dot{M}^{slag}$.

$$\dot{M}^{slag} = \sum_{w} \dot{m}_{w}^{slag} \tag{3.56}$$

where,

$$w = \{Al_2O_3,\ CaO,\ MgO,\ Mn,\ S,\ SiO_2\}$$

The formation of slag involves a very complex set of reaction equations. The basic premise is that the basic components molecularly attach themselves to the acidic components and form slag. These reactions form new complex molecules and therefore the actual slag mass is slightly different than the balance in Equation 3.56 [34]. It is assumed that the difference between Equation 3.56 and the actual slag mass is negligible [29].

Five components of the overall mass balance in Equation 3.42 have yet to be explained. This includes the variables $\dot{M}^{coke}$, $\dot{M}^{oil}$, $\dot{M}^{steam}$, $\dot{V}^{air}$, and $\dot{V}^{top\ gas}$. If balances on hydrogen, oxygen, and carbon were completed, the five mentioned flow rates would enter into the equations. Also, if an overall energy balance were done, all variables in Equation 3.42 would be included.

The blast furnace is a very complex operation. The number of reactions involved is numerous and therefore energy and mass balances on hydrogen, oxygen, and carbon are very difficult to develop from first principles. However, in order for the optimization results to be practical, establishing these relationships is very important.

Modeling of Blast Furnace Relationships

The strategy of obtaining missing mass and energy balances is to build simplified relationships from an existing blast furnace model. The model to be used has many inputs and outputs including the variables in Equation 3.42 [29]. The problem is that the equations are not accessible, and therefore, it is a "black box" in which inputs can be specified and upon simulating, outputs are reported.

By manipulating the various inputs and solving for the outputs, a data set of blast furnace operating scenarios can be generated from the "black box" model. A regression on this data set can then be completed to build the missing mass and energy equations through an empirical model.

In order to accomplish this task, the "black box" model inputs are divided into manipulated inputs and constant inputs. The manipulated inputs are those that are changed in a Design of Experiment (DOE) fashion to represent various blast furnace operating conditions. The constant inputs are those that remain unchanged for every scenario. The final data set will therefore capture the effect of the manipulated inputs on the outputs, under the conditions represented by the constant inputs. The model manipulated and constant inputs are shown in Tables 3.8 and 3.9 along with new variable definitions.

Table 3.8: Classification of blast furnace "black box" model manipulated inputs.

Manipulated Input		Manipulated Input	
Pellet mass rate	$\dot{m}_{pellet}^{model}$	Oil mass rate	$\dot{m}_{oil}^{model}$
Silica from acid pellets	$\dot{m}_{Silica}^{model}$	Steam mass rate	$\dot{m}_{steam}^{model}$
Ash mass rate	$\dot{m}_{Ash}^{model}$	Dolomite addition rate	$\dot{m}_{dol}^{model}$
Iron mass rate	$\dot{m}_{iron}^{model}$	Hot metal P mass rate	$\dot{m}_{hot,P}^{model}$
Coke carbon content	$x_{coke,C}^{model}$	Hot metal Si mass rate	$\dot{m}_{hot,Si}^{model}$
Limestone mass rate	$\dot{m}_{lime}^{model}$	Hot metal C mass rate	$\dot{m}_{hot,C}^{model}$
		Hot metal Mn mass rate	$\dot{m}_{hot,Mn}^{model}$

Table 3.9: Classification of blast furnace "black box" model constant inputs.

Constant Inputs
Slag temp.
Hot metal temp.
Heat losses

Based on discussion with practitioners, it is assumed that strict constraints exist on the temperature of the slag and hot metal. If these are held constant, the final simplified regression model will represent blast furnace operation at the appropriate exit temperatures. Heat losses are assumed to be constant for the various scenario solutions. This is a good assumption so long as the resulting regression model is not used to predict conditions where the production rates are vastly different than those used to build the model.

Based on the "black box" inputs, the model computes overall mass and component balances and an energy balance on the blast furnace to determine the five variables in Table 3.10.

Table 3.10: List of blast furnace"black box" model outputs.

Black Box Model Solution Output	Variable
Hot metal mass rate	$\dot{m}_{hot}^{model}$
Slag mass rate	$\dot{m}_{slag}^{model}$
Blast air volumetric rate	$\dot{V}_{air}^{model}$
Top gas volumetric rate	$\dot{V}_{top\ gas}^{model}$
Coke mass rate	$\dot{m}_{coke}^{model}$

A 2_{IV}^{13-6} design of experiments was generated for the 13 input variables listed in Table 3.8. Using a fractional factorial design makes the total number of model input scenarios manageable. In a resolution IV design, three factor or higher interactions are aliased with the individual model input terms. Two factor interactions are aliased with one another as well. In this respect, some information is lost, however, the design still determines the impact of the individual inputs as well as some information about the interaction between the variables [32]. A total of 128 data points were entered into the "black box" model, and in each case the output variables listed in Table 3.10 were recorded. This resulting database provides the information from which empirical relationships can be built to complete the mass balances of carbon, oxygen, and hydrogen, as well as an overall furnace energy balance.

Predicting the slag and hot metal mass rates from this data set is not necessary. This is because the "black box" model does so in the same manner as shown in Equations 3.56 and 3.87, which will be discussed later in Section 3.4. Therefore, only three of the five output variables need to be predicted. Due to the correlation among the prediction variables, PLS-2 regression was completed on the data generated from the design of experiments to build a single model of the following form.

$$y^{BF} = (r^{BF})^T \beta_{BF} \tag{3.57}$$

where,

$$y^{BF} = \left[\dot{V}_{air}^{model}, \dot{V}_{top\ gas}^{model}, \dot{m}_{coke}^{model}\right]^T$$

$$r^{BF} = \left[1, \dot{m}_{pellet}^{model}, \dot{m}_{Silica}^{model}, \dot{m}_{Ash}^{model}, \dot{m}_{iron}^{model}, x_{coke,C}^{model}, \dot{m}_{steam}^{model}, \dot{m}_{dol}^{model}\right.$$
$$\left.\dot{m}_{lime}^{model}, \dot{m}_{oil}^{model}, \dot{m}_{hot,P}^{model}, \dot{m}_{hot,Si}^{model}, \dot{m}_{hot,C}^{model}, \dot{m}_{hot,Mn}^{model}\right]^T$$

The regression results, using Prosensus Multivariate 10.02, are shown in Figures 3.17 and 3.18 for the prediction of $\dot{m}_{coke}^{model}$ and $\dot{V}_{air}^{model}$. The same modeling procedure, as described in Section 3.2.2, was applied to blast furnace regression modeling. In these figures, the "observed" values are from the detailed "black box" model, and the predicted values are from the linear model in Equation 3.57.

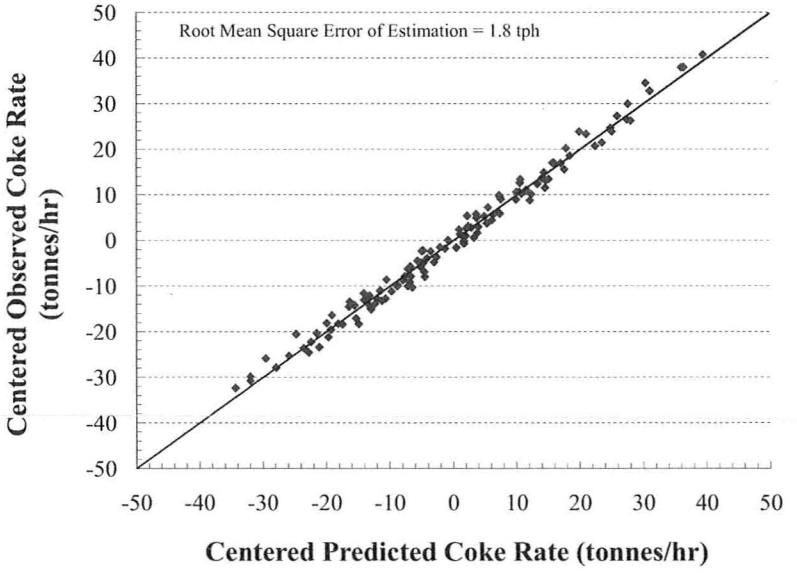

Figure 3.17: Observed vs. predicted results for coke rate addition model.

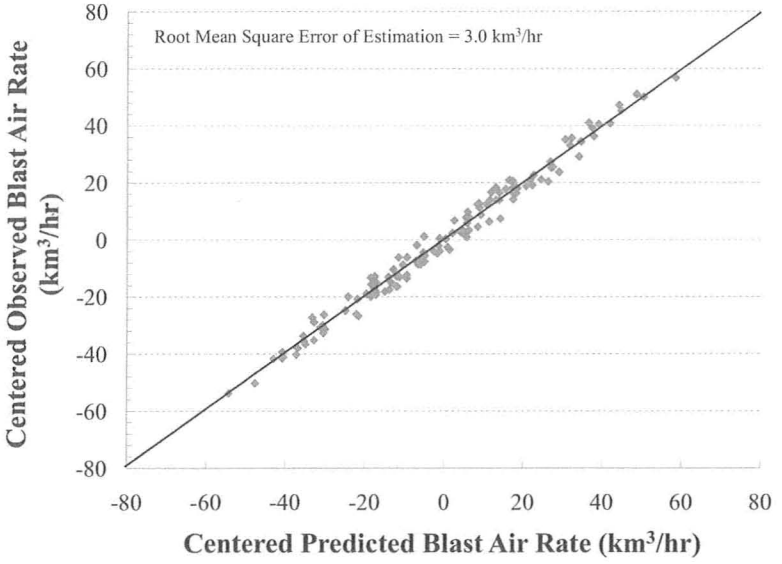

Figure 3.18: Observed vs. predicted results for blast air addition model.

The Q^2 value for this model is 0.982 meaning the predictive capability is excellent. The accuracy of the predictions shows that the linearity assumption is valid for the "black box" model. Therefore, approximating the blast furnace as a linear model, as in Equation 3.57, is appropriate.

In the case of coke PLS models, constraints were added to limit the extent of extrapolation to unsupported raw data regions. These are not needed for the blast furnace model since bounds on the input variables exist in the optimizer that are tighter than the range of raw data used in the model building.

Integrating Simplified Blast Furnace Model into the Optimization Formulation

In order to use the blast furnace model expressed by Equation 3.57, it is important to define the "black box" variables in terms of the optimization variables defined up to this point. Beginning with the r-vector in Equation 3.57, the pellet mass rate is equal to the summation of individual pellets added as expressed in the Equation 3.58.

$$\dot{m}_{pellet}^{model} = \sum_{p} \dot{m}_{p}^{pell} \tag{3.58}$$

Iron pellets can be categorized as either flux or acid. Flux pellets contain a higher percentage of calcium oxide, whereas acid pellets contain more silica. The silica in acid pellets is in a different molecular form than the silica in flux pellets. Therefore, required to reduce this silica is different, which is accounted for in the "black box" model [29].

The set of pellet types p can be split into two subsets; p_f for fluxed pellets and p_a for acid pellets. The silica entering from acid pellets is calculated in Equation 3.59.

$$\dot{m}_{Silica}^{model} = \sum_{p_a} x_{p_a,SiO_2}^{pell} \dot{m}_{p_a}^{pell} \tag{3.59}$$

In this equation, the variable x_{p_a,SiO_2}^{pell} represents the mass fraction of silica in the acid pellet p_a. The variable $\dot{m}_{p_a}^{pell}$ defines the mass addition rate of pellet type p_a.

The input variable $\dot{m}_{Ash}^{model}$ is the total mass of alumina, calcium oxide, magnesium oxide, and silica that enters through flux pellets only.

$$\begin{aligned}\dot{m}_{Ash}^{model} = &\underbrace{\sum_{p}\left(x_{p,CaO}^{pell}\cdot\dot{m}_{p}^{pell}\right) + x_{CaO}^{lime}\cdot\dot{M}^{lime} + x_{CaO}^{dol}\cdot\dot{M}^{dol}}_{\text{Calcium oxide input}} \\ &\underbrace{+ x_{Al_2O_3}^{coke}\cdot\dot{M}^{coke} + \sum_{p}\left(x_{p,Al_2O_3}^{pell}\cdot\dot{m}_{p}^{pell}\right)}_{\text{Alumina input}} + \underbrace{x_{SiO_2}^{coke}\cdot\dot{M}^{coke} + \sum_{p_f}\left(x_{p_f,SiO_2}^{pell}\cdot\dot{m}_{p_f}^{pell}\right)}_{\text{Silica input}} \\ &\underbrace{+ \sum_{p}\left(x_{p,MgO}^{pell}\cdot\dot{m}_{p}^{pell}\right) + x_{MgO}^{dol}\cdot\dot{M}^{dol}}_{\text{Magnesium oxide input}}\end{aligned} \tag{3.60}$$

The remaining manipulated input variables in Table 3.8 are exactly equal to formulation variables already defined. Additionally, the elements of the y-vector in Equation 3.57 are equal to the variables originally specified in Equation 3.42. These equalities are expressed through the Equations 3.61 to 3.73.

$$\dot{m}_{iron}^{model} = \dot{m}_{Fe}^{hot} \tag{3.61}$$

$$x_{coke,C}^{model} = x_{C}^{coke} \tag{3.62}$$

$$\dot{m}_{lime}^{model} = \dot{M}^{lime} \tag{3.63}$$

$$\dot{m}_{dol}^{model} = \dot{M}^{dol} \tag{3.64}$$

$$\dot{m}_{steam}^{model} = \dot{M}^{steam} \tag{3.65}$$

$$\dot{m}_{oil}^{model} = \dot{M}^{oil} \tag{3.66}$$

$$\dot{m}_{hot,P}^{model} = \dot{m}_{P}^{hot} \tag{3.67}$$

$$\dot{m}_{hot,Si}^{model} = \dot{m}_{Si}^{hot} \tag{3.68}$$

$$\dot{m}_{hot,C}^{model} = \dot{m}_{C}^{hot} \tag{3.69}$$

$$\dot{m}_{hot,Mn}^{model} = \dot{m}_{Mn}^{hot} \tag{3.70}$$

$$\dot{V}_{air}^{model} = \dot{V}^{air} \tag{3.71}$$

$$\dot{V}_{top\ gas}^{model} = \dot{V}^{top\ gas} \tag{3.72}$$

$$\dot{m}_{coke}^{model} = \dot{M}^{coke} \tag{3.73}$$

This model, in addition to the mass balances, comprises an approximate heat and mass balance on the blast furnace that is suitable for use in the optimization formulation.

3.3.2 Inequality Constraints

Silica and alumina are removed with the slag which is formed by the addition of magnesium and calcium oxides. In order for this slag to float on top of the exiting blast furnace hot metal, it must be of a certain basicity [34].

Slag basicity measures the ratio of basic to acidic components and is desired to be between a value of b^{low} and b^{up} [34].

$$b^{low} \leq \frac{\dot{m}_{CaO}^{slag} + \dot{m}_{MgO}^{slag}}{\dot{m}_{SiO_2}^{slag} + \dot{m}_{Al_2O_3}^{slag}} \leq b^{up} \tag{3.74}$$

Similar to the case of coal usage, the amount of a particular pellet added must be of a minimum quantity. Operators prefer that flux and acid pellets are always mixed during processing and at most a fraction, p^{up}, can be added.

$$\frac{\sum_{p_a} \dot{m}_{p_a}^{pell}}{\sum_p \dot{m}_p^{pell}} \leq p^{up} \tag{3.75}$$

$$\frac{\sum_{p_f} \dot{m}_{p_f}^{pell}}{\sum_p \dot{m}_p^{pell}} \leq p^{up} \tag{3.76}$$

Similar to cokemaking, it would be impractical for a solution to call for a pellet addition rate of an insignificant amount. Integer variables are not required in this case as during simulations, the solution never called for impractically small amounts of pellets to be added.

Sulphur is removed at the Desulphurization facility with the total mass removed denoted by the variable $\dot{M}_S^{De.}$. This was previously shown in the sulphur balance in Equation 3.44. The extent of sulphur removal must be such that the exit hot metal content is less than s^{up}.

$$\frac{\dot{m}_S^{hot} - \dot{M}_S^{De.}}{\dot{M}^{metal}} \leq s^{up} \tag{3.77}$$

Upper limits on the hot metal composition of carbon, manganese, phosphorous, and silicon also exist. These components are represented by the set i and their upper and lower concentration limits are shown in Equation 3.78.

$$x_i^{min} \leq \frac{\dot{m}_i^{hot}}{\dot{M}^{metal}} \leq x_i^{max} \quad \forall\, i \tag{3.78}$$

where,

$$i = \{\text{C, Fe, Mn, P, S, Si}\}$$

The hot metal manganese, phosphorous, and silicon can also be removed downstream in the steelmaking process. However, there are limitations as to the amount of each impurity that can be extracted at this stage and, for this reason, it is desired that the hot metal from ironmaking not exceed the limits listed in Equation 3.78.

It was previously described that oil combustion could account for any energy deficit not provided by coke addition in the blast furnace, though this is only true to a certain extent. Coke must still provide a physical support for the descending pellets and thus it is important that an oil to hot metal ratio not be exceeded. This is enforced by Equation 3.79 which requires that the oil consumption to hot metal rate not exceed a ratio of r^{oil}.

$$\frac{\dot{M}^{oil}}{\dot{M}^{hot}} \leq r^{oil} \tag{3.79}$$

Equations 3.74, 3.75, 3.76, 3.77, and 3.78 are nonlinear in this formulation due to the ratio term but can be easily manipulated into linear inequality constraints. This can be done by multiplying the sides of the inequalities by the denominator appearing in the ratio of variables.

The blast air intake also presents a physical process constraint because there is a maximum volumetric rate, $\dot{V}^{max}$, that can be supplied to the furnace.

$$\dot{V}^{air} \leq \dot{V}^{max} \tag{3.80}$$

Finally, the total mass of pellet type p used during the time period should be less than mass purchased, represented by B_p^{pell}.

$$\dot{m}_p^{pell} \cdot T_{length} \leq B_p^{pell} \quad \forall\, p \tag{3.81}$$

3.3.3 Ironmaking Summary

A background of the ironmaking process has been given. Most component mass balances were developed from first principles. Balances for components such as hydrogen, oxygen, and carbon, as well as the overall energy balance were developed from an existing model. This complex model was simplified for the purposes of this thesis, and the results yield a nearly perfect representation of the existing model. The relationship between furnace inputs and outputs is clearly defined, and physical operation constraints are imposed on the formulation.

3.4 Steelmaking

Hot metal exiting the Desulphurization Facility is transported to the Basic Oxygen Furnace which is operated as a batch process. An overview is shown in Figure 3.19.

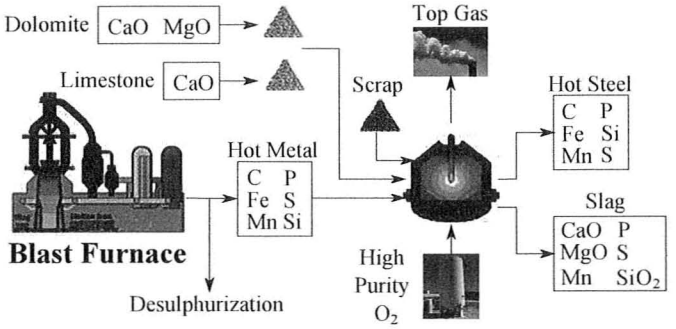

Figure 3.19: Overview of steelmaking process.

The objective of the final primary steelmaking stage is to oxidize and remove remaining impurities to very low levels yielding steel of high purity iron. Furthermore, this stage is used to adjust the hot metal temperature in preparation for casting into final steel slabs.

Oxidation of impurities is done by blowing pure oxygen through the furnace for an extended period of time in a batch vessel. Similar to the blast furnace operation, fluxing agents of lime and dolomite are added in order for slag to form and remove the oxidized impurities.

Steel grades produced in the BOF differ mainly with respect to final carbon content. Due to confidentiality, the three grade carbon contents considered in this thesis are not reported; they are denoted as G_A, G_B, and G_C. The lower the carbon content, the longer the batch duration and thus more oxygen that is consumed. Other factors that differentiate grades of steel include the temperature at which they exit the BOF and the alloys added to the batch at the downstream Ladle Metallurgy Facility (LMF). Table 3.11 lists these specifications for the three steel grades mentioned, relative to those values of G_A.

Table 3.11: Steel grade product classification with respect to grade G_A.

Grade type g	Final Temp. Deviation from G_A ($^\circ C$)	Alloy Addition Deviation from G_A (kg/batch)
G_A	0	0
G_B	-70	16
G_C	-65	288

The alloy addition is important to note since upon leaving the Ladle Metallurgy Facility, it is desired for the exit steel to be 320 tonnes in total. Thus, if 1 tonne of alloys are to be added, the BOF operation must be adjusted such that after all impurities are removed, 319 tonnes of liquid steel exist.

The input hot metal exits the furnace at approximately 1450°C and heats up considerably in the presence of exothermic oxidation and combustion reactions. These reactions and their respective energy outputs at blast furnace temperature and pressure conditions are listed below [34].

$$\mathrm{Si} + \mathrm{O_2} \rightarrow \mathrm{SiO_2} \qquad \Delta H^f_{SiO_2} = -911 \text{ KJ/kmol}$$

$$\mathrm{Mn} + \frac{1}{2}\mathrm{O_2} \rightarrow \mathrm{MnO} \qquad \Delta H^f_{MnO} = -385 \text{ KJ/kmol}$$

$$\mathrm{C} + \frac{1}{2}\mathrm{O_2} \rightarrow \mathrm{CO} \qquad \Delta H^f_{CO} = -111 \text{ KJ/kmol}$$

$$\mathrm{CO} + \frac{1}{2}\mathrm{O_2} \rightarrow \mathrm{CO_2} \qquad \Delta H^f_{CO_2} = -394 \text{ KJ/kmol}$$

In order to control the exit temperature to meet the specifications in Table 3.11, scrap steel is added to the vessel. Not only is the utilization of scrap an effective recycling technique, the added cold steel melts and acts as a heat sink. Depending on the hot metal quality and steel grade to be produced, an appropriate scrap quantity is added to meet the target exit temperature.

The quality of scrap steel poses a possible problem for steel makers. Common scrap impurities such as chromium, copper, and nickel cannot be oxidized in the BOF. These undesirable

components end up in the product steel, where maximum limits exist as to their respective concentrations. Intuitively, this means that the scraps charged to the furnace should be done in an intelligent manner so as to avoid violating this constraint. However, in this thesis, the set point for scrap addition is merely a total mass target, and not one based on specific scrap types. Ignoring the particular quality of scrap is justified because of the dilution that occurs when hot metal is added to the BOF. Since the hot metal charge is over three times that of scrap metal, the impact of these impurities is considered to be negligible [7].

This method of scrap selection is in stark contrast to that done in Electric Arc Furnace (EAF) steelmaking. In this parallel process, scrap steel and flux are the only furnace inputs. The electric arc melts the scraps and in the meantime slag forms and removes the oxidized impurities. There is no dilution method by which to lower the non-oxidized impurities in this case and so the charged scraps must be carefully selected based on their individual qualities. In steel plants which feature both a BOF and EAF, the scraps are separated based on quality and used accordingly.

The outlet streams of the BOF include the top gas, hot steel, and slag. In total, each BOF batch delivers 320 tonnes of hot steel with final steel composition being highly concentrated in iron and low in impurities. Table 3.12 gives an approximate composition of the steel.

Table 3.12: Approximate final steel composition.

Component	Mass Percent [7]
C	$< 0.04\%$
Fe	$> 99\%$
Mn	$< 0.3\%$
P	$< 0.01\%$
S	$< 0.0005\%$
Si	$< 0.01\%$
Other	$< 0.13\%$

Modeling of this process is illustrated in Figure 3.20 which shows the necessary variables.

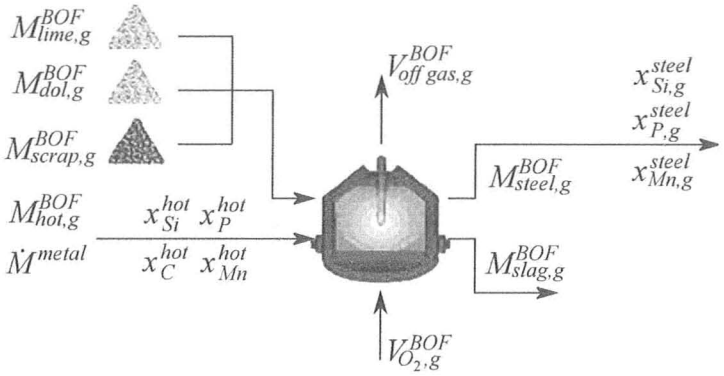

Figure 3.20: Variable definition diagram for steelmaking.

3.4.1 Equality Constraints

An overall mass balance is written in Equation 3.82 for a single batch of steel grade g.

$$M^{BOF}_{in,g} = M^{BOF}_{out,g} \; \forall \; g \tag{3.82}$$

where,

$$M^{BOF}_{in,g} = M^{BOF}_{hot,g} + M^{BOF}_{scrap,g} + \rho_{O_2} V^{BOF}_{O_2,g} + M^{BOF}_{dol,g} + M^{BOF}_{lime,g} \; \forall \; g$$
$$M^{BOF}_{out,g} = M^{BOF}_{slag,g} + M^{BOF}_{steel,g} + \rho^{BOF}_{off\ gas,g} V^{BOF}_{off\ gas,g} \; \forall \; g$$

The inputs include hot metal $M^{BOF}_{hot,g}$, scrap $M^{BOF}_{scrap,g}$, high purity oxygen $V^{BOF}_{O_2,g}$, dolomite $M^{BOF}_{dol,g}$, and limestone $M^{BOF}_{lime,g}$. Batch processing produces an off-gas $V^{BOF}_{off\ gas,g}$, a slag stream $M^{BOF}_{slag,g}$, and the desired hot liquid steel $M^{BOF}_{steel,g}$.

The net steel obtained from each batch, $M^{BOF}_{steel,g}$, is treated as a constant parameter for each grade, not an optimization variable, and is dependent upon the amount of alloys added downstream of the BOF.

Equation 3.82 is not used directly in the formulation but serves to outline the major inputs and outputs. Similar to the blast furnace, BOF operation involves many reactions,

thus deriving mass and energy balances is very challenging. To overcome this difficulty, a simplified empirical model is to be built from an already existing model [7]. Again, the equations governing the existing model are not known, and it is therefore considered to be a "black box". A design of experiments is to be employed to generate a dataset from which the simplified empirical model is to be built. A list of the model inputs and outputs are listed in Table 3.13.

Table 3.13: BOF "black box" model inputs and outputs.

Manipulated Inputs		Model Outputs		Constant Inputs	
Metal Si content	x_{Si}^{hot}	Hot metal mass	$M_{hot,g}^{BOF}$	Hot metal temp.	
Metal P content	x_{P}^{hot}	Scrap mass	$M_{scrap,g}^{BOF}$	Hot steel temp.	
Metal Mn content	x_{Mn}^{hot}	Oxygen volume	$V_{O_2,g}^{BOF}$	Alloy addition	
Metal C content	x_{C}^{hot}	Dolomite mass	$M_{dol,g}^{BOF}$	Steel C content	$x_{C,g}^{steel}$
Steel Si content	$x_{Si,g}^{steel}$	Lime mass	$M_{lime,g}^{BOF}$	Steel output	$M_{steel,g}^{BOF}$
Steel P content	$x_{P,g}^{steel}$				
Steel Mn content	$x_{Mn,g}^{steel}$				

The "black box" model differs depending on the steel grade to be produced. As listed earlier in Table 3.11, the hot steel temperature, alloy addition, and carbon content define each grade type. These three variables must be kept constant while the various inputs are manipulated in the design of experiment used to generate data. Therefore, three simplified models are to be built, one for each grade in the set g. The models will make predictions of the outputs, based on the inputs, subject to the constant parameters that define a particular steel grade. The proposed linear model structure is shown in Equation 3.83.

$$y_g^{BOF} = (r_g^{BOF})^T \beta_g \quad \forall\, g \tag{3.83}$$

where,

$$y_g^{BOF} = \left[M_{hot_g}^{BOF}, M_{scrap_g}^{BOF}, V_{O_{2g}}^{BOF}, M_{dol_g}^{BOF}, M_{lime_g}^{BOF}\right]^T \tag{3.84}$$

$$r_g^{BOF} = \left[1, x_{Mn}^{hot}, x_{P}^{hot}, x_{Si}^{hot}, x_{C}^{hot}, x_{Mn,g}^{steel}, x_{P,g}^{steel}, x_{Si,g}^{steel}\right]^T \tag{3.85}$$

The y_g^{BOF} prediction vector does not contain all of the specified variables in Equation 3.82. It is missing the slag and off-gas mass quantities; however, the "black box" model does calculate these variables but does not report them. Therefore, they cannot be included in the simplified model.

Both Table 3.13 and the r_g^{BOF} input vector are missing the hot metal and steel mass fractions of sulphur and iron. Sulphur is not included in the "black box" model due to its insignificant impact on the overall energy and mass balances. While it is present in the slag and steel exit streams, its concentration is extremely low since it has already passed through the Desulphurization facility. At this point, sulphur is no longer a concern for the steelmaking process, and accordingly, the model considers its presence to be negligible. Iron is not included simply because its mass fraction can be determined directly from the components specified in vector r_g^{BOF}; thus, including the iron content of the steel and hot metal streams is unnecessary.

A 3^7 design of experiments was completed meaning that all seven input variables were assigned high, medium, and low values. Every combination of these inputs was tested on the "black box" model to generate regression data. The scenario size was not reduced, as in the case of the blast furnace model, since information could be sent to the model and received in an automated manner. A single model was built to predict the variables in Equation 3.84 using PLS-2 regression and the Prosensus Multivariate 10.02 software package. The same model building procedure, as outlined in Section 3.2.2, was applied. Figures 3.21 and 3.22 show the model prediction performance for $M_{hot_{G_A}}^{BOF}$ and $M_{scrap_{G_A}}^{BOF}$ only. The observed values in the figures represent the "black box" outputs from the design of experiments while the predicted values are calculated from Equation 3.83.

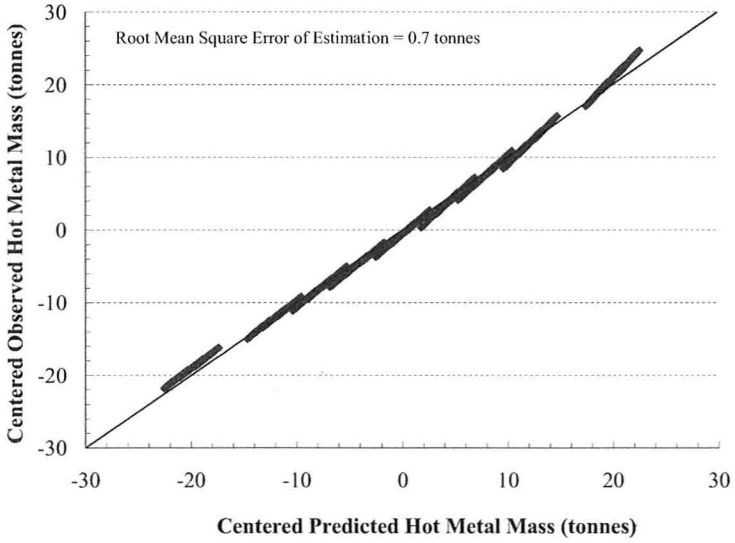

Figure 3.21: Observed vs. predicted results for BOF hot metal addition model.

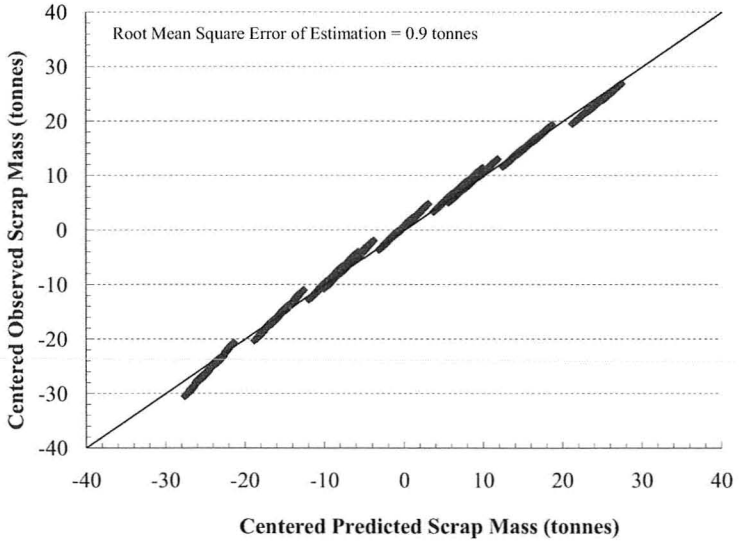

Figure 3.22: Observed vs. predicted results for BOF scrap addition model.

In both plots, the predictions seem to cluster into separate lines. Since a total of 3^7 data points were used in the model building, reproducing this many data points on a figure bunches the observations together, appearing as solid lines. Separation of the lines is a result of the design of experiment procedure with each cluster representing a different region of black box model inputs.

Plots for the other prediction variables were omitted since the overall model fit is very good, indicated by the large overall Q^2 scores for each grade. These statistics are shown in Table 3.14.

Table 3.14: Model results for BOF prediction models.

Model g	Q^2
Grade G_A	0.997
Grade G_B	0.997
Grade G_C	0.997

After specifying the hot metal composition and desired final steel composition, prediction is completed of the required BOF inputs that satisfy all component mass balances as well as the overall energy balance.

$$\begin{bmatrix} M^{BOF}_{hot_g} \\ M^{BOF}_{scrap_g} \\ V^{BOF}_{O_{2g}} \\ M^{BOF}_{dol_g} \\ M^{BOF}_{lime_g} \end{bmatrix} = \begin{bmatrix} 1, \underbrace{x^{hot}_{Mn}, x^{hot}_{P}, x^{hot}_{Si}, x^{hot}_{C}}_{x^{hot}_f = \frac{\dot{m}^{hot}_f}{\dot{M}^{metal}}}, x^{steel}_{Mn,g}, x^{steel}_{P,g}, x^{steel}_{Si,g} \end{bmatrix}^T \beta_g$$

The model introduces three new optimization decision variables: $x^{steel}_{Mn,g}$, $x^{steel}_{P,g}$, and $x^{steel}_{Si,g}$. Blast furnace hot metal composition is also a model input, and was previously denoted by the set i in the blast furnace model development. Since sulphur is ignored, and iron considered to be the balance of the hot metal, compositions of only four of the six elements in set i need to be calculated. This subset, f, represents carbon, manganese, phosphorous, and silicon. Equation 3.86 shows the calculation of these hot metal component mass fractions.

$$\frac{\dot{m}^{hot}_f}{\dot{M}^{metal}} = x^{hot}_f \quad \forall\, f \tag{3.86}$$

where,

$$f = \{\text{C, Mn, P, Si }\}$$

The batches of steel grade g to be produced during the optimization period are denoted by $D_{BOF,g}$. This is an integer value that is input into the formulation before optimizing and represents the steel demand for grade g. The required production rate from the blast furnace depends on the number of BOF batches to be made and the mass of metal added to each steel batch represented by $M_{hot_g}^{BOF}$. Equation 3.87 ensures that the blast furnace produces enough hot metal for the total steel demand to be satisfied.

$$\dot{M}^{metal} = \frac{\sum_g M_{hot_g}^{BOF} \cdot D_{BOF,g}}{T_{length}} \tag{3.87}$$

3.4.2 Inequality Constraints

There are specifications for the quality of steel produced in each BOF batch which depend on the steel grade type g being made. For specified upper and lower limits $X_{max,ig}^{steel}$ and $X_{min,ig}^{steel}$ respectively, the quality constraint can be written as given in Equations 3.88 - 3.90.

$$X_{min,Mn,g}^{steel} \leq x_{Mn,g}^{steel} \leq X_{max,Mn,g}^{steel} \quad \forall\, g \tag{3.88}$$

$$X_{min,P,g}^{steel} \leq x_{P,g}^{steel} \leq X_{max,P,g}^{steel} \quad \forall\, g \tag{3.89}$$

$$X_{min,Si,g}^{steel} \leq x_{Si,g}^{steel} \leq X_{max,Si,g}^{steel} \quad \forall\, g \tag{3.90}$$

The amount of dolomite and limestone added to each batch is constrained by upper limits. These are shown in Equations 3.91 and 3.92.

$$M_{dol_g}^{BOF} \leq M_{dol}^{BOF,max} \quad \forall\, g \tag{3.91}$$

$$M_{lime_g}^{BOF} \leq M_{lime}^{BOF,max} \quad \forall\, g \tag{3.92}$$

Scrap metal is the only raw material associated with BOF production, and the total mass used must not exceed the amount purchased, represented by B^{scrap}.

$$\sum_g M_{scrap,g}^{BOF} \cdot D_{BOF,g} \leq B^{scrap} \tag{3.93}$$

3.4.3 Steelmaking Summary

The process outline of steelmaking has been defined. Modeling of BOF batch operation was done by building a simplified regression model from already existing relationships. The simplified model is of good quality and thus provides reliable results to be used in the formulation. Constraints defining the end steel product specifications were also listed.

3.5 Objective Function Development

The optimization goal is to minimize the net cost of steel production based on satisfying a defined steel demand quantity for one week. This can be achieved by determining the raw materials to be purchased and the conditions under which they are processed. Since the steel production throughput is a fixed requirement, revenue generated from its sale is not considered. A revenue stream does, however, exist; it is regarding the collection of off-gas during coke production. The objective function can be separated into three categories; purchasing costs, operation costs, and coke by-product revenue.

The objective function and decision variables are described in the following diagram.

Min Production Cost = Purchasing Cost + Operation Cost
- By-product Revenue

Integer Decision Variables

- Which coals to use in production

Continuous Decision Variables

- Quantities and proportions of raw materials purchased and used
- Plant operation variables

Many parameters are required to express all costs in the objective function. Table 3.15 lists these costs along with the units for each parameter.

Table 3.15: Primary steelmaking scaled production costs.

Parameter	Parameter Description	Units
c_c^{coal}	Cost of purchasing coal c	\$/tonne
c_p^{pell}	Cost of purchasing pellet p	\$/tonne
c^{scrap}	Cost of purchasing scrap metal	\$/tonne
c_c^{coal}	Cost of purchasing coal c	\$/tonne
c^{oil}	Cost of blast furnace fuel oil	\$/tonne
c^{lime}	Cost of limestone use	\$/tonne
c^{dol}	Cost of dolomite use	\$/tonne
c^{O_2}	Cost of high purity oxygen supply	\$/Km^3
c^{air}	Cost of heating inlet blast furnace air	\$/Km^3
c^{steam}	Cost of steam consumption	\$/tonne
$c^{De.}$	Cost of removing sulphur in desulphurization facility	\$/kg
$p^{*By-prod.}$	Revenue from collecting coking by-products	\$/tonne

Coal, iron ore pellets, and scrap steel are bought on the open market in quantities represented by the variables B_c^{coal}, B_p^{pell}, and B^{scrap}. The total purchasing cost can be calculated from these three variables.

$$\text{Purchasing Cost} = \sum_c c_c^{coal} \cdot B_c^{coal} + \sum_p c_p^{pell} \cdot B_p^{pell} + c^{scrap} \cdot B^{scrap} \tag{3.94}$$

The major costs of the blast furnace operation are represented by steam, blast air, and oil consumption, as well as dolomite and limestone usage. For the BOF, costs are incurred through high purity oxygen and fluxing agent addition. No production costs are associated with cokemaking because the ovens are operated under constant conditions, so that these costs are not changed by the optimization solver.

$$\text{Operation Cost} = \underbrace{\sum_{g} \left(c^{O_2} V_{O_2,g}^{BOF} + c^{dol} M_{dol,g}^{BOF} + c^{lime} M_{lime,g}^{BOF} \right) D_{BOF,g}}_{\text{BOF operating cost}}$$
$$+ \underbrace{\left(c^{lime} \dot{M}^{lime} + c^{dol} \dot{M}^{dol} + c^{air} \dot{V}^{air} + c^{steam} \dot{M}^{steam} + c^{oil} \dot{M}^{oil} + c^{De.} \dot{M}_S^{De.} \right) \cdot T_{length}}_{\text{Blast furnace operating cost}} \tag{3.95}$$

In this equation, the blast furnace operating cost variables are written as mass or volumetric flows. In order to determine the total amount used, each term must be multiplied by T_{length} which is the length of said time period.

During the cokemaking process, volatile matter is driven off from the coals and collected for re-use in the plant. The mass that can be collected from each batch is represented by the variable $M_{V.M.,removed}$. Depending on the number of coke batches made, A^{coke}, the total revenue can be calculated using the market selling price, $p^{*By-prod.}$, of the by-products.

$$\text{By-product Revenue} = p^{*By-prod.} \cdot A^{coke} \cdot M_{V.M.,removed} \tag{3.96}$$

Equation 3.96 does not account for the aromatics that can be collected from the off-gas. Since the concentration is approximately 0.1% volume, the revenue from aromatic collection is considered negligible in this study.

The decision variables are considered to be completely independent of all other variables. In order for the plant to operate, these variables must be first specified and can be either continuous or integer. Vector K lists these variables.

$$K = \Big[\underbrace{\delta_c^{use}, B_c^{coal}, m_c^{coal}}_{\text{Cokemaking}}, \underbrace{B_p^{pell}, \dot{m}_p^{pell}, \dot{M}^{coke}, \dot{M}^{lime}, \dot{M}^{dol}, \dot{M}^{steam}, \dot{M}^{oil}, \dot{V}^{air}}_{\text{Ironmaking}}, \underbrace{x_{Mn,g}^{steel}, x_{P,g}^{steel}, x_{Si,g}^{steel}, B^{scrap}}_{\text{Steelmaking}}\Big]$$

3.6 Integrated Formulation and Problem Size

The objective function, minimizing the total production cost, is combined with the primary steelmaking model and denoted as Problem 1. This includes previously defined equality and inequality constraints listed in this chapter.

PROBLEM 1

$$\min_{K} \underbrace{\sum_{g}\left(c^{O_2}V_{O_2,g}^{BOF} + c^{dol}M_{dol,g}^{BOF} + c^{lime}M_{lime,g}^{BOF}\right)D_{BOF,g}}_{\text{BOF operating cost}} - \underbrace{p^{*By-prod.}\cdot A^{coke}\cdot M_{V.M.,removed}}_{\text{By-product revenue}}$$

$$+\underbrace{\left(c^{lime}\dot{M}^{lime} + c^{dol}\dot{M}^{dol} + c^{air}\dot{V}^{air} + c^{steam}\dot{M}^{steam} + c^{oil}\dot{M}^{oil} + c^{De.}\dot{M}_{S}^{De.}\right)\cdot T_{length}}_{\text{Blast furnace operating cost}}$$

$$+\underbrace{\sum_{c} c_c^{coal}\cdot B_c^{coal} + \sum_{p} c_p^{pell}\cdot B_p^{pell} + c^{scrap}\cdot B^{scrap}}_{\text{Purchasing cost}}$$

Subject to,

Equalities		**Equation Reference #**										
Cokemaking	→	3.6	3.7	3.8	3.9	3.11	3.12	3.13	3.27			
		3.28	3.29	3.30	3.31	3.32	3.33	3.34	3.38			
Ironmaking	→	3.42	3.43	3.44	3.45	3.46	3.47	3.48	3.49	3.50	3.51	
		3.52	3.56	3.53	3.54	3.55	3.57	3.58	3.59	3.60	3.61	3.62
		3.63	3.64	3.65	3.66	3.67	3.68	3.69	3.70	3.71	3.72	3.73
Steelmaking	→	3.83	3.86	3.87								

Inequalities		**Equation Reference #**							
Cokemaking	→	3.15	3.16	3.17	3.18	3.19	3.20	3.21	
		3.35	3.36	3.37	3.39	3.40	3.41		
Ironmaking	→	3.74	3.75	3.76	3.77	3.78	3.79	3.79	3.81
Steelmaking	→	3.88	3.89	3.90	3.91	3.92	3.93		

with,

$$K = \Big[\delta_c^{use}, B_c^{coal}, m_c^{coal}, B_p^{pell}, \dot{m}_p^{pell}, \dot{M}^{coke}, \dot{M}^{lime}, \dot{M}^{dol}, \dot{M}^{steam}, \dot{M}^{oil}, \dot{V}^{air}, x_{Mn,g}^{steel}, x_{P,g}^{steel}, x_{Si,g}^{steel}, B^{scrap}\Big]$$

A breakdown of the total number of variables and equations which comprise the formulation is given in Table 3.16. The values are given with respect to the number of coals available (C), pellets available (P), and grades of steel to produce (G).

Table 3.16: Variable and equation size of final formulation.

	Total
Continuous Variables	$144 + 2C + 2P + 8G$
Discrete Variables	C
Equality Constraints	$137 + 5G$
$\hookrightarrow$ Linear	$121 + 5G$
$\hookrightarrow$ Nonlinear	16
Inequality Constraints	$28 + 2C + P + 8G$
$\hookrightarrow$ Linear	$21 + 2C + P + 8G$
$\hookrightarrow$ Nonlinear	7

A degrees of freedom analysis can be determined by subtracting the total number of variables from the total number of equality constraints.

$$\begin{aligned} D.O.F &= (144 + 3C + 2P + 8G) - (137 + 5G) \\ &= 7 + 3C + 2P + 3G \end{aligned}$$

The degrees of freedom can be explained in further detail and are equivalent to the decision variables specified in vector K.

$$D.O.F. \begin{cases} 7 \rightarrow \text{Blast furnace inputs and scrap purchase: } \dot{M}^{coke}, \dot{M}^{lime}, \dot{M}^{dol}, \dot{M}^{steam}, \dot{M}^{oil}, \dot{V}^{air}, B^{scrap} \\ 3C \rightarrow \text{Coal usage and purchasing: } m_c^{coal}, \delta_c^{use}, B_c^{coal} \\ 2P \rightarrow \text{Pellet usage and purchasing: } \dot{m}_p^{pell}, B_p^{pell} \\ 3G \rightarrow \text{Desired end steel specifications: } x_{Mn,g}^{steel}, x_{P,g}^{steel}, x_{Si,g}^{steel} \end{cases}$$

In this study, 7 coals (C=7) and 3 pellets (P=3) are available for purchase on the open market. Three steel grades are produced during each optimization period (G=3), which is consistent with that of a typical steel plant [7].

3.7 Problem Structure and Solution Method

The formulation is both nonlinear in structure and contains integer variables. It is therefore classified as a mixed-integer nonlinear program (MINLP).

Nonlinearities exist in numerous equations but are only of three different types; bilinear, conic and logarithmic. The prediction model for coke oven wall pressure is of a logarithmic relationship. Second order conic constraints were given in Section 3.2.2 limiting the domain in which the coke prediction models could be used. Bilinear terms were introduced in equations where component mass balances were written.

It is possible to employ a linearization technique to the logarithmic nonlinearity by introducing more integer variables. However, the bilinear mass balance equations cannot be linearized with great accuracy and therefore all equations are left nonlinear.

This problem is relatively small in size and is non-convex in structure due to the bilinear nonlinearities. Consequently, an optimal solution can only be considered globally optimal if a global MINLP solver is employed.

The formulation was coded in GAMS 23.3.3, employing the commercial MINLP solver SBB Level 006 on a Dell XPS 420 computer with Intel 2.40 GHz CPU and 4GB RAM. SBB is a local MINLP solver which uses CONOPT3 to solve relaxed NLP problems in a branch and bound algorithm.

3.8 Chapter Summary

In this chapter background information on primary steelmaking was provided. The three areas comprising steel production were described in detail, and modeling completed.

Cokemaking involved developing mass balances for the various components in both coals and coke. It was assumed that sulphur and volatile matter are partially released into the off-gas during coking and an experimental data set of 450 coke batches was used to determine the percent loss for these components. Constraints exist with respect to coke CSR, stability, and oven wall pressure in order to ensure the final coke is of adequate strength and does not exert immense pressure inside the oven. Linear PLS regression was employed on an experimental data set of 77 observations in order to develop three separate empirical models. The Q^2 model predictability value for CSR and stability were 0.72 and 0.81 respectively. A logarithmic transformation was applied to the wall pressure raw data, yielding a model with a Q^2 value of 0.75. In each case, the quality of fit is not ideal; however, considering the error involved in experiment design and measurement, the models are adequate for the purposes of this thesis.

Ironmaking was modeled by a combination of rigorous material balances and empirical relationships. Mass balances were written for components entering through pellets, coke, limestone, flux, and dolomite. A industrially developed blast furnace model was then used to generate a database of steady state blast furnace operating scenarios. This information was then used to build a simplified linear PLS regression model in order to develop the blast furnace energy balance. As a result, the model Q^2 value was 0.98, validating the linearity assumption. The model was not tuned to actual operating data; thus, there is no quantitative analysis as to how well the model performs.

A similar modeling approach was undertaken for steelmaking in that an existing industrial BOF model was used to build empirical mass and energy relationships. Separate models were built for different grades of steel, which are defined by their respective carbon contents. Each model receives inputs of the hot metal quality fed to the BOF, and the desired end

point composition. The models then determine the hot metal, scrap, oxygen, and flux addition required. The linear PLS models each have Q^2 values of 0.997 indicating nearly perfect fit with the industrial model used to supply the regression data. Again, the model was not tuned to plant data and therefore cannot be validated with respect to actual plant performance.

Integrating the models of cokemaking, ironmaking, and steelmaking yields a complete model of primary steelmaking based on the production of three grades of steel from a single blast furnace and coke oven. An objective function was developed that calculates the total cost of raw material purchasing and plant operation. Embedding this objective function with the primary steelmaking model yields a non-convex MINLP problem which is small enough to be solved by a commercial solver.

Chapter 4

Centralized Optimization

This chapter reports on case studies in which raw material purchasing decisions along with process operating conditions are made. The formulation developed in the previous chapter is used to make these decisions under both nominal and uncertain conditions that arise in actual production. Finally, the benefit of optimizing over the entire primary steelmaking process is studied in comparison to optimization of the three sub-areas individually.

In this chapter, only parts of the solution important to discussion are presented. This includes both variable values and marginal costs for inequality constraints. Appendix B displays a more comprehensive listing of the variable and inequality constraint results for all case studies in this chapter.

4.1 Cost Parameters and Assumptions

The models and formulation given in the preceding chapter provide a framework in which planning decisions can be made for the steel plant. Before demonstrating the benefits of such a tool, the problem parameters must first be defined.

Raw material is available from a number of different vendors. Each coal vendor supplies a unique coal type along with specifications relating to its chemical, rheological, and petrographical qualities. The case studies involve seven coal types, and the specifications are given in Table A.1 in Appendix A.

Three different iron pellets are available for purchase which include two flux pellets (Pellet A and Pellet B) and one acid pellet (Pellet C). The specifications of all three pellets are also given in Table A.2 in Appendix A.

Costs for these raw materials, including that of scrap steel, are listed in Table 4.1. All values are scaled by dividing by a constant factor; this factor is not reported so that confidential business information is not divulged. By scaling all costs in the objective function by the same factor, the optimal values for the variables are not influenced. Also, the costs in Table 4.1, the optimal objective function, and marginal costs are all scaled; therefore, their relative values are unchanged and useful for results interpretation.

Table 4.1: Primary steelmaking raw material scaled cost values.

Cost Item	Parameter	Scaled Cost
Coal A	c_A^{coal}	\$5/tonne
Coal B	c_B^{coal}	\$6/tonne
Coal C	c_C^{coal}	\$5/tonne
Coal D	c_D^{coal}	\$5/tonne
Coal E	c_E^{coal}	\$4.9/tonne
Coal F	c_F^{coal}	\$4.7/tonne
Coal G	c_G^{coal}	\$4.3/tonne
Pellet A	c_A^{pell}	\$13/tonne
Pellet B	c_B^{pell}	\$13/tonne
Pellet C	c_C^{pell}	\$12.70/tonne
Scrap	c^{scrap}	\$20/tonne

Production costs related to processing of raw materials are not included in Table 4.1 due to confidentiality of these values. The revenue obtained from the volatile matter released in the coke oven off-gas is valued in accordance with the price of natural gas. In practice, if the flow of this stream is too low, natural gas is burned to make up for the heating deficit. Using an approximate lower heating value of by-product gas $L.H.V.^{By-prod.}$, and the market value of natural gas $p^{*Nat.\ Gas}$, the associated revenue, $p^{*By-prod.}$, can be calculated as in Equation 4.1.

$$L.H.V.^{By-prod.}\left(\frac{GJ}{tonne}\right)\cdot p^{*Nat.\ Gas}\left(\frac{\$}{GJ}\right)=p^{*By-prod.}\left(\frac{\$}{tonne}\right) \tag{4.1}$$

Since only scaled costs are given, cost benefits with respect to different case studies will be reported as a percent improvement from a base case. A 1% reduction in cost yields approximately \$3.6M in annual savings for a typical plant producing 3 million of steel per year [25]. The case studies used in this chapter are based on a smaller steel production rate of approximately 1.7 million tonnes per year [34], however, it is assumed that percent savings discussed would scale to the 3 million tonnage plant. This means if a case study result demonstrated a 1% overall cost reduction, it would still be accrued for the 3 million tonnage plant.

The optimization period is considered to be a single lumped planning period with the dynamics of the actual steel plant ignored. Any solution, therefore, provides the steady state plant operation for a one week time period. This assumption also impacts the BOF steel production. In practice, the day to day processing of steel requires a more detailed approach than that given in Chapter 3. For example, the steel produced by the BOF is sent to be cast into solid steel slabs. Different grades of steel are cast at different speeds so attention must be paid to the order at which each batch is cast. Considering a lumped planning period ignores these scheduling complexities and also assumes that the steel produced can always be processed downstream.

4.2 Optimization With No Uncertainty

The initial case studies investigated deal with no uncertainty present in the problem. This means the compositions of the coals and pellets are exactly equivalent to those values listed in Appendix A, and the integrated model presented in Chapter 3 is exact.

Input to the optimizer is the total demand of batches for each steel grade. For all case studies in this chapter, 35 batches of each grade are made. Since each batch produces 320 tonnes of steel, the total production for the week is 33,600 tonnes. This production rate is based on a standard, single blast furnace, steel plant [34].

4.2.1 Problem 1a Results

The problem is first formulated by considering that only Coals A, B, C, and D are available for purchase. Given the costs listed in Table 4.1, and for a demand of 35 batches of all three grades of product steel, optimization is completed to select the appropriate raw material mix and plant operating settings. This case study is denoted as Problem 1a, and the optimization result yields an overall scaled cost of $23.30 per tonne of steel produced. The solution for coal purchasing and coke production is given in Table 4.2.

Table 4.2: Cokemaking results for Problem 1a.

Coal Blend		Coke Composition	
Coal A	0%	Al_2O_3	2.54%
Coal B	19.1%	C	90.50%
Coal C	38.5%	P_2O_5	0.0503%
Coal D	42.4%	S	0.0415%
		SiO_2	4.99%
		Volatile Matter	0.50%

The optimizer chose to purchase Coals B, C, and D, thus mixing the most expensive coal

with the cheapest coals. The resulting coke composition has a fairly high carbon percentage of 90.5% meaning it has good fuel value with respect to blast furnace operation. The P_2O_5 content is high at 0.0503%, which can be detrimental to other decisions in this case.

Phosphorous cannot be removed in the blast furnace; therefore, the only means of controlling the exit hot metal content at this stage is by using low phosphorous pellets. The subsequent pellet blend is given in Table 4.3.

Table 4.3: Ironmaking results for Problem 1a.

Pellet Blend Percentage		Blast Furnace Operating Settings	
Pellet A	0%	$\dot{M}^{coke}$	521.9 kg/thm
Pellet B	37.6%	$\dot{M}^{pell}$	1.52 tonnes/thm
Pellet C	62.4%	$\dot{M}^{dol}$	85.9 kg/thm
		$\dot{V}^{air}$	919.9 km^3/thm
		$\dot{M}^{slag}$	195.6 kg/thm

Pellet C constitutes the majority of the blend with Pellet B being the remainder. Since Pellet C is 2.3% cheaper than the other two options, using it in such a great quantity is clearly cost effective. Pellet B has a lower iron content than Pellet A meaning more has to be purchased per tonne of hot metal produced. The reason for using this pellet, however, is the fact that both pellets A and C have high phoshporous contents. Pellet B addition is required to lower the input phosphorous amount in order to satisfy the exit hot metal upper limit.

Table 4.3 also lists the blast furnace operating conditions for this case study. The results show that producing one tonne of hot metal requires just over two tonnes of pellets and coke.

Results relating to BOF steelmaking are summarized in Table 4.4. Of note is the small amount of scrap metal added to each batch of steel grade G_A. This is due to the fact the exit temperature requirement of this grade is very high. Since the scrap mass acts as a heat

sink, less is added to the batch. As a result, more hot metal is charged, requiring more dolomite and limestone to float off the impurities.

Table 4.4: Steelmaking results for Problem 1a.

Variable	Steel Grade g		
	G_A	G_B	G_C
$M^{BOF}_{scrap,g}$	278.4 kg/thm	354.4 kg/thm	348.2 kg/thm
$M^{BOF}_{dol,g}$	18.6 kg/thm	6.3 kg/thm	4.3 kg/thm
$M^{BOF}_{lime,g}$	20.4 tonnes/thm	16.2 kg/thm	17.3 kg/thm
$V^{BOF}_{O_2,g}$	63 m^3/thm	62 m^3/thm	62 m^3/thm

A subset of inequality constraints are shown in Table 4.5 along with their respective marginal scaled costs. The slack value of each constraint is listed in order to show which constraints are active. The marginal costs are given in dollars per tonne of steel produced, meaning that the original value (in scaled dollars) was then divided by the total tonnes of steel produced during the optimization period. Dividing these values by the steel production output keeps the marginal costs consistent with how the overall cost was reported, being \$23.30 per tonne. Normally, marginal costs are given in dollars per unit of measure. In some cases, the costs were divided by a smaller factor than 1 to represent the true magnitude of the constraint. For example, nominal hot metal phosphorous content is less than 0.05%. Reporting a marginal cost per 1% change in the constraint is not as meaningful as a 0.01% change since in practice a change of 1% would never be considered.

Table 4.5: Important active inequality constraints for Problem 1a.

Description	Slack Value	Equation Number	Constraint Type	Marginal Scaled Cost
Coke CSR	8.3%	3.19	Min	-
Coke Stability	7.2%	3.20	Min	-
Oven wall pressure	0 lb/in^2	3.21	Max	-\$0.33/lb/in^2/tonne steel
CSR SPE-X	0	3.39	Max	-\$0.47/tonne steel
Hot metal exit P	0%	3.78	Max	-\$1.69/0.01%/tonne steel
Hot metal exit C	0%	3.78	Max	-\$0.019/%/tonne steel
Hot metal exit Si	0%	3.78	Min	\$0.015/0.1%/tonne steel

The upper limit on coke oven wall pressure is active for this particular coal blend meaning that increasing this coke property will damage the interior lining of the oven more than is deemed acceptable. Further increasing this constraint by 1 lb/in^2 would lower the cost by 1.4% of its base case optimal value but come at an increased cost of oven repair.

The coal blend also pushes the CSR squared prediction error to the furthest possible distance off the model plane in the latent space. Figure 4.1 shows the error contribution for each CSR model input variable.

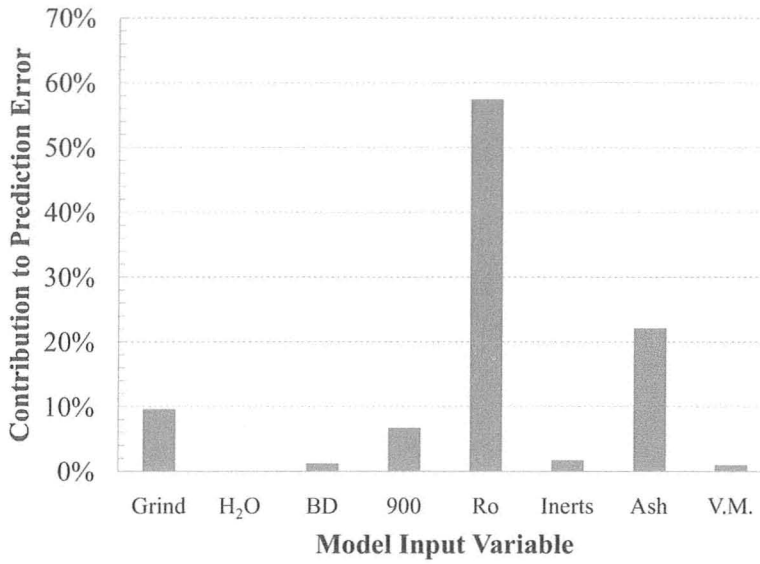

Figure 4.1: CSR model input SPE-X contributions.

The main contributor is that of the coal reflectance and suggests the model is unable to explain this variable in the latent space. The reason for this can be determined by first looking at the properties of the coal blend charged to the oven, compared to the data used to build the CSR model.

Table 4.6: Coal blend properties for CSR model in Problem 1a.

Blend Property	Problem 1a Optimum	Raw Data Mean	Raw Data Standard Deviation
Ro	1.35%	1.23%	0.06%
Inerts	26.8%	22.8%	2.1%
Ash	6.9%	6.4%	1.1%
V.M.	23.2%	26.8%	2.3%
H_2O	6.5%	6.3%	2.5%

Table 4.6 shows that the optimum solution was abnormal for three reasons: Ro was high, Inerts was high, and Volatile Matter content low. The fourth latent variable explains most of the variance in Ro, and therefore is most influential in the large prediction error observed.

In this latent variable, Ro and Inerts are negatively correlated, while Ro and V.M. are positively correlated. This means that in the raw data used to build the model, whenever Ro was large in magnitude, Inerts was low and V.M. was high. In the Problem 1a solution, this correlation structure was broken as the optimizer tried to reverse these trends. The model has no information about coal blends of low V.M. content and high Ro and Inerts values, and thus in the latent space this optimal data point is far off the model plane and constrained by Equation 3.39. If new experiments were conducted based on the correlation structure selected by the optimizer, a new model could be built which would explain the previously missing information. Embedding this into the formulation could then possibly prevent constraint Equation 3.39 from being active and thus reduce cost.

The remaining active constraints in Table 4.5 relate to blast furnace operation. Both the exit phosphorous and carbon contents are at their maximum levels. The marginal cost for increasing the upper limit on carbon content is nearly negligible. In contrast, the benefits of raising the constraint on phosphorous content would be very large. Increasing this constraint by 0.01% mass reduces the scaled cost by \$1.69 per tonne of steel.

The new coal blend is comprised of Coals A, D, and E. Only Coal D remains from the initial blend. The optimizer took full advantage of the newly available cheap coal and decided to use it as the major component in the coke batches. The pellet blend also changed significantly as the maximum acid addition of 80% Pellet C was used with the remainder being Pellet A. Low phosphorous Pellet B was not used in the new solution since the new coke composition was of a far lower phosphorous oxide content.

The major differences in solution variables between Problem 1b and 1a are shown in Table 4.7 to reflect how plant operation and purchasing change according to the addition of a single raw material.

Table 4.7: Comparison of Problem 1b and Problem 1a results.

	Problem 1b	Problem 1a
Scaled Cost	\$22.71/tonne steel	\$23.30/tonne steel
x_C^{coke}	91.22%	90.50%
$x_{P_2O_5}^{coke}$	0.0388%	0.0503%
$\dot{M}^{coke}$	517.3 kg/thm	521.9 kg/thm
$\dot{M}^{dol}$	91.6 kg/thm	85.9 kg/thm
$\dot{M}^{slag}$	198.3 kg/thm	195.6 kg/thm

The cost reduction of 2.5% from Problem 1a to 1b is largely due to the cheaper coal blend that was used and the chain reaction it had on the process. Coal E allowed for the very expensive Coal B to be eliminated from the blend. As a result, the coke carbon content was raised and thus the amount consumed per tonne of hot metal was lowered by 4.6 kg. The coke phosphorous content was decreased significantly which, as mentioned, allowed for the two pellets with the highest iron contents to be used. The ash contents of Pellets A and C, namely silica and manganese, are higher than that of Pellet B. Therefore, in Problem 1b, the dolomite addition was increased as well as the subsequent slag mass flow.

The active constraints for Problem 1b are listed in Table 4.8.

Table 4.8: Important active constraints and marginal costs per tonne for Problem 1b.

Description	Slack Value	Equation Number	Constraint Type	Marginal Cost
Coke CSR	0%	3.19	Min	-$0.028/%/tonne steel
Coke Stability	2.4%	3.20	Min	-
Oven wall pressure	0.763 lb/in^2	3.21	Max	-
CSR SPE-X	4.55	3.39	Max	-
Hot metal exit P	0%	3.78	Max	-$0.033/0.01%/tonne steel
Hot metal exit C	0%	3.78	Max	-$0.026/%/tonne steel
Hot metal exit Si	0%	3.78	Min	$0.017/0.1%/tonne steel

Similar to Problem 1a, the constraints relating to hot metal components of phosphorous, carbon, and silicon are all active. The marginal cost for the exit phosphorous constraint is far lower than that of Problem 1a where it was equal to -$1.69/0.01%/tonne. In Problem 1a, this constraint restricted the usage of the cheap acid pellets whereas in Problem 1b, the maximum amount of Pellet C is used. Since no more Pellet C can be added to the blend, the marginal cost represents savings that could be accrued by selecting a higher phosphorous content coal blend in coke production.

The marginal cost of reducing coke CSR is -$0.027/%/tonne. Lowering CSR comes at a cost of blast furnace operating efficiency as the heating profile of the furnace is impacted. The relationship between added fuel consumption and CSR must be studied before adjusting this lower strength limit.

4.2.3 Problem 1c Results - New Coal Availability: Coal F and Coal G

The problem parameters from Problem 1b remain unchanged except that two additional coals are available for purchase, Coal F and Coal G, with their scaled costs being $4.7 and $4.3 per tonne, respectively. These two coals are significantly cheaper than any other, but each possesses positive and negative attributes.

Coal F has good strength properties; using this coal alone in the blend would yield a CSR value 20% above the minimum allowable level. Also, the volatile matter content is quite low at 21%. While this has a negative impact with regards to the revenue generating by-product stream, it does increase the yield of coke per batch. The major problem with Coal F is that it has a very large ash content at nearly 10%; therefore, coke produced from this coal has a very low carbon content of 87.8%.

Coal G has numerous positive qualities. For example, it has a very low ash content and high carbon content. The resulting coke produced from this coal is 92.5% which would require a lower than normal addition rate to the blast furnace. It also has excellent strength properties, yielding CSR and stability values of 16% and 18% above the minimum requirements, respectively. The largest drawback of this coal is its high coal reflectance value of 1.67%; using this coal alone in the blend would create a coke oven wall pressure 6.5 lb/in^2 above the maximum limit.

Purchasing decisions regarding these two new coals are quite complex considering the constraints of the problem and the consequences of the resulting coke on the process. To determine whether or not these coals are to be purchased, they are added to the formulation which is resolved as Problem 1c. The new minimum scaled cost is \$22.60/tonne, compared with \$22.71/tonne for Problem 1b, representing a 0.48% reduction. The changes with respect to coal and pellet selection are shown in Figure 4.4.

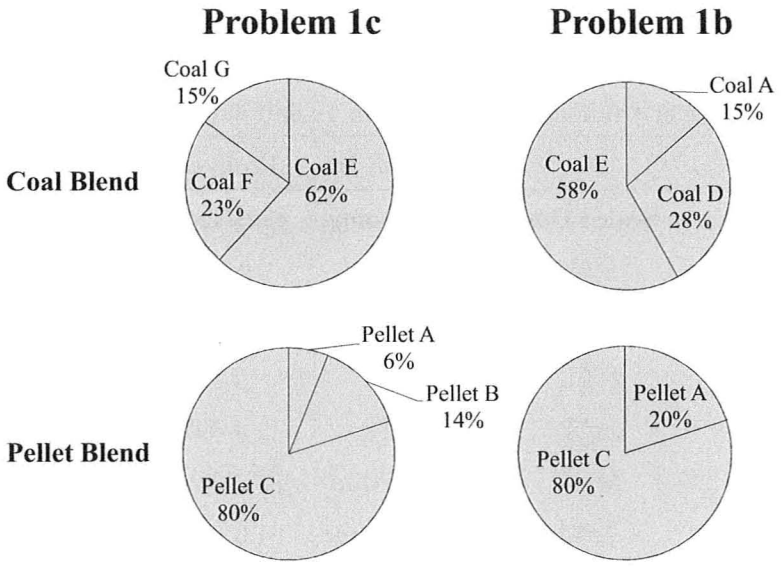

Figure 4.4: Problem 1c and 1b raw material selection comparison.

Both Coal F and Coal G are added to the new coal blend. However, Coal E remains the major addition to the blend. This has to do with both its high carbon and volatile matter content. The poor strength properties of Coal E are alleviated by taking advantage of Coals F and G. All three coals are blended in proper ratios in order to meet the lower specifications on coke strength.

The phosphorous content of coke produced in Problem 1c is higher than that of Problem 1b; hence, Pellet B is added to lower the total phosphorous input to the blast furnace. Unlike Problem 1a, however, Pellet A is still used as the coke phosphorous content is not high enough to require only Pellet B to be used.

Table 4.9 lists the major differences between Problem 1b and the new optimal operation.

Table 4.9: Comparison of Problem 1c and Problem 1b results.

	Problem 1c	Problem 1b
Scaled Cost	\$22.60/tonne	\$22.71/tonne
x_C^{coke}	90.34%	91.23%
$x_{P_2O_5}^{coke}$	0.043%	0.0388%
$x_{Al_2O_3}^{coke}$	2.54%	2.36%
$x_{SiO_2}^{coke}$	5.00%	4.43%
$\dot{M}^{coke}$	518 kg/thm	517.3 kg/thm
$\dot{M}^{dol}$	99.4 kg/thm	91.6 kg/thm
$\dot{M}^{slag}$	203 kg/thm	198.3 kg/thm

Despite the relatively low cost of Coals F and G, the overall cost was only reduced by 0.50%. The new coal blend produced a lower carbon and higher ash content coke. Due to the increase in alumina and silica coke content, more dolomite had to be added to control the slag basicity. This dolomite increased both the subsequent slag rate and coke consumption. These properties are all costly with respect to operation, and so, it may not be apparent to a human decision maker that the new coals should be purchased. The optimizer understands that the added operating costs can be recovered by purchasing the new coals and thus makes a better decision.

The active constraints for the Problem 1c solution are shown in Table 4.10.

Table 4.10: Important active constraints and marginal costs per tonne for Problem 1c.

Description	Slack Value	Equation Number	Constraint Type	Marginal Cost
Coke CSR	0%	3.19	Min	-\$0.014/%/tonne steel
Coke Stability	0%	3.20	Min	-\$2.7 $\times 10^{-4}$/%/tonne steel
Oven wall pressure	0.989 lb/in^2	3.21	Max	-
CSR SPE-X	2.133	3.39	Max	-
Hot metal exit P	0%	3.78	Max	-\$0.32/0.01%/tonne steel
Hot metal exit C	0%	3.78	Max	-\$0.023/%/tonne steel
Hot metal exit Si	0%	3.78	Min	-\$0.017/0.1%/tonne steel

The marginal scaled costs with respect to hot metal carbon and silicon contents are similar to those of the previous cases. Additionally, the CSR and stability constraints are active for this operation with similarly minuscule marginal costs.

The inequality constraint on hot metal phosphorous content is also active; increasing the upper limit by 0.01% reduces the overall scaled cost by \$0.32 per tonne of steel. Phosphorous enters the blast furnace through pellets and coke only. Figure 4.4 shows that low phosphorous Pellet B was used in Problem 1c but not Problem 1b. This illustrates that it is possible for the phosphorous constraint to be met without using Coals F and G. The optimizer recognized the tradeoff between using the new coals and not adding Pellet B and realized it was optimal to incur a higher pellet cost to save money with respect to coal purchasing.

4.2.4 Summary

The results show the strong connection between cokemaking, ironmaking, and steelmaking. The optimizer responds to changes to a single raw material availability by modifying several optimization decisions simultaneously. Changes in purchasing decisions lead to changes in active constraints, which subsequently required operation to be altered. Clearly, the

optimization can answer questions about raw material purchasing and operation that are far from obvious to a human decision maker.

4.3 Optimization Under Uncertainty

In Section 4.2, the raw material compositions were assumed to be equal to their respective nominal values. In practice, this assumption is not exact because specifications listed by raw material vendors are rarely the same as those actually delivered. Therefore, there exists uncertainty with respect to the actual raw material quality.

This uncertainty can have a considerable impact on production. For example, a coal blend could be processed that has low CSR and stability properties. If the coal composition is slightly different than that assumed during the optimization, both strength constraints could be violated. Another example is that of the exit hot metal from the blast furnace; uncertain pellet and coke compositions mean that the hot metal composition could differ from predictions. This composition impacts BOF production because the scrap, flux, and oxygen additions are highly correlated. Not accounting for this uncertainty could require additional costs to be incurred in the BOF in order to prevent violation of the end product specifications. A method to account for uncertainty is proposed in the following sections, and the production impact is compared to the case where uncertainty is not considered.

4.3.1 Two-Stage Stochastic Programming

Stochastic two-stage optimization separates the variables into two classes: first and second stage. First stage variables are those which must be implemented immediately, while second stage decisions can be delayed until the uncertainty is realized and measured. Figure 4.5 shows a time line of the two-stage approach.

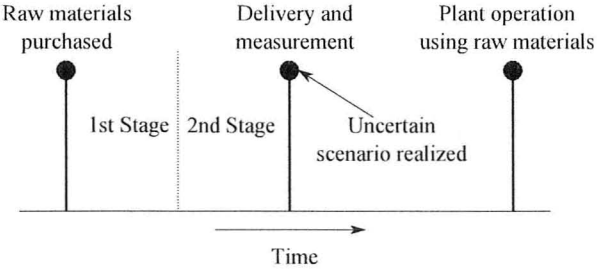

Figure 4.5: Time line of two-stage stochastic programming.

Once the first stage decision has been made, order and delivery of the raw materials occurs. Upon arrival, uncertainty is realized and the raw materials can be measured on site in the plant. This formulation assumes that coal and iron pellet properties are measured in the second stage without error. Naturally, this is not possible when handling large quantities of material; however, it is a common assumption in the two stage approach. After measuring, the plant must process the raw materials. It is at this step where the impact of uncertainty is felt and so that the preliminary operating decisions from stage one should be reconsidered.

As uncertainty in this case study is considered to be found in only the pellet and coal properties, it is logical to categorize the raw material purchasing variables as first stage, and operation related variables as second stage. This division is illustrated in Figure 4.6.

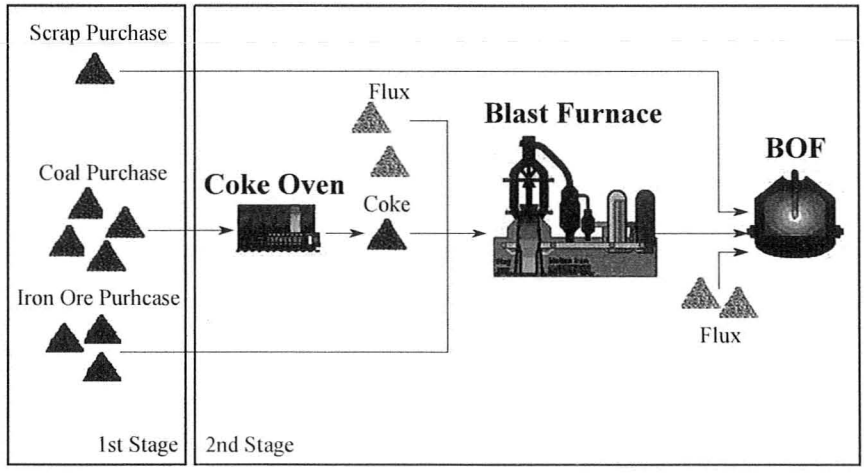

Figure 4.6: Two-stage stochastic separation of variables.

This categorization of first and second stage variables represents actual operation quite accurately. In practice, raw materials are purchased knowing only the approximate quality values. Once the raw materials are received and production begins, the operations would be manipulated in order to account for the actual raw material properties. Depending on the compositional breakdown of raw materials fed to the processes, mass and energy balances still need to be maintained, requiring a different solution of the second stage variables for every uncertain scenario. For example, if iron ore pellets arrive with a higher than expected silica content, more dolomite would be added in order to separate the excess silica. In response, a greater energy input to the furnace would be needed, thereby raising the coke and hot blast air inputs.

It is assumed that, after purchasing, the raw material uncertainty can be classified by different scenarios using the set S. Each element of S represents a unique scenario where the raw material compositions are random values within known, continuous uncertainty probability distributions.

The stochastic two-stage formulation is given below [47].

$$\underset{x_1, x_{2s}}{min}\ \text{Cost} = \underbrace{c_1^T x_1}_{1^{st}\text{ stage costs}} + \underbrace{\sum_{s}^{N^{scen.}} \frac{c_2^T x_{2s}}{N^{scen.}}}_{2^{nd}\text{ stage costs}}$$

Subject to,

$$h(x_1) \leq 0$$

$$h_s(x_1, x_{2s}) \leq 0 \quad \forall\, s$$

$$g(x_1) = 0$$

$$g_s(x_1, x_{2s}) = 0 \quad \forall\, s$$

The objective function is split into two parts, one for the first stage costs and one for the second stage costs. A total of $N^{scen.}$ scenarios are considered to possibly occur. For each scenario (actual material properties), there exists a solution for the second stage variables x_{2s} that satisfies all constraints and minimizes the cost for the scenario. The cost associated with each variable must be included in the objective function and weighted according to

the probability of its occurrence. In the above case, dividing by $N^{scen.}$ attributes equal probability to each scenario.

The formulation given in Chapter 3 must be transformed into the two-stage stochastic framework. The problem constraints are first broken down according to their classification in the two-stage framework.

First Stage Inequalities $h(x_1) \leq 0$

A new first stage binary variable, δ_c^{buy}, is introduced which decides whether or not coal c is to be purchased. This variable is required to enforce the constraint that at most four coals can be stored in the plant:

$$\sum_c \delta_c^{buy} \leq N^{coal} \tag{4.2}$$

This constraint was previously enforced by Equation 3.18 with the binary variable δ_c^{use}. In the two-stage approach, the variable δ_c^{use} becomes a second stage variable $\delta_{c,s}^{use}$ which is still needed to ensure a minimum coal mass is added to each blend.

If coal c is not purchased, meaning δ_c^{buy} is equal to zero, the purchasing amount must also be equal to zero. This is enforced by the constraint below.

$$B_c^{coal} \leq \delta_c^{buy} \cdot M \quad \forall\, c \tag{4.3}$$

In this equation, the variable M is a large number, and represents the upper purchasing limit for coal c. In this problem, no maximum purchase amount exists, and so, the exact value is not important as long as it is sufficiently large.

The rest of the equations given in Chapter 3 remain in the new formulation. Except for the first stage raw material purchasing variables, all other previously defined variables are redefined to have a separate value for each element, s in the set S, and considered to be second stage. Similarly, all constraint equations must be written for all scenarios in the set

S. The classification of constraints in the new formulation is summarized in the following headings.

Second Stage Inequalities $h_s(x_1, x_{2s}) \leq 0$

$$\delta_{c,s}^{use} \cdot m_{min}^{coal} \leq m_{c,s}^{coal} \leq \delta_{c,s}^{use} \cdot m_{max}^{coal} \qquad \forall\, c, s \qquad (4.4)$$

$$\dot{M}_s^{coke} \cdot T_{length} \leq M_{out,s}^{coke} \cdot A_s^{coke} \qquad \forall\, s \qquad (4.5)$$

$$m_{c,s}^{coal} \cdot A_s^{coke} \leq B_{c,s}^{coal} \qquad \forall\, c, s \qquad (4.6)$$

$$y_s^{CSR} \geq y_{min}^{CSR} \qquad \forall\, s \qquad (4.7)$$

$$y_s^{Stab.} \geq y_{min}^{Stability} \qquad \forall\, s \qquad (4.8)$$

$$y_s^{W.P.} \leq y_{max}^{Pressure} \qquad \forall\, s \qquad (4.9)$$

$$\sum_{i=1}^{4} \frac{{T_{CSR,i,s}^*}^2}{s_{CSR,i}^2} \leq T_{max,CSR}^2 \qquad \forall\, s \qquad (4.10)$$

$$\sum_{i=1}^{3} \frac{{T_{Stab.,i,s}^*}^2}{s_{Stab.,i}^2} \leq T_{max,Stab.}^2 \qquad \forall\, s \qquad (4.11)$$

$$\sum_{i=1}^{2} \frac{{T_{W.P.,i,s}^*}^2}{s_{W.P.,i}^2} \leq T_{max,W.P.}^2 \qquad \forall\, s \qquad (4.12)$$

Second Stage Inequalities $h_s(x_1, x_{2s}) \leq 0$ continued...

$$\sum_{k \in k_{CSR}} \left(r^*_{CSR,s}(k) - \hat{r}^*_{CSR,s}(k)\right)^2 \leq \epsilon_{CSR} \qquad \forall\, s \qquad (4.13)$$

$$\sum_{k \in k_{Stab.}} \left(r^*_{Stab.,s}(k) - \hat{r}^*_{Stab.,s}(k)\right)^2 \leq \epsilon_{Stab.} \qquad \forall\, s \qquad (4.14)$$

$$\sum_{k \in k_{W.P.}} \left(r^*_{W.P.,s}(k) - \hat{r}^*_{W.P.,s}(k)\right)^2 \leq \epsilon_{W.P.} \qquad \forall\, s \qquad (4.15)$$

$$b^{low} \leq \frac{\dot{m}^{slag}_{CaO,s} + \dot{m}^{slag}_{MgO,s}}{\dot{m}^{slag}_{SiO_2,s} + \dot{m}^{slag}_{Al_2O_3,s}} \leq b^{up} \qquad \forall\, s \qquad (4.16)$$

$$\frac{\sum_{p_a} \dot{m}^{pell}_{p_a,s}}{\sum_p \dot{m}^{pell}_{p,s}} \leq p^{up} \qquad \forall\, s \qquad (4.17)$$

$$\frac{\sum_{p_f} \dot{m}^{pell}_{p_f,s}}{\sum_p \dot{m}^{pell}_{p,s}} \leq p^{up} \qquad \forall\, s \qquad (4.18)$$

$$\frac{\dot{m}^{hot}_{S,s} - \dot{M}^{De.}_{S,s}}{\dot{M}^{metal}_s} \leq s^{up} \qquad \forall\, s \qquad (4.19)$$

$$x^{min}_i \leq \frac{\dot{m}^{hot}_{i,s}}{\dot{M}^{metal}_s} \leq x^{max}_i \qquad \forall\, i, s \qquad (4.20)$$

$$\frac{\dot{M}^{oil}_s}{\dot{M}^{hot}_s} \leq r^{oil} \qquad \forall\, s \qquad (4.21)$$

$$\dot{V}^{air}_s \leq \dot{V}^{max} \qquad \forall\, s \qquad (4.22)$$

$$\dot{m}^{pell}_{p,s} \cdot T_{length} \leq B^{pell}_{p,s} \qquad \forall\, p, s \qquad (4.23)$$

$$X^{steel}_{min,Mn,g} \leq x^{steel}_{Mn,g,s} \leq X^{steel}_{max,Mn,g} \qquad \forall\, g, s \qquad (4.24)$$

$$X^{steel}_{min,P,g} \leq x^{steel}_{P,g,s} \leq X^{steel}_{max,P,g} \qquad \forall\, g, s \qquad (4.25)$$

$$X^{steel}_{min,Si,g} \leq x^{steel}_{Si,g,s} \leq X^{steel}_{max,Si,g} \qquad \forall\, g, s \qquad (4.26)$$

$$M^{BOF}_{dol_{g,s}} \leq M^{BOF,max}_{dol} \qquad \forall\, g, s \qquad (4.27)$$

$$M^{BOF}_{lime_{g,s}} \leq M^{BOF,max}_{lime} \qquad \forall\, g, s \qquad (4.28)$$

Second Stage Equalities $g_s(x_1, x_{2s}) = 0$

$$0.94 \cdot M_{out,s}^{coke} + M_{H_2O,removed,s} = M_{coal,in} - \sum_q M_{q,removed,s} \qquad \forall\, s \qquad (4.29)$$

$$M_{H_2O,removed,s} = x_{H_2O,s}^{blend} \cdot M_{coal,in} \qquad \forall\, s \qquad (4.30)$$

$$M_{S,removed,s} = \frac{25.85\%}{100\%} \cdot x_{S,s}^{blend} \cdot M_{coal,in} \qquad \forall\, s \qquad (4.31)$$

$$M_{V.M.,removed,s} = \frac{98.33\%}{100\%} \cdot x_{V.M.,s}^{blend} \cdot M_{coal,in} \qquad \forall\, s \qquad (4.32)$$

$$x_{H_2O,s}^{blend} = \frac{\sum_c \left(x_{c,H_2O}^{coal} \cdot m_{c,s}^{coal} \right)}{M_{coal,in}} \qquad \forall\, s \qquad (4.33)$$

$$x_{q,s}^{blend} = \frac{\sum_c \left(x_{c,q}^{coal} \cdot m_{c,s}^{coal} \right)}{M_{coal,in}} \qquad \forall\, q, s \qquad (4.34)$$

$$x_{q,s}^{coke} = \frac{\left(x_{q,s}^{blend} \cdot M_{coal,in} \right) - M_{q,removed,s}}{M_{out}^{coke}} \qquad \forall\, q, s \qquad (4.35)$$

$$y_s^{CSR} = (r_{CSR,s})^T \beta_{CSR} \qquad \forall\, s \qquad (4.36)$$

$$y_s^{Stab.} = (r_{Stab.,s})^T \beta_{Stab.} \qquad \forall\, s \qquad (4.37)$$

$$\ln \left(y_s^{W.P.} \right) = (r_{W.P.,s})^T \beta_{W.P.} \qquad \forall\, s \qquad (4.38)$$

$$u_{h,s}^{blend}(j) = \sum_c \left(\frac{m_{c,s}^{coal}}{M_{coal,in}} \cdot X_{c,j}^{prop} \right) \qquad \forall\, j, h, s \qquad (4.39)$$

$$r_{CSR,s}^*(k) = \frac{r_{CSR,s}(k) - r_{CSR}^{\mu}(k)}{r_{CSR}^{\sigma}(k)} \qquad \forall\, k \in k_{CSR}, s \qquad (4.40)$$

$$r_{Stab.,s}^*(k) = \frac{r_{Stab.,s}(k) - r_{Stab.}^{\mu}(k)}{r_{Stab.}^{\sigma}(k)} \qquad \forall\, k \in k_{Stab.}, s \qquad (4.41)$$

$$r_{W.P.,s}^*(k) = \frac{r_{W.P.,s}(k) - r_{W.P.}^{\mu}(k)}{r_{W.P.}^{\sigma}(k)} \qquad \forall\, k \in k_{W.P.}, s \qquad (4.42)$$

$$T_{h,s}^* = (r_{h,s}^*)^T \cdot W_h^* \qquad \forall\, h, s \qquad (4.43)$$

$$(\hat{r}_{h,s}^*)^T = T_{h,s}^* \cdot P_h^T \qquad \forall\, h, s \qquad (4.44)$$

Second Stage Equalities $g_s(x_1, x_{2s}) = 0$ continued...

$$\dot{M}_s^{in} = \dot{M}_s^{out} \qquad \forall\ s \quad (4.45)$$

$$\dot{M}_s^{pell} = \sum_p \dot{m}_{p,s}^{pell} \qquad \forall\ s \quad (4.46)$$

$$\dot{M}_s^{hot} = \dot{M}_s^{metal} + \dot{M}_{S,s}^{De.} \qquad \forall\ s \quad (4.47)$$

$$\dot{M}_s^{hot} = \sum_i \dot{m}_{i,s}^{hot} \qquad \forall\ s \quad (4.48)$$

$$\sum_p \left(x_{p,Fe}^{pell} \cdot \dot{m}_{p,s}^{pell} \right) = \dot{m}_{Fe,s}^{hot} \qquad \forall\ s \quad (4.49)$$

$$\sum_p \left(x_{p,Mn}^{pell} \cdot \dot{m}_{p,s}^{pell} \right) = \dot{m}_{Mn,s}^{hot} + \alpha_{Mn} \dot{m}_{MnO,s}^{slag} \qquad \forall\ s \quad (4.50)$$

$$\frac{\alpha_{Mn} \cdot \dot{m}_{MnO,s}^{slag}}{\dot{m}_{Mn,s}^{hot}} = r_{Mn}^{slag} \qquad \forall\ s \quad (4.51)$$

$$\dot{m}_{P,s}^{hot} - \sum_p \left(x_{p,P}^{pell} \cdot \dot{m}_{p,s}^{pell} \right) = \alpha_P \cdot x_{P_2O_5}^{coke} \cdot \dot{M}_s^{coke} \qquad \forall\ s \quad (4.52)$$

$$\frac{\dot{m}_{Si,s}^{hot}}{\alpha_{Si}} + \dot{m}_{SiO_2,s}^{slag} = x_{SiO_2,s}^{coke} \cdot \dot{M}_s^{coke} + \sum_p \left(x_{p,SiO_2}^{pell} \cdot \dot{m}_{p,s}^{pell} \right) \qquad \forall\ s \quad (4.53)$$

$$x_{S,s}^{coke} \cdot \dot{M}_s^{coke} + \sum_p \left(x_{p,S}^{pell} \cdot \dot{m}_{p,s}^{pell} \right) = \dot{m}_{S,s}^{hot} + \dot{m}_{S,s}^{slag} \qquad \forall\ s \quad (4.54)$$

$$\frac{\dot{m}_{S,s}^{slag}}{\dot{m}_{S,s}^{hot}} = r_S^{slag} \qquad \forall\ s \quad (4.55)$$

$$\dot{M}_s^{slag} = \sum_w \dot{m}_{w,s}^{slag} \qquad \forall\ s \quad (4.56)$$

$$\dot{m}_{Al_2O_3,s}^{slag} - x_{Al_2O_3,s}^{coke} \cdot \dot{M}_s^{coke} = \sum_p \left(x_{p,Al_2O_3}^{pell} \cdot \dot{m}_{p,s}^{pell} \right) \qquad \forall\ s \quad (4.57)$$

$$\dot{m}_{CaO,s}^{slag} - \sum_p \left(x_{p,CaO}^{pell} \cdot \dot{m}_{p,s}^{pell} \right) = x_{CaO}^{lime} \cdot \dot{M}_s^{lime} + x_{CaO}^{dol} \cdot \dot{M}_s^{dol} \qquad \forall\ s \quad (4.58)$$

$$\dot{m}_{MgO,s}^{slag} = \sum_p \left(x_{p,MgO}^{pell} \cdot \dot{m}_{p,s}^{pell} \right) + x_{MgO}^{dol} \cdot \dot{M}_s^{dol} \qquad \forall\ s \quad (4.59)$$

$$y_s^{BF} = (r_s^{BF})^T \beta_{BF} \qquad \forall\ s \quad (4.60)$$

$$\dot{m}_{pellet,s}^{model} = \sum_p \dot{m}_{p,s}^{pell} \qquad \forall\ s \quad (4.61)$$

$$\dot{m}_{Silica,s}^{model} = \sum_{p_a} x_{p_a,SiO_2}^{pell} \dot{m}_{p_a,s}^{pell} \qquad \forall\ s \quad (4.62)$$

Second Stage Equalities $g_s(x_1, x_{2s}) = 0$ continued...

$$\dot{m}^{model}_{MgO,s} = \sum_p \left(x^{pell}_{p,MgO} \cdot \dot{m}^{pell}_{p,s} \right) + x^{dol}_{MgO} \cdot \dot{M}^{dol}_s \qquad \forall\, s \qquad (4.63)$$

$$\dot{m}^{model}_{CaO,s} = \sum_p \left(x^{pell}_{p,CaO} \cdot \dot{m}^{pell}_{p,s} \right) + x^{lime}_{CaO} \cdot \dot{M}^{lime}_s + x^{dol}_{CaO} \cdot \dot{M}^{dol}_s \qquad \forall\, s \qquad (4.64)$$

$$\dot{m}^{model}_{MgO,s} = x^{coke}_{Al_2O_3,s} \cdot \dot{M}^{coke}_s + \sum_p \left(x^{pell}_{p,Al_2O_3} \cdot \dot{m}^{pell}_{p,s} \right) \qquad \forall\, s \qquad (4.65)$$

$$\dot{m}^{model}_{SiO_2,s} = x^{coke}_{SiO_2,s} \cdot \dot{M}^{coke}_s + \sum_{p_f} \left(x^{pell}_{p_f,SiO_2} \cdot \dot{m}^{pell}_{p_f,s} \right) \qquad \forall\, s \qquad (4.66)$$

$$\dot{m}^{model}_{Ash,s} = \dot{m}^{model}_{MgO,s} + \dot{m}^{model}_{CaO,s} + \dot{m}^{model}_{MgO,s} + \dot{m}^{model}_{SiO_2,s} \qquad \forall\, s \qquad (4.67)$$

$$\dot{m}^{model}_{iron} = \dot{m}^{hot}_{Fe,s} \qquad \forall\, s \qquad (4.68)$$

$$x^{model}_{coke,C,s} = x^{coke}_{C,s} \qquad \forall\, s \qquad (4.69)$$

$$\dot{m}^{model}_{lime,s} = \dot{M}^{lime}_s \qquad \forall\, s \qquad (4.70)$$

$$\dot{m}^{model}_{dol,s} = \dot{M}^{dol}_s \qquad \forall\, s \qquad (4.71)$$

$$\dot{m}^{model}_{steam,s} = \dot{M}^{steam}_s \qquad \forall\, s \qquad (4.72)$$

$$\dot{m}^{model}_{oil,s} = \dot{M}^{oil}_s \qquad \forall\, s \qquad (4.73)$$

$$\dot{m}^{model}_{hot,P,s} = \dot{m}^{hot}_{P,s} \qquad \forall\, s \qquad (4.74)$$

$$\dot{m}^{model}_{hot,Si,s} = \dot{m}^{hot}_{Si,s} \qquad \forall\, s \qquad (4.75)$$

$$\dot{m}^{model}_{hot,C,s} = \dot{m}^{hot}_{C,s} \qquad \forall\, s \qquad (4.76)$$

$$\dot{m}^{model}_{hot,Mn,s} = \dot{m}^{hot}_{Mn,s} \qquad \forall\, s \qquad (4.77)$$

$$\dot{V}^{model}_{air,s} = \dot{V}^{air}_s \qquad \forall\, s \qquad (4.78)$$

$$\dot{V}^{model}_{top\ gas,s} = \dot{V}^{top\ gas}_s \qquad \forall\, s \qquad (4.79)$$

$$\dot{m}^{model}_{coke,s} = \dot{M}^{coke}_s \qquad \forall\, s \qquad (4.80)$$

$$y^{BOF}_{g,s} = (r^{BOF}_{g,s})^T \beta_g \qquad \forall\, g, s \qquad (4.81)$$

$$\frac{\dot{m}^{hot}_{f,s}}{\dot{M}^{metal}_s} = x^{hot}_{f,s} \qquad \forall\, f, s \qquad (4.82)$$

$$\dot{M}^{metal}_s = \frac{\sum_g M^{BOF}_{hot_{g,s}} \cdot D_{BOF,g}}{T_{length}} \qquad \forall\, s \qquad (4.83)$$

The decision variables can be categorized as either first or second stage. The vector K_s contains all second stage decision variables for every scenario s.

$$K_s = \Big[(\delta_{c,s}^{use})^T, (m_{c,s}^{coal})^T, (\dot{M}_s^{coke})^T, (\dot{m}_{p,s}^{pell})^T, (\dot{M}_s^{lime})^T, (\dot{M}_s^{dol})^T, (\dot{M}_s^{steam})^T, \\ (\dot{M}_s^{oil})^T, (\dot{V}_s^{air})^T, (x_{Mn,g,s}^{steel})^T, (x_{P,g,s}^{steel})^T, (\dot{x}_{Si,g,s}^{steel})^T\Big]^T$$

For a total of $N^{scen.}$ scenarios, the complete second stage decision variable vector $K^{2^{nd}}$ can be written:

$$K^{2^{nd}} = \left[K_1^T, K_2^T, ..., K_{N^{scen.}}^T\right]^T$$

The new first stage variable δ_c^{buy} is considered a decision variable and is added to the scrap, coal, and pellet purchasing decision variables. Combining these variables with the vector $K^{2^{nd}}$ yields the complete decision variable vector K^{stoch}.

$$K^{stoch} = \left[(\delta_c^{buy})^T, (B_c^{coal})^T, (B_p^{pell})^T, B^{scrap}, (K^{2^{nd}})^T\right]^T$$

The new objective function gives equal probability to each scenario s occurring and is written below.

PROBLEM 2

$$\min_{K^{stoch}} \sum_{s=1}^{N^{scen.}} \Bigg[\sum_{g} \left(c^{O_2} V_{O_2,g,s}^{BOF} + c^{dol} M_{dol,g,s}^{BOF} + c^{lime} M_{lime,g,s}^{BOF} \right) D_{BOF,g}$$

$$- p^{*By-prod.} \cdot A_s^{coke} \cdot M_{VM,removed,s}$$

$$+ \left(c^{lime} \dot{M}_s^{lime} + c^{dol} \dot{M}_s^{dol} + c^{air} \dot{V}_s^{air} + c^{steam} \dot{M}_s^{steam} + c^{oil} \dot{M}_s^{oil} + c^{De.} \dot{M}_{S,s}^{De.} \right) \cdot T_{length} \Bigg] / N^{scen.}$$

$$+ \sum_{c} c_c^{coal} \cdot B_c^{coal} + \sum_{p} c_p^{pell} \cdot B_p^{pell} + c^{scrap} \cdot B^{scrap}$$

Subject to,

		Equation Reference #									
$h(x_1) \leq 0$	$\rightarrow$	4.2	4.3								
$h_s(x_1, x_{2s}) \leq 0$	$\rightarrow$	4.4	4.5	4.6	4.7	4.8	4.9	4.10	4.11	4.12	
		4.13	4.14	4.15	4.16	4.17	4.18	4.19	4.20		
		4.21	4.21	4.23	4.24	4.25	4.26	4.27	4.28		
$g_s(x_1, x_{2s}) = 0$	$\rightarrow$	4.45	4.46	4.47	4.48	4.49	4.50	4.51	4.52	4.53	4.54
		4.55	4.56	4.57	4.58	4.59	4.60	4.61	4.62	4.63	4.64
		4.65	4.66	4.67	4.68	4.69	4.70	4.71	4.72	4.73	4.74
		4.75	4.76	4.77	4.78	4.79	4.80	4.81	4.82	4.83	

where,

$$K^{stoch} = \left[(\delta_c^{buy})^T, (B_c^{coal})^T, (B_p^{pell})^T, B^{scrap}, (K^{2^{nd}})^T \right]^T$$

4.3.2 Two-Stage Stochastic Optimization Case Study

In this case study, uncertainty is considered in only the coal and pellet compositions, and more specifically, only specific components. The uncertain mass fractions are assumed to

belong to standard normal distributions. For each component, its mean value is reported in Appendix A. The corresponding standard deviations are given in Table 4.11 and are assumed to be equal among all the different coal and pellet types. In this respect, it is assumed the raw material suppliers provide an equally uncertain product. In order to ensure the mass fractions add to one, the sum of mass fractions are set equal to 1 by adjusting the carbon content for coal and iron content for pellets.

Table 4.11: Standard deviation of uncertain components in coals and pellets.

Raw Material	Component	σ wt. %
Coal	Ash	0.8%
	H_2O	0.5%
	P_2O_5	0.001%
	Volatile Matter	1%
Pellets	Mn	0.3%
	P	0.001%
	SiO_2	0.3%

The standard deviation values were chosen arbitrarily for this study, based on advice from an industrial contact [18].

The total number of possible scenarios in this case is infinite since the uncertainty distributions are continuous. Optimizing with respect to many scenarios would expand the problem size immensely and make the problem computationally intractable. Thus, for this study, a total of 50 uncertain scenarios are considered. The compositions of the raw materials are generated randomly from their respective standard normal distributions. The random values are never allowed to be further than three standard deviations away from the respective means of each component. This sampling procedure is repeated 50 times building a scenario database.

The availability of raw materials is considered to be the same as Problem 1c in Section 4.2.3 in that seven coals and three pellets can be purchased. The optimization solution is given

in Table 4.12 for the first stage variables only. Also listed are the purchasing decisions for the nominal case in which uncertainty is ignored. All mass quantities are given in kg of raw material per tonne of steel produced, and scaled costs given per tonne of steel produced.

Table 4.12: First stage purchasing comparison of stochastic and nominal solutions.

Raw Material	Two-Stage Purchase Problem 2a (kg/tonne steel)	Nominal Purchase Problem 1c (kg/tonne steel)
Coal C	38	0
Coal E	183	370
Coal F	160	139
Coal G	188	90
Pellet A	460	74
Pellet B	223	171
Pellet C	970	980
Scrap	251	255
Purchasing Scaled Cost	\$21.87/tonne	\$21.72/tonne

The first stage purchasing scaled cost term in the above table does not represent solely the costs of buying raw materials. As mentioned, there is a revenue stream related to the by-product released from the coals that, if not considered, would make the two-stage purchasing solution appear to be less costly than that of the nominal solution. Consequently, it was assumed that all the coals purchased in the above table would be processed and the volatile matter collected. The revenue from this was then subtracted from the raw purchasing cost, resulting in the reported costs in Table 4.12. This costing calculation was not done in either solving Problems 1c or 2c or in the simulation results reported later. It was only completed to compare the first stage purchasing differences.

The purchasing decision for each raw material is different when uncertainty is considered. Coal E is very profitable with respect to generating by-product off gas. Only about half of Coal E in the nominal case is purchased in the stochastic case. This is replaced by purchasing more of Coals F and G as well as previously unused Coal C. Coals F and G have excellent

strength attributes and therefore are blended in greater quantities in order to guard against the CSR and stability coke constraints. Coal C has a fairly low phosphorous content and its addition is likely decided upon by the optimizer to back-off from the phosphorous upper limit constraint in the blast furnace.

A greater amount of low phosphorous and silica Pellet B was purchased in the two-stage solution. This low ash pellet reduces the dolomite consumption in the blast furnace and also contributes to the back-off from the phosphorous upper limit constraint. The impact on BOF production is positive, and thus, less phosphorous is required to be oxidized and removed. A reduction in phosphorous oxidation means less scrap needs to be added to the BOF batches in order to control the final steel temperature; hence, less scrap was purchased in the two-stage solution.

The first stage cost of the nominal solution is 0.71% cheaper than that of the two-stage approach. This makes sense because the decisions become more conservative when considering uncertainty. Table 4.13 shows the difference in production if the raw materials were used and nominal raw material compositions were encountered.

Table 4.13: Nominal and two-stage production comparison if no uncertainty were present.

	Two-Stage Purchase (Problem 2a)	Nominal Purchase (Problem 1c)
$x^{coke}_{P_2O_5}$	0.038%	0.043%
Coke stability slack	5.4%	0%
Coke CSR slack	6.8%	0%
Hot metal P slack	0.0122%	0%

The conservativeness of the two-stage solution is illustrated in Table 4.13. The optimizer essentially backs off from the CSR and stability constraints as well as the upper limit on exit hot metal phosphorous content by altering the coal and pellet purchasing decisions. As a result, a different coal blend is chosen, highlighted by the coke phosphorous composition in Table 4.13 .

In order to determine the benefits of the more conservative two-stage approach, the solution, along with the nominal solution, must be implemented on the plant. Figure 4.7 shows the approach taken to compare these two methods.

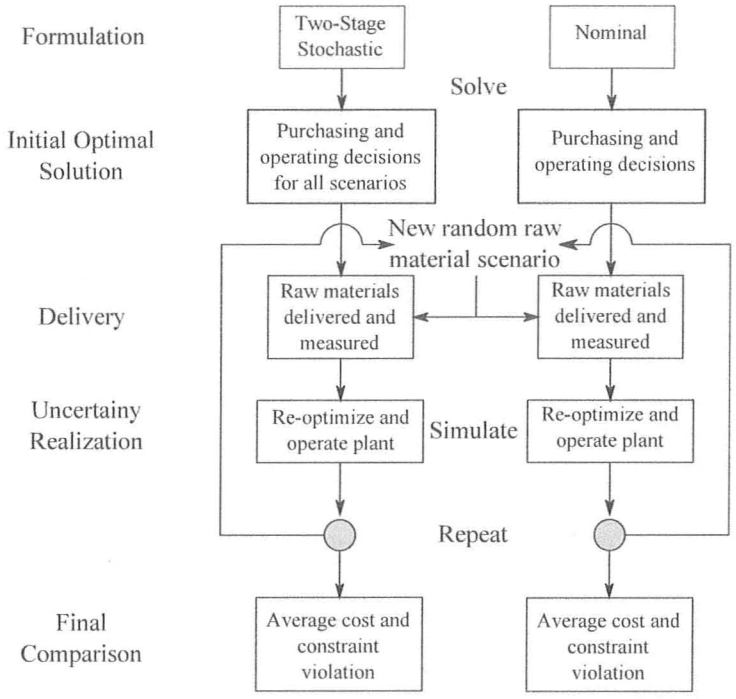

Figure 4.7: Uncertainty method comparison approach for nominal and two-stage operation.

The proposed testing method fixes the purchasing decisions for both the nominal and two-stage solutions after the initial optimization. The materials are then delivered to the plant for storage. A random scenario is generated based on the standard normal distributions of the raw material components. The problem is then re-optimized with the purchasing decisions fixed and the constraints relating to stream compositions and coke strength softened. The cost of resulting operation in dollars, and each constraint violation, are recorded and the process repeated with a new random scenario. Depending on the uncertainty realization, not all original purchased raw material may be used. In these instances, only the material processed is considered in the overall cost.

The degree of constraint violation is added to the objective function and assigned a weighting in order to force the optimizer to attempt to minimize the violation if possible. This

method is called goal programming in which the weights must be selected based on the relative importance of each constraint [45]. The objective is equal to the exact same cost function as in Problem 2, plus the cost of each slack variable s_m. The first stage purchasing decisions are included in this objective function, but are considered to be fixed variables and not manipulated by the optimizer. The penalty value of slack m is represented by ρ_m. The softened constraints in Problem 2 are replaced by new slack constraints in which the variables s_m are added. The new objective function and slack constraints are given in the following formulation.

$$min \quad \text{Cost} = \text{Cost}_{Problem\ 2} + \sum_{m}^{M} \rho_m s_m$$

Subject to,

- Non-softened constraints from Problem 2
- Fixed purchasing decisions

$$f_m(x, \beta) \geq RHS_m - s_m \qquad \forall\ m$$

$$s_m \geq 0,\ \rho_m \geq 0 \qquad \forall\ m$$

$$m = \{\text{CSR, Stability, Wall Press., P}\}$$

The softened constraints are comprised of the original equation, $f_m(x, \beta)$, and the right hand side of the constraint RHS_m. In this study, the weights, ρ_m, were assigned values of 1, placing almost no penalty for operating outside the constraints. The effect of this small penalty is the optimizer will satisfy the softened inequality constraints if possible with essentially no cost. In a later study in this section, results with much larger penalty values will be reported.

The procedure outlined in Figure 4.7 was simulated a total of 500 times with both s_m and $\text{Cost}_{Problem\ 2}$ recorded. The average cost of the two-stage solution was \$22.78/tonne compared to \$22.62/tonne for the nominal case in Problem 1c, representing a 0.71% cost increase. The constraint violations were averaged as well and are presented in Table 4.14.

Table 4.14: Constraint violation for plant simulations of nominal and two-stage solutions.

Constraint	Equation#	Violation Information	Two-Stage Solution (Problem 2a)	Nominal Solution (Problem 1c)
Coke CSR	3.19	Avg. Frequency	2%	51%
		Avg. Magnitude	1.1%	3.0%
Coke stability	3.20	Avg. Frequency	0%	52%
		Avg. Magnitude	0%	0.13%
Oven wall pressure	3.21	Avg. Frequency	0%	0%
		Avg. Magnitude	0 lb/in^2	0%
Hot metal P content	3.78	Avg. Frequency	12%	48%
		Avg. Magnitude	0.0007%	0.001%

The reduction in constraint violation is very significant in the two-stage approach; the coke quality rarely went off-spec with CSR violating the constraint a mere 2% of the time. The stability constraint was never exceeded whereas the nominal solution produced sub-standard coke half of the time. The hot metal phosphorous constraint was violated 12% of the time for the two-stage solution. This may seem large but is still a dramatic improvement over the nominal solution. The result points to the drastic impact of phosphorous variance on blast furnace operation. In the cases of CSR and phosphorous, the two-stage solution also reduced the average magnitude of violation by 63% and 30% respectively.

The wall pressure constraint was never violated for either solution. This is most likely attributed to the fact that wall pressure is related more to the coke oven operating conditions, which are unaffected by uncertainty, than the particular coal compositions. Additionally, the coal blends decided upon in the nominal and two-stage solutions do not approach the constraint on wall pressure, indicating perturbations in the coal compositions never caused this constraint to be exceeded.

4.3.3 Two-Stage Scenario Size Study

Choosing a scenario size of 50 in the previous case study was done arbitrarily. Using more scenarios would represent the overall uncertainty distribution more accurately, but come at a cost of increased computation time. Additionally, the two-stage solution is highly dependent on the exact 50 scenarios used. In theory, if 50 different scenarios were used, the solution could change. It is desired that the solution be fairly robust with respect to both the scenario choices and the overall scenario size. This was tested by simulating various two-stage solutions along with the nominal solution of Problem 1c. Each solution was simulated 500 times, and the results summarized in Table 4.15.

Table 4.15: Varying scenario size results for simulated two-stage solutions.

Problem	Scenario Size	First Stage Computing Time	Average Cost $c^{avg.}$ ($/tonne)	Average Constraint Violations			
				CSR	Stability	Wall Press.	P
1c	1	0.3 s	$22.62	51%	52%	0%	49%
2a	50	296 s	$22.78	2%	0%	0%	12%
2b	50	181 s	$22.78	1%	0%	0%	13%
2c	50	81 s	$22.79	2%	0%	0%	8%
2d	50	142 s	$22.81	1%	0%	0%	10%
2e	50	611 s	$22.84	5%	0%	0%	4%
2f	100	2,472 s	$22.86	2%	0%	0%	4%
2g	125	3,970 s	$22.83	1%	0%	0%	10%
2h	150	>12 hr	-	-	-	-	-

The two-stage solution was solved using 50 scenarios four additional times. The computation times varied from approximately one to ten minutes. The average costs fluctuate 0.26% among the five trials, and there is not much difference between the CSR and phosphorous constraint violations. Problem 2f used 100 scenarios in total, increasing the average cost to $22.86 per tonne of steel. The scenarios used in this case likely captured the extreme un-

certainty conditions to a greater extent, and subsequently, the computation time increased. The high cost decisions made in Problem 2f were beneficial in the sense that the lowest number of constraint violations were incurred. Problem 2g used 125 scenarios and took well over an hour to find a solution. The cost, in this case, was 0.13% less than Problem 2f which can be explained as the 125 scenarios are chosen at random and therefore could not stretch the uncertainty space as much as the 100 scenarios in Problem 2f. Again, this smaller cost came at a price of more constraint violations.

As the scenario size was increased to 150, the problem size became intractable as no solution was found after 12 hours of computation. The results show that choosing anywhere from 50 to 125 scenarios results in a formulation that can be solved within a reasonable time length. Additionally, the solutions have very similar costs, averaging $22.81/tonne, and performance with respect to minimizing constraint violation. In all cases from Problem 2a to Problem 2g, the same slate of coals and pellets were purchased but in slightly different ratios. Therefore, regardless of the specific random scenarios used, one can be confident that at least the proper raw materials are being purchased. Moreover, in comparison to the nominal case of Problem 1c, the constraint violations were significantly reduced for all two-stage solutions.

4.3.4 Goal Programming Constraint Violation Penalty Study

The previous study determined the constraint violation for various two-stage solutions when a very small objective function penalty was added for constraint violations of CSR, stability, wall pressure, and hot metal phosphorous content. It may be such that the two-stage methods have the flexibility to remain within the constraints but not the economic incentive to actually operate in a feasible manner. The following study examines the cost and performance of the plant in the situation where minimizing constraint violation is of greater importance.

The objective function penalties were chosen to give approximately equal weight in the

objective function compared to other purchasing and production costs.

$$\text{CSR Penalty}(\rho_{CSR}) = \$1 \times 10^6/\%\ \text{CSR}$$

$$\text{Stability Penalty}(\rho_{Stab.}) = \$1 \times 10^6/\%\ \text{Stability}$$

$$\text{Wall Press. Penalty}(\rho_{W.P.}) = \$1 \times 10^6/\text{lb/in}^2$$

$$\text{Phos. Penalty}(\rho_P) = \$1 \times 10^7/0.01\%\ \text{Phosphorous}$$

Table 4.16 lists the average magnitude of violation, $s_m^{avg.}$, that would be experienced in practice, and the subsequent cost of violation. This calculation shows the approximate impact on the objective function for each violation relative to $\text{Cost}_{Problem\ 2}$.

Table 4.16: Approximate cost value of constraint violations in objective function.

Slack Constraint m	Avg. Violation Magnitude $s_m^{avg.}$	Approx. Percent of Overall Cost $\frac{s_m^{avg.} \cdot \rho_m}{\text{Cost}_{Problem\ 2}} \cdot 100\%$
CSR	1%	8.3%
Stability	0.1%	0.83%
Wall Pressure	0.1 lb/in^2	0.83%
P	0.001%	8.3%

These new penalty values were added to the objective function and 500 simulations carried out. The results are summarized in Table 4.17.

Table 4.17: Increased constraint penalty simulation results for two-stage solutions.

Problem	Scenario Size	Average Cost $c^{avg.}$ ($/tonne)	Average Constraint Violations			
			CSR	Stability	Wall Press.	P
1c	1	$23.08	46%	51%	0%	0%
2a	50	$22.82	0%	0%	0%	0%
2b	50	$22.81	0%	0%	0%	0%
2c	50	$22.86	0%	0%	0%	0%
2d	50	$22.83	0%	0%	0%	0%
2e	50	$22.81	0%	0%	0%	0%
2f	100	$22.86	0%	0%	0%	0%
2g	125	$22.82	0%	0%	0%	0%

On average, for the two-stage solutions, the overall cost increased from $22.81/tonne to $22.83/tonne in comparison to where almost no penalty was placed on constraint violation. This added cost came with the benefit of a reduction in violation for both CSR and phosphorous. In the 500 simulations, no two-stage solution exceeded any inequality constraints. Table 4.17 illustrates that increasing the violation penalties for the two-stage solutions results in a minimal increase in cost with a significant decrease in constraint violation.

In Problem 1c, as the penalties were increased, the overall cost increased from $22.62/tonne to $23.08/tonne. As a result, the CSR violation frequency was reduced slightly and phosphorous violations never occurred. In most cases over the 500 simulations, the hot metal phosphorous constraint was controlled by changing the total amount of coke added to the blast furnace. To make up for the energy deficit normally provided by coke, oil consumption was increased. Since oil is costly, this action raised the overall cost to the point where it was greater than that of all the two-stage solutions. The CSR and stability violations could not be avoided since these are a function of coal blend types only. If the wrong coals are purchased initially, the plant cannot order a different slate of coals and instead must use what is in the first stage decision to somehow minimize the extent of constraint violation.

Being able to place an exact dollar value on constraint violation would help in the analysis of optimization under uncertainty. In most industrial operations, determining these penalties is difficult, and therefore, plant personnel should be consulted in developing the weights to be used in the objective function.

4.3.5 Summary

A method has been presented which accounts for the inherent uncertainty in raw material purchasing. Using two-stage stochastic optimization, the original formulation was modified in order to separate the purchasing and operating variables. Each uncertainty outcome was considered to be a unique scenario, and assuming each scenario occurred with equal probability, the optimizer purchased a slate of raw materials that could be processed for most scenarios.

Comparing the results shows that a more conservative set of purchasing decisions must be made in order to accommodate the fluctuations in raw material composition. In the case of optimizing with respect to 50 scenarios, the two-stage approach makes a first stage raw material purchase that is 0.69% more costly than the nominal case where uncertainty is not considered. The benefits of this approach are observed when applying the purchasing solution to plant operation. In this situation, coke stability and CSR constraints were almost never violated. Furthermore, on average the hot metal phosphorous upper limit was violated 12% of the time. By comparison, in the nominal case, these three constraints were violated approximately 50% of the time.

Additional two-stage solutions were obtained using 50, 100, and 125 scenarios. The computing times for solving these problems ranged from approximately 1 to 66 minutes. As the scenario size was increased to 150, solving the two-stage problem became intractable with GAMS 23.3.3. When simulated under uncertain raw material conditions, the two-stage solutions exhibited similar low frequency constraint violations and overall cost.

The penalties on constraint violation were then increased from nearly negligible values in

order to encourage the optimizer to remain feasible during plant simulation. The two-stage solutions reduced all constraint violations to 0% frequency and increased the average overall cost from \$22.81/tonne to \$22.83/tonne. The nominal case of Problem 1c reduced phosphorous violations to 0% frequency but raised the overall cost by 2%. Due to lack of production information, the actual costs of constraint violation are not known. Therefore, a decision by plant operators must be made on their willingness to save purchasing costs versus incurring added costs when constraints are violated in production.

4.4 Centralized vs. Decentralized Optimization

This section compares the benefit of the proposed integrated centralized optimizer in Chapter 3 to that of a decentralized approach that separates decisions made for each of the three main areas of primary steelmaking. For this study, no mismatch exists between model predictions and actual plant operation. The problem parameters with respect to steel demand and available coals are exactly the same as in Problem 1c.

Decentralized optimization, with respect to the steelmaking process, allows optimization for individual units to share information with one another, but in a limited manner. The order of the decision making process it outlined in Figure 4.8.

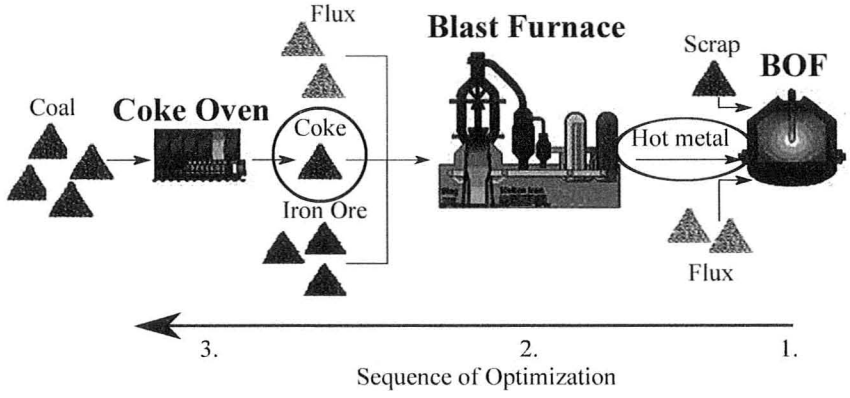

Figure 4.8: Decentralized optimization solution sequence.

The two streams of coke and hot metal connect the primary steelmaking units as shown in Figure 4.8. Steelmaking planners make an assumption about the approximate quality of hot metal that will be received from the blast furnace. Ideally the BOF would like hot metal of low impurity and carbon content as it would reduce several steelmaking costs. The amount of oxygen consumed to oxidize the impurities would be smaller and less scrap would be purchased, since its main purpose is to limit high temperatures generated from impurity oxidation. Fluxing agent consumption would be subsequently reduced since the hot metal is of a higher purity iron. Realizing that the blast furnace is unlikely to supply a very high

quality feed, steelmaking assumes the hot metal composition x_f^{hot} is equal to an average composition represented by $x_{hot,f}^{asmp.}$.

$$x_f^{hot} = x_{hot,f}^{asmp.} \quad \forall\, f \tag{4.84}$$

Depending on the steel grades to be made, this information is used to optimize BOF operation minimizing scrap purchasing, oxygen consumption, lime addition, and dolomite addition. The formulation for this sub-problem is shown below.

Step 1. - Steelmaking Optimization

$$\min_{K_{Steel}} \sum_g \left(c^{O_2} V_{O_2,g}^{BOF} + c^{dol} M_{dol,g}^{BOF} + c^{lime} M_{lime,g}^{BOF} \right) D_{BOF,g} + c^{scrap} \cdot B^{scrap}$$

Subject to,

Equation Reference #

3.83 3.86 3.87 3.88 3.89 3.90 3.91 3.92 3.93 4.84

with,

$$K_{Steel} = \left[x_{Mn,g}^{steel}, x_{P,g}^{steel}, x_{Si,g}^{steel}, B^{scrap} \right]$$

Note that this optimization determines the required hot metal tonnage rate of the blast furnace, $\dot{M}^{metal}$, which is dependent on the decision variables in K_{Steel}. This hot metal output is communicated to the ironmaking optimization as a fixed parameter.

The ironmaking optimization receives the demand quantity from steelmaking, but it does not provide the exact quality of hot metal that was previously assumed by $x_{hot,i}^{asmp.}$. In the centralized model, the upper limits on hot metal impurity levels are represented by x_i^{max}. Since the decentralized optimizer does not use an integrated model, the ironmaking optimization imposes new upper limits, $x_{max,i}^{asmp.}$, that are more conservative than x_i^{max}. These tighter constraints are more costly to ironmaking but are needed to prevent the optimizer from producing exceedingly poor hot metal. The ironmaking optimization must also assume

a quality of coke received by the upstream coke oven represented by $x_{coke,q}^{asmp.}$. Equations 4.85 and 4.86 illustrate these new quality constraints.

$$x_i^{min} \leq x_i^{hot} \leq x_{max,i}^{asmp.} \quad \forall\, i = C, Mn, P, Si \tag{4.85}$$

$$x_q^{coke} = x_{coke,q}^{asmp.} \quad \forall\, q \tag{4.86}$$

Adding these equations to the constraints written in Section 3.3 finalizes the ironmaking optimization formulation.

Step 2. - Ironmaking Optimization

$$\min_{K_{Iron}} \left(c^{lime}\dot{M}^{lime} + c^{dol}\dot{M}^{dol} + c^{air}\dot{V}^{air} + c^{steam}\dot{M}^{steam} + c^{oil}\dot{M}^{oil} + c^{De.}\dot{M}_S^{De.} \right) \cdot T_{length} + \sum_p c_p^{pell} \cdot B_p^{pell}$$

Subject to,

Equation Reference #

3.42	3.43	3.44	3.45	3.46	3.47	3.48	3.49	3.50	3.51	3.52
3.56	3.53	3.54	3.55	3.57	3.58	3.59	3.60	3.61	3.62	
3.63	3.64	3.65	3.66	3.67	3.68	3.69	3.70	3.71	3.72	
3.73	3.74	3.75	3.76	3.77	3.79	3.79	3.81	4.85	4.86	

with,

$$K_{Iron} = \left[\dot{M}^{coke}, B_p^{pell}, \dot{m}_p^{pell}, \dot{M}^{lime}, \dot{M}^{dol}, \dot{M}^{steam}, \dot{M}^{oil}, \dot{V}^{air} \right]$$

The result of this optimization determines the selection of pellets to be purchased, plant operating conditions, and the coke demand, $\dot{M}^{coke}$, to be issued to cokemaking.

The final step in the decentralized solution is that of cokemaking optimization which seeks to produce coke in the cheapest manner possible. Similar to ironmaking, the impact of coke on the blast furnace is taken into consideration. Phosphorous, for example, is difficult to maintain within the hot metal quality limits and therefore cokemaking sets a maximum

phosphorous limit on it's own operation represented by $x_{P_2O_5}^{max}$. This is shown in Equation 4.87.

$$x_{P_2O_5}^{coke} \leq x_{P_2O_5}^{max} \tag{4.87}$$

The optimization goal for cokemaking is to minimize cost with respect to coal purchasing and by-product revenue. The formulation is completed by fixing the required coke demand from the ironmaking optimization, and adding Equation 4.87 to the constraints listed in Section 3.2.

Step 3. Cokemaking Optimization

$$\min_{K_{Coke}} \sum_{c} c_c^{coal} \cdot B_c^{coal} - p^{*By-prod.} \cdot A^{coke} \cdot M_{V.M.,removed}$$

Subject to,

Equation Reference #

3.6	3.7	3.8	3.9	3.11	3.12	3.13	3.27	3.28	3.29
3.30	3.31	3.32	3.33	3.34	3.38	3.15	3.16	3.17	3.18
3.19	3.20	3.21	3.35	3.36	3.37	3.39	3.40	3.41	4.87

with,

$$K_{Coke} = \left[\delta_c^{use}, B_c^{coal}, m_c^{coal}\right]$$

The solution to Step 3 purchases an appropriate slate of coals as per the decision variables in vector K_{Coke}.

In this decentralized framework the flow of information is opposite to that of production. The solution procedure is outlined below and is denoted as Problem 3.

PROBLEM 3

1. Steelmaking Optimization
2. Ironmaking Optimization
3. Cokemaking Optimization

By contrast, the centralized approach makes all decisions simultaneously and considers the impact of operation on all areas of the plant. Section 4.4.1 studies the benefits of centralized optimization in the context of primary steelmaking.

4.4.1 Problem 3a: Centralized vs. Decentralized Optimization No Uncertainty

In the decentralized approach, the assumptions made by the three primary steelmaking areas have a significant impact on the overall cost of implementing the decentralized solution. This case study employs nominal assumptions meaning that the units are neither overly optimistic or pessimistic about the coke and hot metal stream qualities. These assumptions were chosen arbitrarily to replicate nominal conditions and are shown below in Table 4.18.

Table 4.18: Decentralized coke and hot metal stream quality assumptions.

Component	Hot Metal Assumption $x_{hot,i}^{asmp.}$ (%)	Coke Assumption $x_{coke,q}^{asmp.}$ (%)
Si	0.7%	-
P	0.027%	-
Mn	0.7%	-
C	4.5%	89%
Al_2O_3	-	2.5%
P_2O_5	-	0.045%
S	-	0.050%
SiO_2	-	5.0%
V.M.	-	0.5%

The ironmaking optimization imposes it's own upper limits on the hot metal quality delivered to steelmaking. These constraints are more conservative than that of the centralized optimization formulation. Since reporting of the actual values is confidential, the new upper limits, $x_{max,i}^{asmp.}$, are reported relative to those of the centralized formulation, x_i^{max}, in Table 4.19.

Table 4.19: Decentralized blast furnace hot metal upper limit deviation from centralized value x_i^{max}.

	Hot Metal Quality
Component	Upper Limit Deviation
	$x_{max,i}^{asmp.}$ - x_i^{max} (%)
C	-0.5%
Mn	0%
P	0%
Si	-0.5%

In comparison to the centralized formulation, the ironmaking formulation backs off from only the carbon and silica constraints. Without these new upper limits, the optimizer would simply raise the hot metal concentration of these components to the maximum allowable amount. This would be cost effective for the blast furnace but not for the BOF and so the constraints act as a means to incorporate the trade off between blast furnace and BOF operating costs.

Cokemaking must also impose an upper limit on phosphorous content so it does not overload the blast furnace and make it impossible to meet the subsequent hot metal upper limit constraint. This new upper limit for cokemaking, represented by $x_{P_2O_5}^{max}$, is equal to 0.045% in this case study.

These nominal values for stream quality assumptions and newly imposed quality upper limits are used in the decentralized formulation. This problem, classified as Problem 3a, is solved and the solution implemented on the plant with no uncertainty. Since implementation

may not result in a consistent system regarding mass balances, re-optimization is completed with certain variables fixed. These variables include the coal (m_c^{coal}) and pellet ($\dot{m}_p^{pell}$) mixes added to the coke oven and blast furnace respectively. Therefore, cokemaking produces coke as originally intended which is then used in the blast furnace. Ironmaking still uses the same pellet mix as decided upon before, however, since the coke is of different quality, the remaining blast furnace variables are allowed to change in order to satisfy the process constraints.

Upon implementation, the original hot metal upper limits used in the centralized formulation are reintroduced. Table 4.20 highlights the differences between the Problem 3a solution and that of the centralized method in Problem 1c.

Table 4.20: Centralized vs. decentralized solution comparison.

	Decentralized Solution (Problem 3a)	Centralized Solution (Problem 1c)
H.M. Si slack	0.2%	0%
$\dot{M}^{dol}$	92.4 kg/thm	99.4 kg/thm
B^{scrap}	347.6 kg/thm	313.4 tonnes/thm
$\dot{m}_A^{pell}$	0 tonnes/thm	91.3 tonnes/thm
$\dot{m}_B^{pell}$	309.4 tonnes/thm	210.4 tonnes/thm
$\dot{M}^{coke}$	520.4 kg/thm	515.8 kg/thm
Scaled Cost	\$22.72/tonne	\$22.60/tonne

The decentralized results show an increase of 0.53% in cost compared to the centralized solution. Table 4.20 highlights several areas where the centralized solution was able to reduce cost. The blast furnace lower limit constraint on silicon was active in the case of Problem 1c but not Problem 3a, meaning the centralized solution removed as much silicon as possible in the blast furnace, using more dolomite in the process. With respect to the decentralized solution, more silicon had to be oxidized and removed in the BOF. Since this releases a great deal of heat, more scrap had to be purchased in Problem 3a. The centralized optimizer recognized the trade off between dolomite usage and scrap purchasing

and decided it was optimal to incurr a higher dolomite cost instead.

The type of pellets purchased is another area where the solutions differed considerably. The decentralized optimizer assumed the coke phosphorous oxide content to be 0.0045% and therefore decided to use a significant amount of low phosphorous Pellet B. The resulting hot metal phosphorous content was 0.0005% below the upper limit. The centralized optimizer knew exactly what the coke phosphorous oxide content was to be and decided it could use a mixture of Pellets A and B and directly meet the upper hot metal phosphorous limit. Using Pellet A is advantageous because it has higher iron content, and as such, less of that pellet is purchased per tonne of hot metal produced.

In Problem 3a, the coke carbon content was assumed to be 89%. The blast furnace requested a coke supply rate of 520.4 kg/thm, approximately 5 kg/thm higher than that of the centralized solution. The actual coke produced by the cokemaking optimization had a carbon content of 90.3% and therefore less coke could have been produced overall to meet the needs of the blast furnace. In Problem 1c, the centralized optimizer decided on a carbon content and coke rate simultaneously, thus lowering the blast furnace coke addition rate and saving cost with respect to coal purchasing.

This case study demonstrates the savings that can be accrued with all the units in complete communication with each other. It is not only the quality of the coke and hot metal streams that is important to overall cost, but also resulting masses of these streams as they determine the purchasing quantities of the raw materials.

4.4.2 Problem 3b - Centralized vs. Decentralized Optimization With Uncertainty

The previous section studied a single case of assumed compositions and upper limits on the coke and hot metal streams. The results do not determine what the cost of the decentralized solution is if these parameters change. It is proposed to solve the decentralized solution for many different assumptions, and then take an average of the overall cost and constraint violations when the solutions are simulated on the plant.

First, each assumed component is assigned a standard deviation. It is assumed the decentralized assumptions vary according to standard normal distributions with the means being equal to those listed in the previous section. The subsequent standard deviations are listed below and were chosen arbitrarily to represent conditions that would exist in an actual decentralized steel plant.

Table 4.21: Decentralized standard deviations for assumptions and upper limits on quality streams.

Component	Coke Quality Upper Limits	Coke Quality Assump. (Table 4.18, col. 3)	Hot Metal Quality Upper Limits (Table 4.19, col. 2)	Hot Metal Quality Assump. (Table 4.18, col. 2)
P_2O_5	0.007%	0.007%	-	-
Al_2O_3	-	0.2%	-	-
S	-	0.005%	-	-
V.M.	-	0%	-	-
C	-	2%	0.2%	0.2%
SiO_2	-	0.25%	0.1%	0.1%
Mn	-	-	0%	0.1%
P	-	-	0%	0.007%

A single decentralized solution has random values selected from the above normal distributions and solved in the sequence as explained in the previous section, denoted as Problem

3b. After obtaining the raw material purchasing and plant operating settings, the solution is then simulated on the plant. The final cost is recorded, along with any constraint violations, and the process is repeated 500 times using violation penalties (ρ_m) of 1.

The averaged results are summarized in Table 4.22 in comparison to the centralized approach of Problem 1c.

Table 4.22: Scaled cost results for Problems 1c and 3b.

	Nominal Centralized (Problem 1c)	Decentralized (Problem 3b)
Scaled Cost per tonne	\$22.60/tonne	\$22.85/tonne

The results show the decentralized solution cost rises in the face of changes in the assumptions made between the units. On average, in comparison to Problem 1c the cost increase is 1.1%. A distribution of the Problem 3b costs for the 500 simulations is given in Figure 4.9.

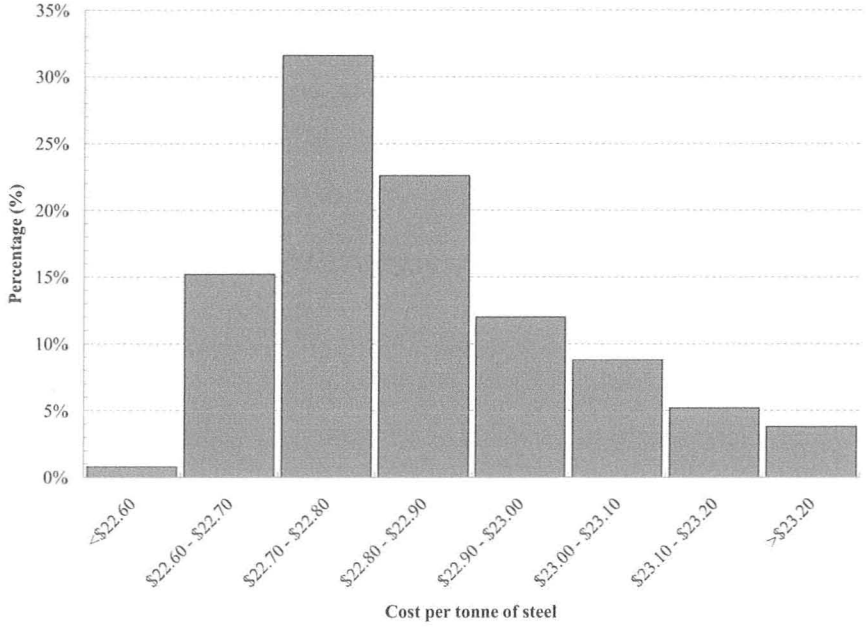

Figure 4.9: Decentralized optimization solution cost distribution for simulation study.

The above distribution shows that the final costs are very sensitive to the assumptions made in the decentralized approach. Also, in comparison to the nominal case of \$22.60/tonne, as the assumptions vary the cost rarely improves as the distribution is skewed towards the higher cost values. There could be many reasons for the high costs incurred in these scenarios. This most likely is that an overly conservative coke phosphorous content assumption is made. This would result in either a lot of Pellet B being used, or a costly coal blend that produced an unnecessarily low phosphorous content coke.

Another source of the high cost values could be related to the carbon, silica, and manganese levels in the hot metal assumed by steelmaking. These could have resulted in a sub-optimal amount of scrap being purchased. This directly impacts the hot metal rate of the blast furnace which relates to a sub-optimal amount of pellets purchased. The pellet addition then has an impact on the coke addition rate which has an effect on the total mass of coals purchased.

Figure 4.9 shows that approximately 1% of the simulations were actually less costly than the centralized case of \$22.60/tonne. In theory, the centralized case includes the most information in a single solution and therefore a cheaper solution cannot exist. Due to the mismatch in assumptions made in the coke and hot metal streams for the decentralized case, inequality constraints had to be relaxed during the 500 simulations to satisfy mass balances and energy relationships. This was implemeted exactly the same as in the two-stage stochastic approach in Section 4.3.2 where the inequality penalties (ρ_m) were set equal to 1. Therefore, the 1% of simulations in Figure 4.9 that are smaller than the centralized case of \$22.60/tonne, represent instances where the decentralized solution was very similar to the centralized solution and had the added benefit of being able to violate constraints to a degree.

4.4.3 Summary

Centralized optimization includes the most information in a simultaneous solution. This allows not only for the qualities of the connected streams to be optimized, but also for the

masses of these streams and the raw material masses used in production. In decentralized optimization, the connected units must make assumptions about the quality of feed they will receive and also operate without knowing the optimal quality of product to output. On average, the centralized approach in Problem 1c yields an improvement of 1.1%.

4.5 Chapter Summary

This chapter demonstrated the benefits that could be obtained by the integrated modeling of primary steelmaking. Decisions on raw material purchasing and subsequent operation can be obtained through optimization of the centralized formulation. The solution yields results which are not inherently obvious to a human planner, giving evidence to the necessity of the optimizer.

Raw material uncertainty was investigated by modifying the formulation into that of a two-stage stochastic approach. The problem was solved for various scenario sizes ranging from 50 to 125 scenarios. On average, the two-stage solutions cost \$22.81/tonne compared to the nominal case which cost \$22.62/tonne. The higher cost in the two-stage case resulted in a different slate of raw materials purchased. Upon plant operation, using these more costly materials resulted in very few constraint violations. In comparison, the nominal case experienced violations for CSR, stability, and phosphorous content nearly 50% of the time.

The constraint violation penalties were then increased significantly in order to force the optimizer to remain feasible upon processing of the uncertain raw materials. In this case, the two-stage approach changed operation slightly, costing \$22.83/tonne, but never incurred a constraint violation. By contrast, the nominal case was able to reduce only the percentage of phosphorous violations by a significant amount, but it came at a 2% increase in cost.

The centralized optimization approach was then compared to that of the current decentralized approach where the three main areas of steelmaking are optimized independently. It was shown that in the presence of nominal conditions and no raw material uncertainty, the decentralized method performed 0.53% worse than the centralized method. As the assump-

tions between the decentralized units were changed, the improvement of the centralized method was increased further to 1.1%.

Chapter 5

Multi-period Planning

The following chapter extends the primary steelmaking planning model from a single time period to a multiple time period model. Raw material pricing discounts are often offered by vendors in order to entice their customers to purchase greater quantities. Purchasing in bulk amounts can save the steel plant a significant amount of money. However, these decisions become quite complex and require managing of inventories over several time periods. The savings opportunities inherent in this purchasing practice require a multi-period approach as given in this chapter. The primary steelmaking units are assumed to operate at steady state within each time period and the units are connected via dynamic inventory models.

5.1 Formulation

Cokemaking

When considering more than one time period, inventory levels must be included in the formulation. This not only exists for coals, pellets, and scrap, but also for the coke which is stored between the coke oven and blast furnace. The coke inventory balance is given in Equation 5.1. Also shown is Equation 5.2 which requires the inventory to always be above a minimum level I_{min}^{coke}.

$$I_t^{coke} = I_{t-1}^{coke} + M_{out,t}^{coke} \cdot A_t^{coke} - \dot{M}_t^{coke} \cdot T_{length} \qquad \forall\, t \qquad (5.1)$$

$$I_t^{coke} \geq I_{min}^{coke} \qquad \forall\, t \qquad (5.2)$$

The coke inventory at the end of time period t is represented by I_t^{coke}. This variable is equal to the initial amount of coke present, I_{t-1}^{coke}, plus the amount produced by the coke oven, minus the coke used in the blast furnace.

Since the coke made during each time period may be of different quality, the composition of the coke inventory pile may change. The variable $d_{q,t}^{coke}$ represents the mass fraction of component q in the coke inventory pile at time t. The quality of coke being produced and added to inventory is represented by $x_{q,t}^{coke}$. The component balance on q is written in Equation 5.3 and assumes that the inventory pile is well mixed.

$$I_t^{coke} d_{q,t}^{coke} = I_{t-1}^{coke} d_{q,t-1}^{coke} + M_{out,t}^{coke} A_t^{coke} x_{q,t}^{coke} - \dot{m}_t^{coke} d_{q,t}^{coke} T_{length} \quad \forall\, q,t \qquad (5.3)$$

In comparison to the single time period approach, coal vendor pricing is considered to be more complex. It is assumed that coals can be purchased at two different pricing tiers. That is, vendors offer a discount after a certain quantity has been purchased. This is illustrated in Figure 5.1.

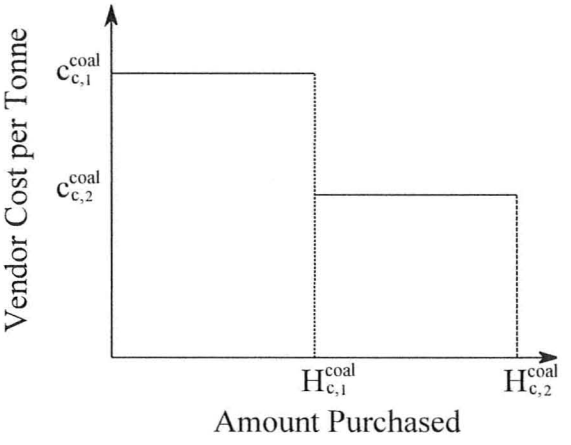

Figure 5.1: Two-tiered vendor raw material pricing for coal c.

In the above figure, $H_{c,1}^{coal}$ represents the purchasing break where the cost lowers from $c_{c,1}^{coal}$ to $c_{c,2}^{coal}$. The parameter $H_{c,2}^{coal}$ is the maximum mass that can be bought. Purchasing in the first tier, $B_{c,1,t}^{coal}$, must be exhausted before buying in the cheaper cost level, $B_{c,2,t}^{coal}$. Tiered purchasing rules are expressed through constraints as shown in Equations 5.4 through 5.6 [21].

$$H_{c,1}^{coal} \cdot \delta_{c,2,t}^{tier} \leq B_{c,1,t}^{coal} \leq H_{c,1}^{coal} \cdot \delta_{c,1,t}^{tier} \qquad \forall\, c,t \qquad (5.4)$$

$$0 \leq B_{c,2,t}^{coal} \leq \left(H_{c,2}^{coal} - H_{c,1}^{coal}\right) \cdot \delta_{c,2,t}^{tier} \qquad \forall\, c,t \qquad (5.5)$$

$$\delta_{c,1,t}^{tier} \geq \delta_{c,2,t}^{tier} \qquad \forall\, c,t \qquad (5.6)$$

The binary variable $\delta_{c,l,t}^{tier}$ is equal to 1 if coal c is to be purchased at tier l during time t. Equation 5.6 forces the order of tiered purchasing meaning if coal c is not purchased at tier 1, it cannot be purchased at tier 2 either.

A mass balance on each coal type c is written in Equation 5.7. The inventory quantity of coal c, at the end of time period t, is represented by $I_{c,t}^{coal}$. This quantity is equal to the initial inventory level $I_{c,t-1}^{coal}$, plus the amount purchased, $B_{c,l,t}^{coal}$, minus the amount used in cokemaking. Coal consumed in coke production is equal to the product of the batch addition amount $m_{c,t}^{coal}$ and the total number of batches made A_t^{coke}. The balance assumes that the amount purchased is equal to the amount delivered, meaning there is no model error and no delay with respect to raw material delivery.

$$I_{c,t}^{coal} = I_{c,t-1}^{coal} + \sum_{l} B_{c,l,t}^{coal} - m_{c,t}^{coal} A_t^{coke} \qquad \forall\, c,t \qquad (5.7)$$

Equation 5.8 requires that a minimum amount of coal, I_c^{min}, is stored in inventory at all times.

$$I_{c,t}^{coal} \geq I_c^{min} \qquad \forall\, c,t \qquad (5.8)$$

The remaining cokemaking equations expressed in Section 3.2 apply to the multi-period formulation. These are written in Equations 5.9 through 5.33.

$$0.94 \cdot M_{out,t}^{coke} + M_{H_2O,removed,t} = M_{coal,in} - \sum_q M_{q,removed,t} \qquad \forall\, t \qquad (5.9)$$

$$M_{H_2O,removed,t} = x_{H_2O,t}^{blend} \cdot M_{coal,in} \qquad \forall\, t \qquad (5.10)$$

$$M_{S,removed,t} = \frac{25.85\%}{100\%} \cdot x_{S,t}^{blend} \cdot M_{coal,in} \qquad \forall\, t \qquad (5.11)$$

$$M_{V.M.,removed,t} = \frac{98.33\%}{100\%} \cdot x_{V.M.,t}^{blend} \cdot M_{coal,in} \qquad \forall\, t \qquad (5.12)$$

$$x_{H_2O,t}^{blend} = \frac{\sum_c \left(x_{c,H_2O}^{coal} \cdot m_{c,t}^{coal} \right)}{M_{coal,in}} \qquad \forall\, t \qquad (5.13)$$

$$x_{q,t}^{blend} = \frac{\sum_c \left(x_{c,q}^{coal} \cdot m_{c,t}^{coal} \right)}{M_{coal,in}} \qquad \forall\, q,t \qquad (5.14)$$

$$x_{q,t}^{coke} = \frac{\left(x_{q,t}^{blend} \cdot M_{coal,in} \right) - M_{q,removed,t}}{M_{out}^{coke}} \qquad \forall\, q,t \qquad (5.15)$$

$$y_t^{CSR} = (r_{CSR,t})^T \beta_{CSR} \qquad \forall\, t \qquad (5.16)$$

$$y_t^{Stab.} = (r_{Stab.,t})^T \beta_{Stab.} \qquad \forall\, t \qquad (5.17)$$

$$\ln\left(y_t^{W.P.} \right) = (r_{W.P.,t})^T \beta_{W.P.} \qquad \forall\, t \qquad (5.18)$$

$$u_{h,t}^{blend}(j) = \sum_c \left(\frac{m_{c,t}^{coal}}{M_{coal,in}} \cdot X_{c,j}^{prop} \right) \qquad \forall\, j,h,t \qquad (5.19)$$

$$T_{h,t}^* = (r_{h,t}^*)^T \cdot W_h^* \qquad \forall\, h,t \qquad (5.20)$$

$$(\hat{r}_{h,t}^*)^T = T_{h,t}^* \cdot P_h^T \qquad \forall\, h,t \qquad (5.21)$$

$$\delta_{c,t}^{use} \cdot m_{min}^{coal} \leq m_{c,t}^{coal} \leq \delta_{c,t}^{use} \cdot m_{max}^{coal} \qquad \forall\, c,t \qquad (5.22)$$

$$\dot{M}_t^{coke} \cdot T_{length} \leq M_{out,t}^{coke} \cdot A_t^{coke} \qquad \forall\, t \qquad (5.23)$$

$$m_{c,t}^{coal} \cdot A_t^{coke} \leq B_{c,t}^{coal} \qquad \forall\, c,t \qquad (5.24)$$

$$y_t^{CSR} \geq y_{min}^{CSR} \qquad \forall\, t \qquad (5.25)$$

$$y_t^{Stab.} \geq y_{min}^{Stability} \qquad \forall\, t \qquad (5.26)$$

$$y_t^{W.P.} \leq y_{max}^{Pressure} \qquad \forall\, t \qquad (5.27)$$

$$\sum_{i=1}^{4} \frac{{T^*_{CSR,i,t}}^2}{s^2_{CSR,i}} \leq T^2_{max,CSR} \qquad \forall\, t \qquad (5.28)$$

$$\sum_{i=1}^{3} \frac{{T^*_{Stab.,i,t}}^2}{s^2_{Stab.,i}} \leq T^2_{max,Stab.} \qquad \forall\, t \qquad (5.29)$$

$$\sum_{i=1}^{2} \frac{{T^*_{W.P.,i,t}}^2}{s^2_{W.P.,i}} \leq T^2_{max,W.P.} \qquad \forall\, t \qquad (5.30)$$

$$\epsilon_{CSR} \geq \sum_{k \in k_{CSR}} \left(r^*_{CSR,t}(k) - \hat{r}^*_{CSR,t}(k)\right)^2 \qquad \forall\, t \qquad (5.31)$$

$$\epsilon_{Stab.} \geq \sum_{k \in k_{Stab.}} \left(r^*_{Stab.,t}(k) - \hat{r}^*_{Stab.,t}(k)\right)^2 \qquad \forall\, t \qquad (5.32)$$

$$\epsilon_{W.P.} \geq \sum_{k \in k_{W.P.}} \left(r^*_{W.P.,t}(k) - \hat{r}^*_{W.P.,t}(k)\right)^2 \qquad \forall\, t \qquad (5.33)$$

Ironmaking

It is assumed that pellets are not available at different pricing tiers like that of coal purchasing. The inventory of pellet p at time t is represented by $I^{pell}_{p,t}$. This variable is equal to the initial pellet level $I^{pell}_{p,t-1}$ plus the purchasing amount $B^{pell}_{p,t}$, minus the pellet addition rate $\dot{m}^{pell}_{p,t}$. The inventory balance is given in Equation 5.34.

$$I^{pell}_{p,t} = I^{pell}_{p,t-1} + B^{pell}_{p,t} - \dot{m}^{pell}_{p,t} \cdot T_{length} \qquad \forall\, p,t \qquad (5.34)$$

Also, Equation 5.35 requires a minimum pellet mass, $I^{pell}_{p,min}$, to be stored in inventory.

$$I^{pell}_{p,t} \geq I^{pell}_{p,min} \qquad \forall\, p,t \qquad (5.35)$$

The remaining ironmaking equations expressed in Section 3.3 apply to the multi-period formulation. These are written in Equations 5.36 through 5.79.

$$b^{low} \leq \frac{\dot{m}^{slag}_{CaO,t} + \dot{m}^{slag}_{MgO,t}}{\dot{m}^{slag}_{SiO_2,t} + \dot{m}^{slag}_{Al_2O_3,t}} \leq b^{up} \qquad \forall\, t \qquad (5.36)$$

$$\frac{\sum_{p_a} \dot{m}^{pell}_{p_a,t}}{\sum_p \dot{m}^{pell}_{p,t}} \leq p^{up} \qquad \forall\, t \qquad (5.37)$$

$$\frac{\sum_{p_f} \dot{m}^{pell}_{p_f,t}}{\sum_p \dot{m}^{pell}_{p,t}} \leq p^{up} \qquad \forall\, t \qquad (5.38)$$

$$\frac{\dot{m}^{hot}_{S,t} - \dot{M}^{De.}_{S,t}}{\dot{M}^{metal}_t} \leq s^{up} \qquad \forall\, t \qquad (5.39)$$

$$x^{min}_i \leq \frac{\dot{m}^{hot}_{i,t}}{\dot{M}^{metal}_t} \leq x^{max}_i \qquad \forall\, i,t \qquad (5.40)$$

$$\frac{\dot{M}^{oil}_t}{\dot{M}^{hot}_t} \leq r^{oil} \qquad \forall\, t \qquad (5.41)$$

$$\dot{V}^{air}_t \leq \dot{V}^{max} \qquad \forall\, t \qquad (5.42)$$

$$\dot{m}^{pell}_{p,t} \cdot T_{length} \leq B^{pell}_{p,t} \qquad \forall\, p,t \qquad (5.43)$$

$$\dot{M}^{in}_t = \dot{M}^{out}_t \qquad \forall\, t \qquad (5.44)$$

$$\dot{M}^{pell}_t = \sum_p \dot{m}^{pell}_{p,t} \qquad \forall\, t \qquad (5.45)$$

$$\dot{M}^{hot}_t = \dot{M}^{metal}_t + \dot{M}^{De.}_{S,t} \qquad \forall\, t \qquad (5.46)$$

$$\dot{M}^{hot}_t = \sum_i \dot{m}^{hot}_{i,t} \qquad \forall\, t \qquad (5.47)$$

$$\sum_p \left(x^{pell}_{p,Fe} \cdot \dot{m}^{pell}_{p,t} \right) = \dot{m}^{hot}_{Fe,t} \qquad \forall\, t \qquad (5.48)$$

$$\sum_p \left(x^{pell}_{p,Mn} \cdot \dot{m}^{pell}_{p,t} \right) = \dot{m}^{hot}_{Mn,t} + \alpha_{Mn} \dot{m}^{slag}_{MnO,t} \qquad \forall\, t \qquad (5.49)$$

$$\frac{\alpha_{Mn} \cdot \dot{m}^{slag}_{MnO,t}}{\dot{m}^{hot}_{Mn,t}} = r^{slag}_{Mn} \qquad \forall\, t \qquad (5.50)$$

$$\dot{m}^{hot}_{P,t} - \sum_p \left(x^{pell}_{p,P} \cdot \dot{m}^{pell}_{p,t} \right) = \alpha_P \cdot x^{coke}_{P_2O_5} \cdot \dot{M}^{coke}_t \qquad \forall\, t \qquad (5.51)$$

$$\frac{\dot{m}^{hot}_{Si,t}}{\alpha_{Si}} + \dot{m}^{slag}_{SiO_2,t} = x^{coke}_{SiO_2,t} \cdot \dot{M}^{coke}_t + \sum_p \left(x^{pell}_{p,SiO_2} \cdot \dot{m}^{pell}_{p,t} \right) \qquad \forall\, t \qquad (5.52)$$

$$\dot{m}_{S,t}^{hot} + \dot{m}_{S,t}^{slag} = x_{S,t}^{coke} \cdot \dot{M}_t^{coke} + \sum_p \left(x_{p,S}^{pell} \cdot \dot{m}_{p,t}^{pell} \right) \qquad \forall\, t \qquad (5.53)$$

$$\frac{\dot{m}_{S,t}^{slag}}{\dot{m}_{S,t}^{hot}} = r_S^{slag} \qquad \forall\, t \qquad (5.54)$$

$$\dot{M}_t^{slag} = \sum_w \dot{m}_{w,t}^{slag} \qquad \forall\, t \qquad (5.55)$$

$$\dot{m}_{Al_2O_3,t}^{slag} = x_{Al_2O_3,t}^{coke} \cdot \dot{M}_t^{coke} + \sum_p \left(x_{p,Al_2O_3}^{pell} \cdot \dot{m}_{p,t}^{pell} \right) \qquad \forall\, t \qquad (5.56)$$

$$\dot{m}_{CaO,t}^{slag} = \sum_p \left(x_{p,CaO}^{pell} \cdot \dot{m}_{p,t}^{pell} \right) + x_{CaO}^{lime} \cdot \dot{M}_t^{lime} + x_{CaO}^{dol} \cdot \dot{M}_t^{dol} \qquad \forall\, t \qquad (5.57)$$

$$\dot{m}_{MgO,t}^{slag} = \sum_p \left(x_{p,MgO}^{pell} \cdot \dot{m}_{p,t}^{pell} \right) + x_{MgO}^{dol} \cdot \dot{M}_t^{dol} \qquad \forall\, t \qquad (5.58)$$

$$y_t^{BF} = (r_t^{BF})^T \beta_{BF} \qquad \forall\, t \qquad (5.59)$$

$$\dot{m}_{pellet,t}^{model} = \sum_p \dot{m}_{p,t}^{pell} \qquad \forall\, t \qquad (5.60)$$

$$\dot{m}_{Silica,t}^{model} = \sum_{p_a} x_{p_a,SiO_2}^{pell} \dot{m}_{p_a,t}^{pell} \qquad \forall\, t \qquad (5.61)$$

$$\dot{m}_{MgO,t}^{model} = \sum_p \left(x_{p,MgO}^{pell} \cdot \dot{m}_{p,t}^{pell} \right) + x_{MgO}^{dol} \cdot \dot{M}_t^{dol} \qquad \forall\, t \qquad (5.62)$$

$$\dot{m}_{CaO,t}^{model} = \sum_p \left(x_{p,CaO}^{pell} \cdot \dot{m}_{p,t}^{pell} \right) + x_{CaO}^{lime} \cdot \dot{M}_t^{lime} + x_{CaO}^{dol} \cdot \dot{M}_t^{dol} \qquad \forall\, t \qquad (5.63)$$

$$\dot{m}_{MgO,t}^{model} = x_{Al_2O_3,t}^{coke} \cdot \dot{M}_t^{coke} + \sum_p \left(x_{p,Al_2O_3}^{pell} \cdot \dot{m}_{p,t}^{pell} \right) \qquad \forall\, t \qquad (5.64)$$

$$\dot{m}_{SiO_2,t}^{model} = x_{SiO_2,t}^{coke} \cdot \dot{M}_t^{coke} + \sum_{p_f} \left(x_{p_f,SiO_2}^{pell} \cdot \dot{m}_{p_f,t}^{pell} \right) \qquad \forall\, t \qquad (5.65)$$

$$\dot{m}_{Ash,t}^{model} = \dot{m}_{MgO,t}^{model} + \dot{m}_{CaO,t}^{model} + \dot{m}_{MgO,t}^{model} + \dot{m}_{SiO_2,t}^{model} \qquad \forall\, t \qquad (5.66)$$

$$\dot{m}_{iron}^{model} = \dot{m}_{Fe,t}^{hot} \qquad \forall\, t \qquad (5.67)$$

$$x_{coke,C,t}^{model} = x_{C,t}^{coke} \qquad \forall\, t \qquad (5.68)$$

$$\dot{m}_{lime,t}^{model} = \dot{M}_t^{lime} \qquad \forall\, t \qquad (5.69)$$

$$\dot{m}_{dol,t}^{model} = \dot{M}_t^{dol} \qquad \forall\, t \qquad (5.70)$$

$$\dot{m}_{steam,t}^{model} = \dot{M}_t^{steam} \qquad \forall\, t \qquad (5.71)$$

$$\dot{m}_{oil,t}^{model} = \dot{M}_t^{oil} \qquad \forall\, t \qquad (5.72)$$

$$\dot{m}_{hot,P,t}^{model} = \dot{m}_{P,t}^{hot} \qquad \forall\, t \qquad (5.73)$$

$$\dot{m}_{hot,Si,t}^{model} = \dot{m}_{Si,t}^{hot} \qquad \forall\, t \qquad (5.74)$$

$$\dot{m}_{hot,C,t}^{model} = \dot{m}_{C,t}^{hot} \qquad \forall\, t \qquad (5.75)$$

$$\dot{m}_{hot,Mn,t}^{model} = \dot{m}_{Mn,t}^{hot} \qquad \forall\, t \qquad (5.76)$$

$$\dot{V}_{air,t}^{model} = \dot{V}_{t}^{air} \qquad \forall\, t \qquad (5.77)$$

$$\dot{V}_{top\ gas,t}^{model} = \dot{V}_{t}^{top\ gas} \qquad \forall\, t \qquad (5.78)$$

$$\dot{m}_{coke,t}^{model} = \dot{M}_{t}^{coke} \qquad \forall\, t \qquad (5.79)$$

Steelmaking

Similar to coal, scrap metal is available at two different pricing tiers. The discount break point occurs when H_1^{scrap} tonnes of scrap are purchased. In total, a maximum of H_2^{scrap} tonnes can be bought over both tiers. The variables $B_{1,t}^{scrap}$ and $B_{2,t}^{scrap}$ represent the amount purchased at tiers 1 and 2 respectively. The binary variable $\delta_{scrap,l,t}^{tier}$ equals 1 if scrap is purchased at tier l during time t, and 0 otherwise. Equations 5.80 through 5.82 show how this practice can be modeled.

$$H_1^{scrap} \cdot \delta_{scrap,2,t}^{tier} \leq B_{1,t}^{scrap} \leq H_1^{scrap} \cdot \delta_{scrap,1,t}^{tier} \qquad \forall\, t \qquad (5.80)$$

$$0 \leq B_{2,t}^{scrap} \leq (H_2^{scrap} - H_1^{scrap}) \cdot \delta_{scrap,2,t}^{tier} \qquad \forall\, t \qquad (5.81)$$

$$\delta_{scrap,1,t}^{tier} \geq \delta_{scrap,2,t}^{tier} \qquad \forall\, t \qquad (5.82)$$

The final inventory level is equal to the initial quantity, I_{t-1}^{scrap}, plus the scrap purchased, $B_{l,t}^{scrap}$, minus the amount used in BOF production $M_{scrap_g}^{BOF}$. A balance on scrap inventory level, I_t^{scrap}, is written in Equation 5.83.

$$I_t^{scrap} = I_{t-1}^{scrap} + \sum_l B_{l,t}^{scrap} - \sum_g M_{scrap_g}^{BOF} \cdot D_{BOF,g,t} \qquad \forall\, t \qquad (5.83)$$

Equation 5.84 indicates that a minimum quantity of scrap, I_{min}^{scrap}, must always remain in inventory.

$$I_t^{scrap} \geq I_{min}^{scrap} \qquad \forall\, t \qquad (5.84)$$

The remaining steelmaking equations expressed in Section 3.4 apply to the multi-period formulation. These are written in Equations 5.85 through 5.92.

$$X^{steel}_{min,Mn,g} \leq x^{steel}_{Mn,g,t} \leq X^{steel}_{max,Mn,g} \qquad \forall\, g,t \qquad (5.85)$$

$$X^{steel}_{min,P,g} \leq x^{steel}_{P,g,t} \leq X^{steel}_{max,P,g} \qquad \forall\, g,t \qquad (5.86)$$

$$X^{steel}_{min,Si,g} \leq x^{steel}_{Si,g,t} \leq X^{steel}_{max,Si,g} \qquad \forall\, g,t \qquad (5.87)$$

$$M^{BOF}_{dol_{g,t}} \leq M^{BOF,max}_{dol} \qquad \forall\, g,t \qquad (5.88)$$

$$M^{BOF}_{lime_{g,t}} \leq M^{BOF,max}_{lime} \qquad \forall\, g,t \qquad (5.89)$$

$$y^{BOF}_{g,t} = (r^{BOF}_{g,s})^T \beta_g \qquad \forall\, g,t \qquad (5.90)$$

$$\frac{\dot{m}^{hot}_{f,t}}{\dot{M}^{metal}_t} = x^{hot}_{f,t} \qquad \forall\, f,t \qquad (5.91)$$

$$\dot{M}^{metal}_t = \frac{\sum_g M^{BOF}_{hot_{g,t}} \cdot D_{BOF,g}}{T_{length}} \qquad \forall\, t \qquad (5.92)$$

The new binary tiered purchasing variables are decision variables and added to the vector K_t which represents the optimization decision variables for period t.

$$K_t = \Big[(\delta^{coal}_{c,l,t})^T, (\delta^{use}_{c,t})^T, (B^{coal}_{c,l,t})^T, (m^{coal}_{c,t})^T, (\dot{M}^{coke}_t)^T, (B^{pell}_{p,t})^T, (\dot{m}^{pell}_{p,t})^T, (\dot{M}^{lime}_t)^T, (\dot{M}^{dol}_t)^T,$$
$$(\dot{M}^{steam}_t)^T, (\dot{M}^{oil}_t)^T, (\dot{V}^{air}_t)^T, (x^{steel}_{Mn,g,t})^T, (x^{steel}_{P,g,t})^T, (x^{steel}_{Si,g,t})^T, (\delta^{scrap}_{l,t})^T, (B^{scrap}_{l,t})^T\Big]^T$$

For a total of t_f periods, the complete decision variable vector K^{multi} can be written:

$$K^{multi} = \Big[K^T_1, K^T_2, ..., K^T_{t_f}\Big]^T$$

The new objective function must consider all purchasing and production costs, as well as the cost of holding inventory. The parameter c^{inv} is used to represent the cost per tonne of inventory per time period. The parameters c^{scrap}_l and $c^{coal}_{c,l}$ denote the new scrap and coal costs for various pricing tiers.

PROBLEM 4a

$$\min_{K^{multi}} \sum_{t}^{t_f} \Bigg[\sum_{g} \left(c^{O_2} V_{O_2,g,t}^{BOF} + c^{dol} M_{dol,g,t}^{BOF} + c^{lime} M_{lime,g,t}^{BOF} \right) D_{BOF,g} - p^{*By-prod.} \cdot A_t^{coke} \cdot M_{VM,removed,t}$$
$$+ \left(c^{lime} \dot{M}_t^{lime} + c^{dol} \dot{M}_t^{dol} + c^{air} \dot{V}_t^{air} + c^{steam} \dot{M}_t^{steam} + c^{oil} \dot{M}_t^{oil} + c^{De.} \dot{M}_{S,t}^{De.} \right) \cdot T_{length}$$
$$+ \sum_{l} \left(\sum_{c} c_{c,l}^{coal} \cdot B_{c,l,t}^{coal} + c_l^{scrap} \cdot B_{l,t}^{scrap} \right) + \sum_{p} c_p^{pell} \cdot B_{p,t}^{pell}$$
$$+ \sum_{c} c_{coal,c}^{inv} I_{c,t}^{coal} + \sum_{p} c_{pell,p}^{inv} I_{p,t}^{pell} + c_{scrap}^{inv} I_t^{scrap} + c_{coke}^{inv} I_t^{coke} \Bigg]$$

Subject to,

Equation Reference #

		5.1	5.2	5.3	5.4	5.5	5.6	5.7	5.8	5.9	
Cokemaking	→	5.10	5.11	5.12	5.13	5.14	5.15	5.16	5.17		
		5.18	5.19	5.20	5.21	5.22	5.23	5.24	5.25		
		5.26	5.27	5.28	5.29	5.30	5.31	5.32	5.33		
		5.34	5.35	5.36	5.37	5.38	5.39	5.40	5.41	5.42	5.43
		5.44	5.45	5.46	5.47	5.48	5.49	5.50	5.51	5.52	
Ironmaking	→	5.53	5.54	5.55	5.56	5.57	5.58	5.59	5.60	5.61	
		5.62	5.63	5.64	5.65	5.66	5.67	5.68	5.69	5.70	
		5.71	5.72	5.73	5.74	5.75	5.76	5.77	5.78	5.79	
		5.80	5.81	5.82	5.83	5.84	5.85	5.86			
Steelmaking	→	5.87	5.88	5.89	5.90	5.91	5.92				

where,

$$K^{multi} = \left[K_1^T, K_2^T, ..., K_{t_f}^T \right]^T$$

5.2 Planning vs. No Planning Case Study

Planning for a year of steel production is to be completed using the formulation in Problem 4a. A total of six time periods, each two months in length, are considered with 325 batches of each grade of steel produced per time period. It is assumed that this steel demand is known with certainty over the entire year of operation.

The cost of inventory per time period is equal to a 5% rate of return of the initial purchase price of the raw material. Ignoring compounding interest, the inventory costs can be calculated as follows:

$$c^{inv}_{coal,c} = \frac{\frac{5\%}{100\%}}{6 \text{ periods}} \cdot c^{coal}_{c,1}$$

$$c^{inv}_{pell,p} = \frac{\frac{5\%}{100\%}}{6 \text{ periods}} \cdot c^{pell}_{p}$$

$$c^{inv}_{scrap} = \frac{5\%}{6 \text{ periods}} \cdot c^{scrap}_{1}$$

For simplicity, only Coals E, F, and G are available for purchase whereas all three pellet types can still be bought, with no raw material uncertainty assumed to exist. For comparison purposes, two different planning approaches are considered:

- Forecast ($t_f = 6$) $\rightarrow$ Optimization is completed for the entire year
- Short sight ($t_f = 1$) $\rightarrow$ Optimization is recomputed six times, once for every 2 month time period

Each method uses the same initial conditions in terms of not just inventory levels, but also the compositional quality of the coke inventory. These are summarized in Table 5.1. Also listed are the minimum inventory levels required for each material throughout the year.

Table 5.1: Minimum inventory requirements and initial inventory and coke quality conditions.

Material	Initial Inv. (tonnes)	Minimum Inv. (tonnes)	Component	$d_{q,t=0}^{coke}$ %
Coal E	50,000	20,000	Al_2O_3	2.5%
Coal F	50,000	20,000	C	90%
Coal G	20,000	4,000	P_2O_5	0.023%
Coke	20,000	20,000	S	0.05%
Pellet A	50,000	10,000	SiO_2	5%
Pellet B	50,000	10,000	V.M.	0.5%
Pellet C	300,000	10,000		
Scrap	20,000	20,000		

Coal and scrap are available for purchase at two pricing tiers. The cost and break points of these discounts differ for each raw material and are listed in Table 5.2.

Table 5.2: Tiered purchasing breakpoints and cost for coal and scrap.

Material	Scaled Cost ($/tonne)		Discount Break	Max Purchase
	Tier 1	Tier2	Point (tonnes)	Amount (tonnes)
Coal E	4.87	4.53	100,000	200,000
Coal F	4.67	4.33	60,000	100,000
Coal G	4.33	4.00	10,000	50,000
Scrap	20	19.67	100,000	175,000

By inserting the above listed initial conditions and tiered pricing values into Problem 4a, optimization can be completed for the two methods of Forecast and Short sight. The results indicate that the Forecast solution yields a 0.39% improvement. The costs are summarized in Table 5.3.

Table 5.3: Summary of scaled costs for multi-period optimization methods.

Cost Type	Short sight ($/tonne)	Forecast ($/tonne)
Pellet Purchase	$13.67	$13.64
Coal Purchase	$2.54	$2.46
Scrap Purchase	$5.18	$5.17
Inventory	$0.06	$0.09
Coal Revenue	-$1.79	-$1.78
Operation	$0.87	$0.87
Total	$20.53	$20.45

The scaled costs for both methods are lower than those of the previous case studies in Chapter 4. In those examples, it was assumed that no raw material existed in inventory. In the multi-period approach, the plant was supplied with initial inventory thus lowering the overall cost of production. If the value of this inventory were included in the objective function of Problem 4a, the overall costs in Table 5.3 would be similar to those reported in Chapter 4.

Figure 5.2 illustrates the major differences between the solutions and is helpful in understanding the scaled costs listed in Table 5.3.

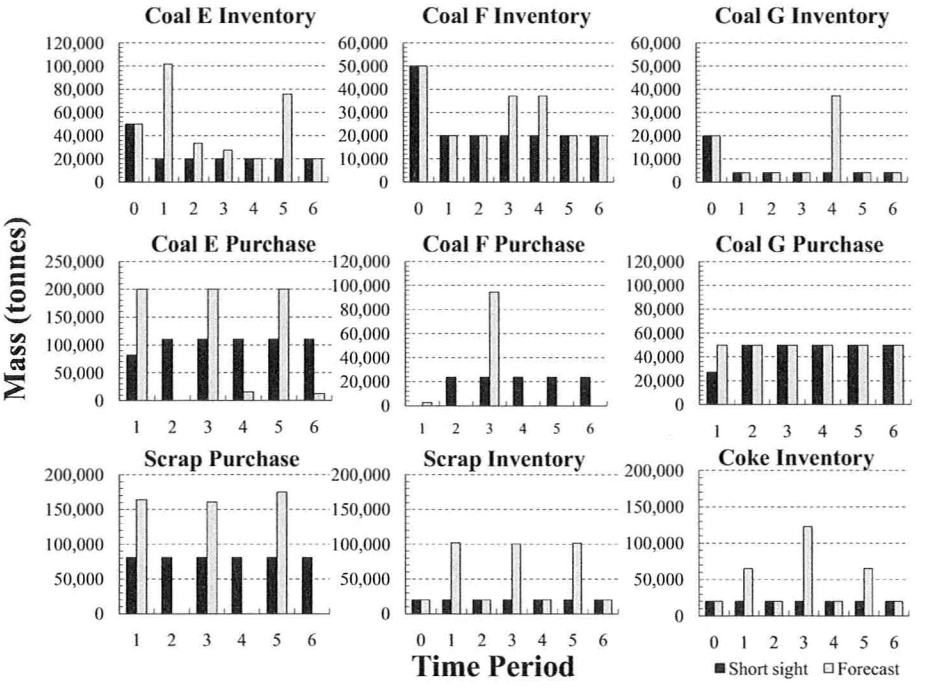

Figure 5.2: Inventory and purchasing result comparison for Problem 4a.

The Short sight method only optimizes with respect to the current demand. Since holding inventory is costly, the optimizer seeks to buy raw material to satisfy the current demand, and then drain the inventory to the minimum allowable levels. The steel demand for this study does not change from period to period, and therefore, the purchasing quantities remain nearly unchanged throughout the simulation as seen in Figure 5.2. In this method, the optimizer still takes advantage of the tiered pricing discounts, but only to a certain degree. Since the problem is defined for only the current time period, the optimizer does not realize that purchasing more material at a discount than currently needed could save cost.

The Forecast solution purchases scrap, as well as coals E and F, intermittently. The strategy in this method is to stock up on raw materials in order to take full advantage of the pricing discounts. Inventory levels rise as a result of bulk purchasing which is why the cost of inventory is larger for the Forecast method. Table 5.3 shows that incurring this higher cost is justified considering the savings gained from coal and scrap purchasing.

Pellets are not offered at tiered discounts, yet the Forecast method spent less money on this material meaning fewer pellets were purchased in total. Using fewer pellets in the blast furnace produces less hot metal in total which requires more scrap to be added in BOF steelmaking. The total purchasing masses of raw materials are given in Table 5.4 per tonne of steel produced.

Table 5.4: Comparison of raw material purchasing quantities for Forecast and Short sight methods.

	Short sight (tonnes/tonne steel)	Forecast (tonnes/tonne steel)
Pellets purchased	1.074	1.071
Coals purchased	0.550	0.548
Scrap purchased	0.259	0.261

Indeed the Forecast solution purchased more scrap and less pellets overall. Less coal was also purchased since the lower blast furnace production rate required less coke and thus less coals to be used. These values give insight to the trade-offs involved in the optimization problem. By looking into the future, the Forecast method decided that not only could it save by purchasing more material at discounted prices, but also by reducing the total mass of two of the raw materials purchased. Despite buying more scrap in total, the Forecast method still spent less money on that purchase, as seen in Table 5.3, since it took advantage of the tiered pricing.

The tiered pricing also caused the two methods to use different coal blends in the production of coke. These are shown in Table 5.5.

Table 5.5: Comparison of coal blending decisions for Forecast and Short sight methods.

Method	Coal Blend	Time Period					
		1	2	3	4	5	6
Forecast	Coal E	60.0%	57.7%	61.8%	57.7%	59.0%	57.7%
	Coal F	13.3%	0%	23.2%	0%	7.0%	0%
	Coal G	26.7%	42.3%	15.0%	42.3%	34.0%	42.3%
Short sight	Coal E	60.5%	60.0%	60.0%	60.0%	60.0%	60.0%
	Coal F	16.2%	12.9%	12.9%	12.9%	12.9%	12.9%
	Coal G	23.3%	27.1%	27.1%	27.1%	27.1%	27.1%

The blend solution for the single time period optimization of Problem 1c was comprised of 61.8% Coal E, 23.2% Coal F, and 15% Coal G. The resulting solutions in Table 5.5 show that tiered pricing changed the composition of the optimal coal blend. Compared to the blend used in Problem 1c, the percentage of G was increased from 15% to 27% in the Short sight method, meaning the optimizer saw great opportunity in the pricing discounts offered for Coal G.

The Forecast solution desired to further increase this percentage to 42.3% by purchasing and storing a greater amount of Coal G. To accomplish this, the optimizer purchased as much coal as possible every time period as well as making a large bulk purchase of Coal F in time period three. The optimizer used Coal F in time periods three and five in order to maximize the usage of Coal G across all six time periods.

5.3 End Point Inventory Condition

In both multi-period planning methods, Figure 5.2 shows that at the end of time period six, the final inventories of coke and raw materials are at their minimum constraint levels. This is because the optimizer assumes that there is no production after time period six and does not require any raw material.

This problem can be remedied by assigning value to the raw material in storage at the end of the multi-period horizon. The objective function can be changed by including the working capital of each raw material. Working capital is defined as the difference between current assets and liabilities. The liability cost with holding inventory has already been defined by the parameter c^{inv}. Therefore, by assigning an asset value to the raw materials, the working capital revenue for coal (w_c^{coal}) and scrap (w^{scrap}) can be calculated. The changed objective function, incorporating working capital, is denoted as Problem 4b.

PROBLEM 4b

$$\min_{K_t} \sum_{t}^{t_f} \Bigg[\sum_{g} \left(c^{O_2} V^{BOF}_{O_2,g,t} + c^{dol} M^{BOF}_{dol,g,t} + c^{lime} M^{BOF}_{lime,g,t} \right) D_{BOF,g} - p^{By-prod.} A^{coke}_{t} M_{VM,removed,t}$$
$$+ \left(c^{lime} \dot{m}^{lime}_{t} + c^{dol} \dot{m}^{dol}_{t} + c^{air} \dot{m}^{air}_{t} + c^{steam} \dot{m}^{steam}_{t} + c^{oil} \dot{m}^{oil}_{t} + c^{De.} \dot{m}^{De.}_{S,t} \right) \cdot T_{length}$$
$$+ \sum_{l} \left(\sum_{c} c^{coal}_{c,l} B^{coal}_{c,l,t} + c^{scrap}_{l} B^{scrap}_{l,t} \right) + \sum_{p} c^{pell}_{p} B^{pell}_{p} + \sum_{p} c^{inv}_{pell,p} I^{pell}_{p,t} + c^{inv}_{coke} I^{coke}_{t} \Bigg]$$
$$+ \sum_{t=1}^{5} \left(\sum_{c} c^{inv}_{coal,c} I^{coal}_{c,t} + c^{inv}_{scrap} I^{scrap}_{t} \right) - \underbrace{\left(\sum_{c} w^{coal}_{c} I^{coal}_{c,t=6} + w^{scrap} I^{scrap}_{t=6} \right)}_{\text{Working capital revenue}}$$

Subject to,

Equation Reference #

		5.1	5.2	5.3	5.4	5.5	5.6	5.7	5.8	5.9	
		5.10	5.11	5.12	5.13	5.14	5.15	5.16	5.17		
Cokemaking	→	5.18	5.19	5.20	5.21	5.22	5.23	5.24	5.25		
		5.26	5.27	5.28	5.29	5.30	5.31	5.32	5.33		
		5.34	5.35	5.36	5.37	5.38	5.39	5.40	5.41	5.42	5.43
		5.44	5.45	5.46	5.47	5.48	5.49	5.50	5.51	5.52	
Ironmaking	→	5.53	5.54	5.55	5.56	5.57	5.58	5.59	5.60	5.61	
		5.62	5.63	5.64	5.65	5.66	5.67	5.68	5.69	5.70	
		5.71	5.72	5.73	5.74	5.75	5.76	5.77	5.78	5.79	
		5.80	5.81	5.82	5.83	5.84	5.85	5.86			
Steelmaking	→	5.87	5.88	5.89	5.90	5.91	5.92				

where,

$$K^{multi} = \left[K^{T}_{1}, K^{T}_{2}, ..., K^{T}_{t_f} \right]^{T}$$

This problem was solved for an initial set of working capital values listed in Table 5.6.

Table 5.6: Initial working capital values for raw materials offered with tiered pricing.

Raw Material	Scaled Working Capital w ($/tonne)
Coal E	4.60
Coal F	4.43
Coal G	4.07
Scrap	19.73

Inputting these working capital values into Problem 4b resulted in no change in the solution with respect to purchasing and operation over the entire time horizon. This means that the credit accrued by having more endpoint inventory than minimally required was sub-optimal. Since the purchasing of raw materials are dependent on one another, the working capital value for each raw material was moved independently from the initial value in Table 5.6. The results are illustrated in Figure 5.3 and show the impact of the working capital on the final inventory levels.

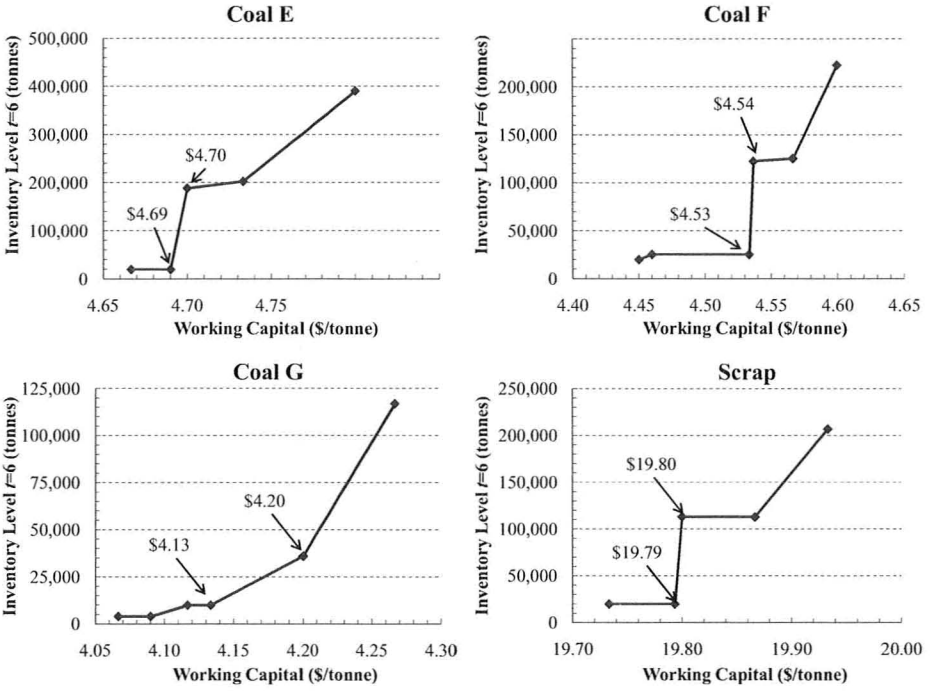

Figure 5.3: Resulting final inventory levels for varying working capital values.

Coals E, F, and scrap metal have break points where the endpoint inventory level increases dramatically. In all cases, this switch occurs between a scaled cost change of \$0.01 per tonne where the optimizer decides to make a bulk purchase in the last time period. While these final purchases inject the plant with a large amount of coal or scrap, they have no impact on plant operation in time periods 1 to 6. As the working capital was increased further, bulk purchases were made in earlier time periods and simply stored in order for the optimizer to incur the final credit in period 6.

Coal G does not experience this trend. This is because, as shown in Figure 5.2, maximum purchasing is already being completed every time period. Thus, no bulk purchase can be made at the end of the time horizon. The rise in endpoint inventory for Coal G, seen in Figure 5.3, occurs as a result of a bulk Coal F purchase. The optimizer decides that since Coal G has a high working capital, it should purchase more Coal F and reduce the amount of Coal G used in blending; thus more remains in inventory at time 6.

The working capital value affects more than just purchasing and operation in the final time periods. If it is increased high enough, the purchasing decision in the first time period could be changed. This is shown in Figure 5.4 where the purchasing quantity of Coal F, in the first time period, is plotted for various working capital values of Coal F. Also included is the final inventory level for this coal only.

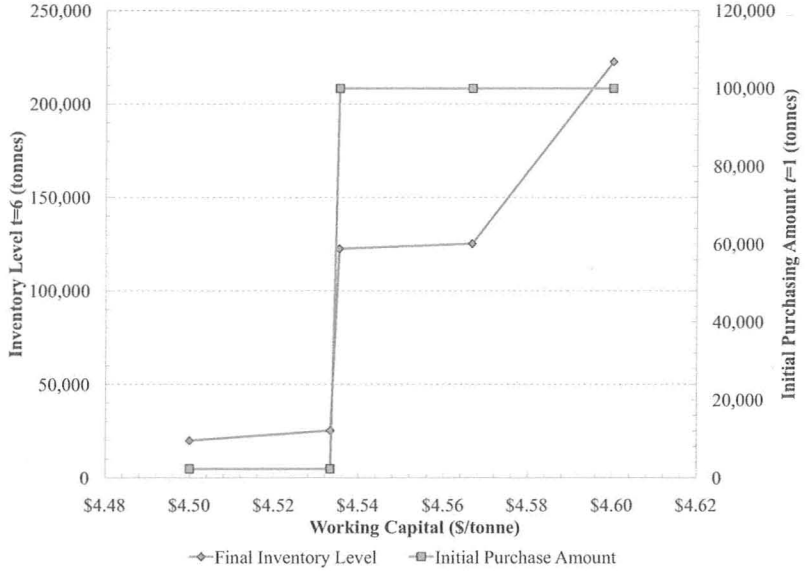

Figure 5.4: Initial purchasing and final inventory level results for varying Coal F working capital values.

The final inventory level of Coal F, for the first working capital data point, is at the minimum level of 20,000 tonnes. The solution purchases zero tonnes of Coal F during the first time period. As the working capital is increased, the final inventory level changes from 20,000 to approximately 25,000 tonnes, while still not purchasing any Coal F in time period one. A further increase in the working capital results in the final inventory level increasing from 25,000 tonnes to 125,000 tonnes. At the same time, the optimizer decides to make a bulk purchase of 100,000 tonnes during time period one. The importance of this trend is that the horizon length is not long enough in order for the decisions of the first time period to be independent of the endpoint inventory conditions. Therefore, the working capital values used in optimization must be selected intelligently in order for the solution to be practical.

5.4 Rolling Horizon Case Study

In the previous section it was shown that the endpoint inventory condition has an effect on the optimization decisions in the first time period. If this is true, the decisions in all subsequent time periods must also be impacted. If this approach were undertaken for the steel plant, decision makers could not simply optimize at the beginning of the year and implement the solution throughout the year. In other words, it is necessary to re-optimize every time period.

At the beginning of the first time period, the current inventory levels must be noted and a demand prediction made. This would be obtained from customer order forecasting models. Demand information would then be inserted into the optimization formulation and solved. The purchasing and operation decisions would be implemented on the plant for the first time period only. When the second time period is reached, the inventory levels would be measured and the horizon rolled one step forward. A new prediction is then made and re-optimization completed. These steps are illustrated below.

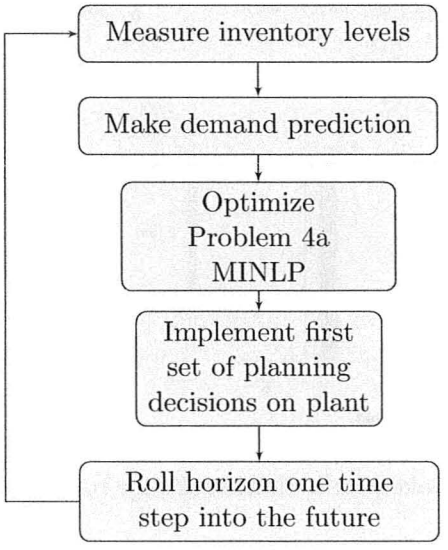

This approach is similar to what would be done in real plant operation as the rolling horizon reacts to changes in the actual market conditions. For example, inaccuracies in the demand forecast would require alterations to purchasing quantities in later time periods. Also,

disturbances in raw material transportation could lead to shortages in delivery and thus reduce the amount of available inventory.

The rolling horizon approach is implemented for Problem 4a where the demand forecast is 325 batches for all three steel grades each time period. The actual demand realized is also 325 batches per steel grade, and therefore, there is no error with respect to the demand prediction. Additionally, there is no uncertainty considered in plant operation, and thus, no model error occurs when the first set of optimization decisions are implemented. No working capital values are used in this case study.

Figure 5.5 illustrates the difference between the solution for the first time period only, and the decisions in each time period for the rolling horizon approach.

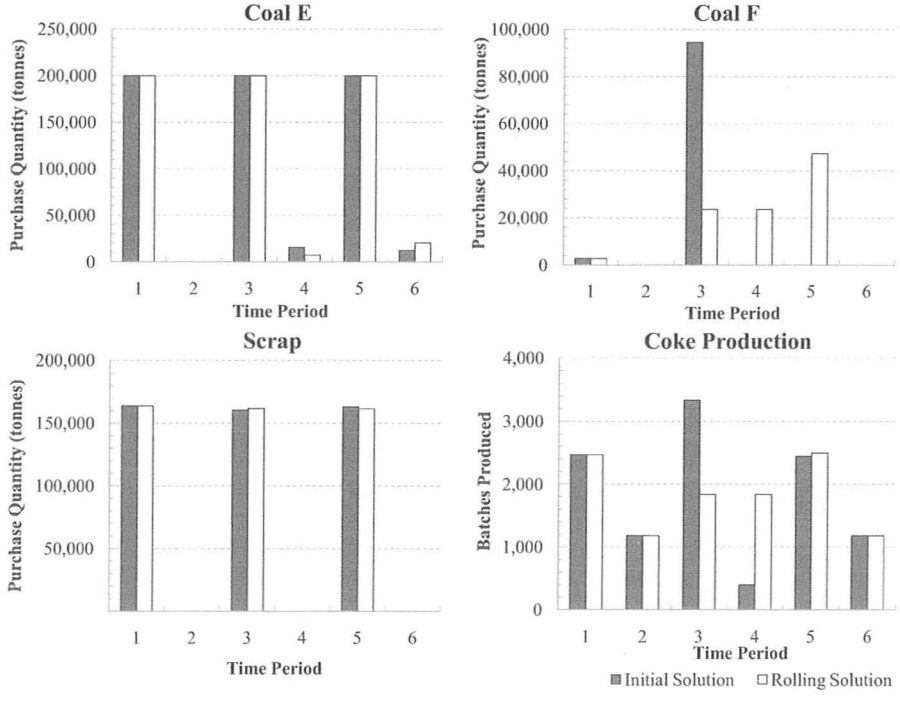

Figure 5.5: Purchasing and coke production results for rolling horizon approach in Problem 4a.

The first time period solution makes decisions for all six time periods; however, only the first set of decisions are implemented. When the horizon rolled forward and implemented

its next decision, Figure 5.5 shows it was identical to that of time period two in the initial solution. In other words, nothing changed when the horizon rolled one step ahead. In time period three, the rolling horizon solution begins to diverge, specifically with a decrease of Coal F purchased and subsequent coke production. Instead of making a large bulk purchase of Coal F in time period three, and slowly processing the material from this large purchase, the optimizer purchased smaller amounts in periods three to five.

This solution divergence illustrates that the plant planners cannot optimize at the beginning of the year and simply implement that solution, even in the presence of no uncertainty. In this case study, the initial solution was only valid for two time periods and re-optimization was completed at the beginning of the third period in order to implement an improved set of decisions.

The presence of uncertain plant conditions suggests that re-optimization should be done every time period in order for the plant to react to changes that occur spontaneously during production. An example of this is that of demand fluctuation. The previous studies considered the demand forecast and actual demand to be equivalent; however, in reality this is rarely true.

It is considered that in the second time period a demand of 370 batches of each steel grade occurs instead of the forecast of 325 batches. This leaves a 45 batch backorder that must then be filled during the next time period. The difference between the forecast and actual demand is illustrated in Figure 5.6.

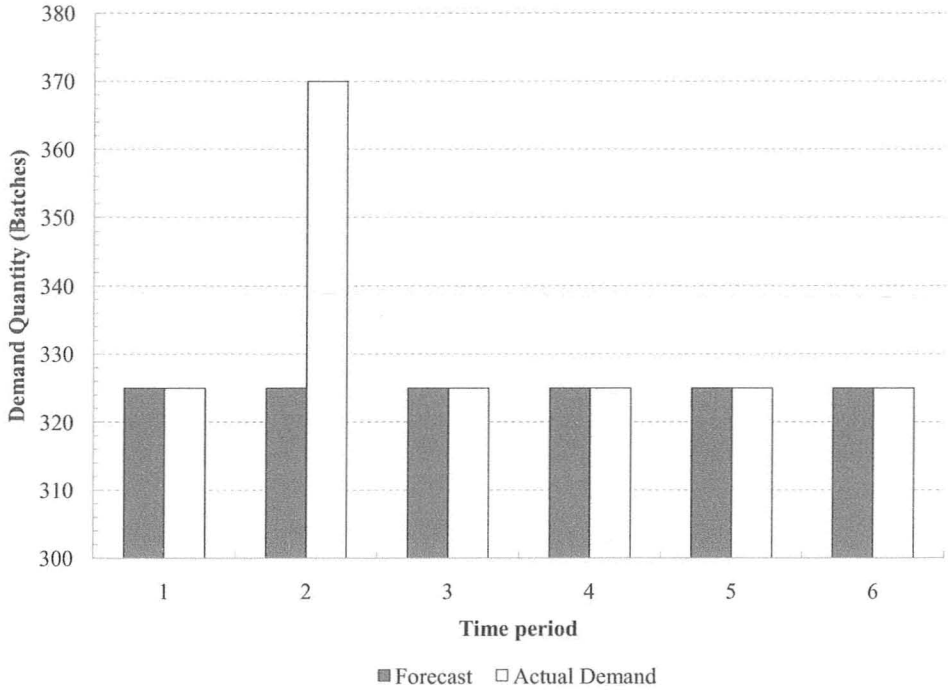

Figure 5.6: Forecast and demand profiles for all three grades of steel.

The rolling horizon approach was implemented for this demand profile in order to determine how the plant should operate to respond to this unexpected demand increase. Figure 5.7 shows the rolling solution in comparison to that for the first time period solution only.

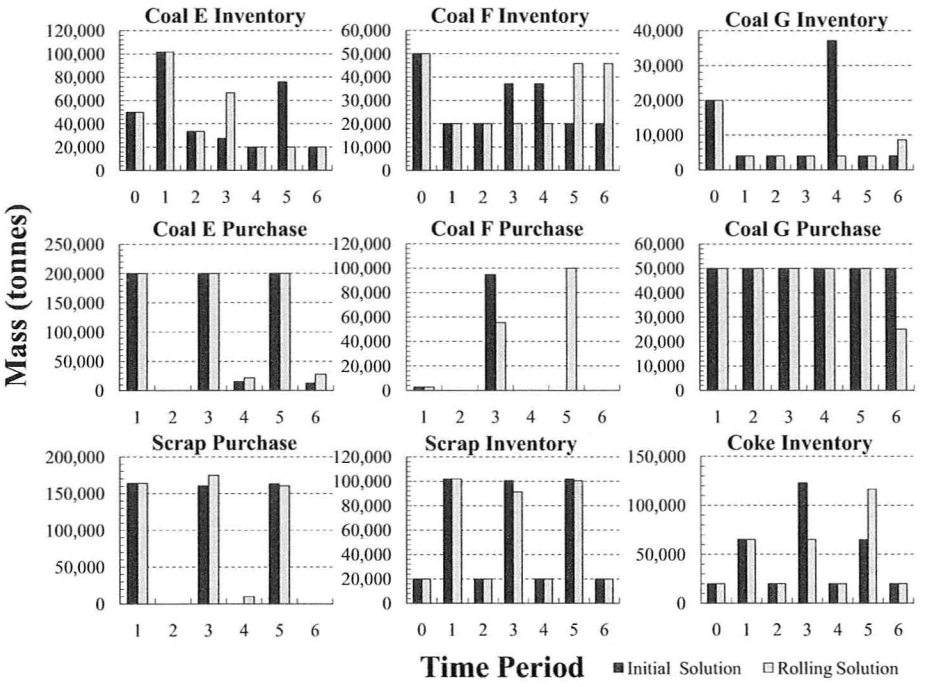

Figure 5.7: Purchasing and inventory solution for rolling horizon demand discrepancy case study.

Since the production of steel was increased to fill the back orders in period three, more scrap metal was purchased. Additionally, the scrap inventory level at the end of the same time period was lower than originally intended meaning a great deal of scrap was consumed in production. The initial solution in time period one desired to make large bulk purchases of coal in time period three and subsequently increase the coke inventory. As the back orders were realized in time period three, this plan was abandoned since coke was required to be consumed immediately. The coke inventory was increased at time period five as the maximum amount of all three coals was purchased. However, only coals E and G were consumed to their respective lower inventory limits with a little over 45,000 tonnes of Coal F remaining in inventory at the end of time five. In the next and final time period, Coal F was not used in the coal blend, thus the inventory level was unchanged.

This may seem illogical as the large Coal F inventory pile sits for two time periods at a cost to the objective function. However, the rolling horizon optimizer, in time period five,

decided make coke using Coal F. Additionally, it looked ahead into time period seven and decided to include Coal F in coke production as well. Therefore, the optimizer decided it was optimal to make a large bulk purchase in time period five, and let the excess inventory sit idle during time period six.

5.5 Chapter Summary

A formulation for multi-period planning was provided in this chapter. This involved the integration of inventory models with the steelmaking model developed in Chapter 3. The method of planning into the future was motivated by the introduction of a new purchasing method offered by coal and scrap vendors. These two raw material types were offered in two different pricing tiers in order to encourage bulk purchasing.

The multi-period formulation was applied to a one year steel production example where demand information was provided on a bimonthly basis. Optimization results were compared to the case where no forecasting is done, and instead optimization is recomputed every two months. The results show that the forecasting method was 0.39% less costly. The optimizer achieved this result by making large bulk purchases of scrap. This cheap scrap allowed for less hot metal to be used in BOF steelmaking which resulted in fewer pellets being purchased for blast furnace use. Since less hot metal was produced, less coke was used, and thus, less coal was purchased.

Due to the cost of inventory in the multi-period problem, the solution resulted in end point inventory levels being at their minimum allowable levels. This is because the optimizer only considers steel demand over the time periods included in the formulation. In reality, this solution is impractical because production continues past the time horizon that is optimized. To remedy this issue, the inclusion of working capital cost was added to the objective function. Credit was given with respect to coal and scrap inventory present at the end of the planning horizon. It was discovered that the working capital values can influence not only the final inventory levels, but also purchasing decisions in the first discrete time

period. The results show the importance of accurately valuing working capital in actual production.

Finally, the presence of plant uncertainty necessitates re-optimization of the original planning solution. As time progresses, and plant conditions change, the multi-period optimization should be updated. This was tested for two cases of demand uncertainty. The first case involves no discrepancy between what is forecast in time period one, and the actual demand encountered throughout the year. The first time period and rolling horizon solutions diverge during time period three. This means that even when the steel demand forecast is perfect, the solution in time period one is only valid for two time periods.

A final case study was completed where the demand forecast underestimated the actual demand by 45 batches for all three steel types in one time period. The optimizer was then forced to fill the outstanding demand in the subsequent time period. The rolling horizon approach optimally manipulated the original solution by rearranging bulk purchasing and storage of several raw materials. Additionally, coke production was altered in order to increase inventory in the time period in which the back orders were filled.

The results indicate that re-optimization is important when planning over an extended time horizon.

Chapter 6

Conclusions and Recommendations

6.1 Conclusions

1. **Modeling of Primary Steelmaking.** An integrated model of primary steelmaking was presented that connected the three areas of cokemaking, ironmaking, and steelmaking. Cokemaking involved writing component mass balances for the transformation of coals to coke. Additionally, models were built in order to predict the final coke stability, CSR, and resulting oven wall pressure, from the particular coal types used. Multivariate PLS models were built in each case using an experimental data set of trial runs completed on a pilot plant coke oven. Ironmaking modeling was completed using a combination of rigorous component mass balances, and multivariate empirical models to express energy relationships. Steelmaking involved building empirical mass and energy models in order to replicate the Basic Oxygen Furnace operation. Connecting the models from each sub-area results in a single primary steelmaking model which can be used to investigate such matters as operational and raw material changes on the resulting process.

2. **Optimization Under Raw Material Uncertainty.** The inherent uncertainty in raw material quality can have a significant impact on plant operation. If ignored, important constraint limits may be exceeded which can subsequently lead to increased

costs in order to correct for the violations. The order in which raw materials are purchased, delivered, and then processed, lends itself to be formulated as a two-stage stochastic programming problem. It was determined that the number of scenarios used to represent uncertainty could be between 50 and 125 and still provide similar purchasing decisions. In comparison to the case where uncertainty was ignored, the two-stage stochastic solution purchased slightly more expensive raw materials that, when used, violated process constraints with far less frequency. When more importance was placed on remaining within the constraints, the two-stage solution was both less costly and less likely to exceed the process limits. The results prove that in steel manufacturing, it is cost beneficial to incorporate uncertainty into raw material purchasing decisions.

3. **Centralized Optimization.** Nominal practice is such that the units involved in steel production make decisions in a decentralized manner. Raw material purchasing is done using rules of thumbs and assumptions about how neighbouring units operate. Centralized optimization over the entire integrated model includes the most information in a simultaneous solution. Comparing the two approaches under no raw material or plant uncertainty, shows that the centralized optimizer outperforms the decentralized solution. When uncertainty in the assumptions is introduced, the gap widens as the centralized optimizer is far less costly. These results indicate the importance of using a single decision maker across the plant when purchasing and processing raw material.

4. **Multi-period Planning.** A formulation was presented to extended the single period optimization problem to multiple time periods. This was motivated by the fact that raw materials are often sold by vendors at different pricing tiers which encourage bulk purchasing. Therefore, demand over several time periods should be considered in order to take advantage of tiered pricing. The mass breakpoints of the pricing tiers differ for each raw material, in addition to the discounts at each tier. With numerous raw materials involved, the purchasing decisions become increasingly unclear and require an optimizer to find the minimum overall cost. The results show that making bulk

purchases intermittently, and storing the material in inventory is optimal. This strategy can only be determined if multiple periods are considered in a single optimization problem. In comparison to completing several single period optimization problems successively, the solution did not take full advantage of the tiered pricing discounts and therefore was outperformed by the multi-period optimizer. It is also concluded that a single multi-period optimization does not provide the optimal solution for all subsequent time intervals. As plant conditions change, updating of initial inventories and re-optimization should be carried out in order to react to new conditions. A rolling horizon optimization approach is therefore outlined to implement this strategy.

6.2 Recommendations for Further Work

Areas in which future research effort should be directed are as follows:

1. **Refinement of Models.** The quality of the three cokemaking PLS models is somewhat poor with respect to predictability. New experiments should be conducted on the coke oven to gather a larger and more comprehensive data set. It would also be advantageous to determine the error involved in measuring stability, CSR, and wall pressure. If the PLS models can be developed such that their respective Root Mean Square Error terms are smaller than the measurement error, then it can be concluded the predictions are at least within the noise of measurement. Additionally, the blast furnace and BOF models should be tuned to real plant data in order to validate that the results determined by the optimizer could be realized in practice. Work could also be dedicated to including the Electric Arc Furnace in the integrated model. Scrap purchasing would be far more complex in this case as quality would have to be considered in order to reserve the lower impurity scraps for EAF use.

2. **Optimization Under Uncertainty.** A great deal of opportunity exists for future work dealing with raw material uncertainty. It is currently not known with statistical proof as to the extent of variation within the raw materials, nor the covariance among

components. This could be solved by measuring the composition of delivered materials on a continuous basis. Not only would this provide the uncertainty within raw material types, but also give indication as to what suppliers offer a more consistent product. Also, a study should be conducted to determine the exact cost impact of constraint violations on the resulting process. If these cost values are added to the objective function, the trade-offs between violations and other costs can be evaluated on a level playing field.

3. **Multi-period Planning.** The formulation developed should be extended to include various unique scenarios that are encountered by long term planning personnel. For example, iron ore pellet delivery is not possible during the winter months as the seaways are frozen. Plans must therefore be developed to stock up inventory levels during these periods. Another example is that of plant shut down. If long term forecasting indicates a decline in steel demand, the operation of multiple blast furnaces may not be necessary. Shut down is a very important decision as, when completed, it usually lasts for months. The multi-period formulation should be used to determine when it is optimal to shut down furnaces, or simply reduce throughput of the on-line furnaces.

List of References

[1] G. Anandalingam. Process Modelling Under Uncertainty: Simulation Analysis of Indian Steel. *Journal of Operational Research Society*, 38(2):115–123, 1987.

[2] G. Baffi, E.B. Martin, and A.J. Morris. Non-linear Projection to Latent Structures Revisited: the quadratic PLS algorithm. *CCHE*, 23(12):395–441, 1999.

[3] R. Bandyopadhyay. Open-Hearth and Basic-Oxygen Furnaces: An Allocation Model for Production Planning. *IEEE Transactions on Systems Science and Cybernetics*, 5(2):115–124, 1969.

[4] A. Bemporad and M. Morari. Control of systems integrating logic, dynamics and constraints. *Automatica*, 35(3):407–427, 1999.

[5] K.P. Bernatzki, M.R. Bussieck, and T. Lindner. Optimal Scrap Combination for Steel Production. *Operation Research Spectrum*, 20:251–258, 1998.

[6] H. Bertling. Coal and Coke for Blast Furnaces. *Iron and Steel Institute of Japan International*, 39(7):617–624, 1999.

[7] K. Boylan. Personal communication, March 2010.

[8] C. Braekman-Danheux, A. Fontana, P. Laurent, and P. Lolivier. Catalytic hydrogenation of polycyclic aromatic hydrocarbons with coke oven gas. *Fuel*, 75:579–584, 1996.

[9] M. Chen and W. Wang. A Linear Programming Model for Integrated Steel Production and Distribution Planning. *Internation Journal of Operations & Production Management*, 17(6):592–610, 1997.

[10] A. Davenport, J. Kalagnanam, C. Reddy, S. Siegel, and J. Hou. An Application of Constraint Programming to Generating Detailed Operations Schedules for Steel Manufacturing. In *Proceedings of the 13th International Conference on Principles and Practice of Constraint Programming*, 2007.

[11] M.A. Diez, R. Alvarez, and C. Barriocanal. Coal for Metallurgical Coke Production: Predictions of Coke Quality and Future Requirements for Cokemaking. *International Journal of Coal Geology*, 50:389–412, 2002.

[12] G. Dutta and R. Fourer. A Survey of Mathematical Programming Applications in Integrated Steel Plants. *Manufacturing & Service Operations Management*, 3(4):387–400, 2001.

[13] L. Eriksson, E. Johansson, N. Kettaneh-Wold, and S. Wold. *Introduction to Multi- and Megavariate Data Analysis using Projection Methods.* Umetrics, 1999.

[14] M.E. Ertem and S. Gurgen. Energy Balance Analysis for Erdemire Blast Furnace Number One. *Applied Thermal Engineering*, 26:1139–1148, 2006.

[15] T. Fabian. A Linear Programming Model of Integrated Iron and Steel Production. *Management Science*, 4(4):415–449, 1958.

[16] T. Fabian. Blast Furnace Production Planning - A Linear Programming Example. *Management Science*, 14(2):B1–B27, 1967.

[17] Z. Gao and L. Tang. A Multi-objective Model for Purchasing of Bulk Raw Materials of a Large-scale Integrated Steel Plant. *International Journal of Production Economics*, 83:325–334, 2003.

[18] H. Gou. Personal communication, November 2009.

[19] I. Grossmann. Enterprise-wide Optimization: A New Frontier in Process Systems Engineering. *AIChE Journal*, 51(7):1846–1857, 2005.

[20] I. Harjunkoski and I. Grossmann. A Decomposition Approach for the Scheduling of a Steel Plant Production. *Computers and Chemical Engineering*, 25:1647–1660, 2001.

[21] S. Heipcke. *Applications of optimization with Xpress-MP.* Dash Optimization Ltd., Warwickshire, United Kingdom, 2003.

[22] A. Jackson. *Steelmaking for Steelmakers.* The United Steel Companies LTD, Sheffield, England, 1960.

[23] A. Jindal, S. Pujari, P. Sandilya, and S. Ganguly. A reduced order thermo-chemical model for blast furnace for real time simulation. *Computers and Chemical Engineering*, 31:1484–1495, 2007.

[24] A. Johansson, A. Medvedev, and D. Widlund. Model-Based Estimation of Decarburization Rate and Carbon Content in the Basic Oxygen Steelmaking Process. In *Industry Applications Conference*, volume 4, pages 2578–2583, 2000.

[25] T. Kono. Economic and Management Implications of Technological Advances in the World Steel Industry. *Technological Forecasting and Social Change*, 16:33–45, 1980.

[26] J.R. Lawrence and A.D.J. Flowerdew. Economic Models for Production Planning. *Operational Research Society*, 14(1):11–29, 1963.

[27] R. D.M. MacRosty and C. L.E. Swartz. Dynamic Optimization of Electric Arc Furnace Operation. *AIChE Journal*, 53:640–653, 2007.

[28] R.D.M. MacRosty and C.L.E. Swartz. Dynamic Modeling of an Industrial Electric Arc Furnace. *Industrial & Engineering Chemistry Research*, 44:8067–8083, 2005.

[29] A. McClure. Personal communication, January 2010.

[30] E. Mestan, M. Turkay, and Y. Arkun. Optimization of Operations in Supply Chain Systems Using Hybrid Systems Approach and Model Predictive Control. *Industrial and Engineering Chemistry Research*, 45(19):6493–6503, 2006.

[31] I. Miletic, R. Garbaty, S. Waterfall, and M. Mathewson. Steel Scrap Purchasing Optimization and Supply Management. In *AIChE Annual Meeting Conference*, San Francisco, 2006.

[32] D.C. Montgomery and G.C. Runger. *Applied Statistics and Probability for Engineers.* Wiley, 2002.

[33] K. Muteki. Mixture Product Design Using Latent Variable Methods. Master's thesis, McMaster University, 2006.

[34] J.G. Peacey and W.G. Davenport. *The Iron Blast Furnace Theory and Practice.* Pergamon Press, 1979.

[35] D.E. Pearson. Influence of Geology on CSR. *Advances in Western Canadian Coal Geoscience*, 103:174–183, 1989.

[36] E. Perea-Lopez, B. E. Ydstie, and I. E. Grossmann. A model predictive control strategy for supply chain optimization. *Computers and Chemical Engineering*, 27:1201–1218, 2003.

[37] ProSensus MultiVariate. *Analysis Methods and Techniques*, 10.02 edition, 2010.

[38] A. Rong and R. Lahdelma. Fuzzy chance constrained linear programming model for optimizing the scrap charge in steel production. *European Journal of Operational Research*, 186:953–964, 2008.

[39] L. Ronholm. Personal communication, November 2009.

[40] E. Sandberg, B. Lennox, and P. Undvall. Scrap Management by Statistical Evaluation of EAF Process Data. *Control Engineering Practice*, 15:1063–1075, 2007.

[41] S. Sen and J.L. Higle. An Introductory Tutorial on Stochastic Linear Programming Models. *Interfaces*, 29:33–61, 1999.

[42] J. Shih and H.C. Frey. Coal Blending Optimization Under Uncertainty. *European Journal of Operational Research*, 83:452–465, 1995.

[43] L. Tang, J. Liu, A. Rong, and Z. Yang. A Review of Planning and Scheduling Systems and Methods for Integrated Steel Production. *European Journal of Operational Research*, 133:1–20, 2001.

[44] T.W. Todoschuk, J.T. Price, and J.F. Gransden. Simulation of Industrial Coking - Phase 2. In *ISS-AIME Ironmaking Conference Proceedings*, 1997.

[45] W.L. Winston. *Operations Research Applications and Algorithms.* Thomson Learning, fourth edition edition, 2004.

[46] S. Wold, M. Sjostroma, and L. Eriksson. PLS-regression: a basic tool of chemometrics. *Chemometrics and Intelligent Laboratory Systems*, 58:109–130, 2001.

[47] F. You, J.M. Wassick, and I.E. Grossmann. Risk Management for a Global Supply Chain Planning Under Uncertainty: Models and Algorithms. *AIChE Journal*, 55(4):931–946, 2009.

[48] S. Zanoni and L. Zavanella. Model and Analysis of Integrated Production-inventory System: The Case of Steel Production. *International Journal of Production Economics*, 93-94:197–205, 2005.

[49] Q. Zhang, X. Wu, A. Feng, and M. Shi. Prediction of Coke Quality at Baosteel. *Fuel Processing Technology*, 86:1–11, 2004.

[50] Y. Zhang, D. Monder, and J.F. Forbes. Real-time optimization under parametric uncertainty: a probability constrained approach. *Computers and Chemical Engineering*, 12:373–389, 2002.

Appendix A

Raw Material Compositions and Variable Definitions

Table A.1: Coal cost and composition parameters.

	Coal A	Coal B	Coal C	Coal D	Coal E	Coal F	Coal G
C (%)	69.18	63.83	60.87	70.07	55.61	62.64	72.91
V.M. (%)	17.06	19.43	27.02	17.94	31.73	21.52	15.25
H_2O(%)	7.5	7.5	6.26	6.16	7.5	7.5	6.23
P_2O_5 (%)	0.028	0.112	0.019	0.017	0.030	0.028	0.023
Ash (%)	6.26	8.78	5.86	5.83	5.16	8.34	5.62
S (%)	0.051	0.026	0.038	0.048	0.046	0.073	0.048
Al_2O_3 (%)	1.84	2.40	1.75	1.65	1.51	2.25	1.52
SiO_2 (%)	3.31	5.25	3.37	3.07	2.89	4.64	2.95
FSI	8.5	7.0	6.5	9.0	7.9	9.0	8.0
Ro	1.59	1.35	1.15	1.54	0.98	1.28	1.67
Inerts (%)	23.8	28.4	35.6	18.1	24.8	23.5	24.0
Scaled Cost \$/tonne	5	6	5	5	4.9	4.7	4.3

Table A.2: Pellet cost and composition parameters.

Component	Pellet A	Pellet B	Pellet C
Fe (%)	63.3	62.4	65.3
P (%)	0.015	0.010	0.015
S (%)	0.011	0.010	0.009
Al_2O_3 (%)	0.5	0.4	0.05
H_2O (%)	3.5	3.5	3.5
CaO (%)	3.68	3.0	0.838
MgO (%)	1.3	1.15	2.03
SiO_2 (%)	3.75	3.25	5.327
Mn (%)	2.02	1.5	0.12
Scaled Cost $/tonne	13	13	12.7

Table A.3: Dependent variable listing and definition.

Dependent Variable	**Variable Definition**	**Units**
A^{coke}	Total number of coke batches made during the optimization period	None
$\dot{M}_S^{De.}$	Mass rate of sulphur removed by the Desulphurization Facility	tonne/hr
$\dot{M}^{slag}$	Total mass rate of slag exiting the blast furnace	tonne/hr
$\dot{m}_w^{slag}$	Mass rate of slag component w exiting blast furnace	tonne/hr
$\dot{M}^{hot}$	Mass rate of exiting hot metal from blast furnace	tonne/hr
$\dot{m}_i^{hot}$	Mass rate of component i in blast furnace exit hot metal	tonne/hr
M_{out}^{coke}	Mass of coke obtained from coke oven batch after quenching	tonne
M_{out}^{dry}	Mass of coke obtained from coke oven batch directly after discharge (pre-quench)	tonne
$M_{H_2O,removed}$	Mass water removed from coals during coke production	tonne
$M_{q,removed}$	Mass component q removed from coals during coke production	tonne
$M_{scrap,g}^{BOF}$	Mass of hot metal added to the BOF in the production of steel grade type g	tonne/batch
$M_{hot_g}^{BOF}$	Mass of hot metal added to the BOF in the production of steel grade type g	tonne/batch
$M_{dol,g}^{BOF}$	Mass of dolomite added to the BOF in the production of steel grade type g	tonne/batch
$M_{lime,g}^{BOF}$	Mass of lime added to the BOF in the production of steel grade type g	tonne/batch

Table A.4: Dependent variable listing and definitions continued.

Dependent Variable	**Variable Definition**	**Units**
$u_h^{blend}(j)$	Value of property j in coal blend input to model h	Various
w^{quench}	Mass of water added during quenching after coke has been pushed from coke oven	tonne
x_q^{blend}	Mass fraction of component q in coal blend charged to coke oven	None
$x_{c,q}^{coal}$	Mass fraction of component q in coal c	None
x_i^{hot}	Mass fraction of component i in hot metal exiting blast furnace	None
x_q^{coke}	Mass fraction of component q in the product coke	None
$x_{i,g}^{steel}$	Mass fraction of component i in steel grade g at the end of the BOF batch	None
y^{CSR}	Coke Strength after Reaction of product coke	%
$y^{Stab.}$	Stability of product coke	%
$y^{W.P.}$	Resulting oven wall pressure exerted by coals	lb/in^2
$V_{O_2,g}^{BOF}$	Volume of oxygen used in the BOF batch production of steel grade type g	Km^3
$V_{off\ gas,g}^{BOF}$	Volume of gas exiting the BOF in the production of steel grade g	Km^3
$V_{off\ gas}$	Volume of off gas from coke batch	Km^3
$\rho_{off\ gas}$	Density of coke oven off gas	$tonne/Km^3$
$\dot{V}_{top\ gas}$	Volumetric rate of top gas exiting blast furnace	Km^3/hr
$\rho_{off\ gas,g}^{BOF}$	Density of off gas exiting the BOF in the production of steel grade g	$tonne/Km^3$
$\rho_{top\ gas}$	Density of blast furnace top gas	$tonne/Km^3$

Table A.5: Independent decision variable and definition listing.

Independent Variable	**Variable Definition**	**Units**
δ_c^{use}	Binary variable deciding if coal c is to be used in the coal blend	None
δ_c^{buy}	Binary variable deciding if coal c is to be purchased	None
B_c^{coal}	Mass of coal c purchased	tonne
B_p^{pell}	Mass of pellet p purchased	tonne
B^{scrap}	Mass of scrap purchased	tonne
m_c^{coal}	Mass of coal type c added to the coke oven	tonne/hr
$\dot{M}^{coke}$	Mass addition rate of coke to blast furnace	tonne/hr
$\dot{M}^{dol}$	dolomite addition rate to blast furnace	tonne/hr
$\dot{M}^{lime}$	limestone addition rate to blast furnace	tonne/hr
$\dot{M}^{oil}$	oil addition rate to blast furnace	tonne/hr
$\dot{m}_p^{pell}$	mass addition rate of pellet p	tonne/hr
$\dot{M}^{steam}$	steam addition rate to blast furnace	tonne/hr
$\dot{V}^{air}$	Volumetric flow of blast air to blast furnace	Km^3/hr

Table A.6: Constant parameter definition listing.

Parameter	**Parameter Definition**	**Units**
α_{Mn}	MnO to Mn conversion factor	tonne Mn/tonne MnO
α_P	P_2O_5 to P conversion factor	tonne P/tonne P_2O_5
b^{low}	Lower slag basicity limit in blast furnace	None
b^{up}	Upper slag basicity limit in blast furnace	None
c^{O_2}	Cost of high purity oxygen supply	\$/Km^3
c^{dol}	Cost of dolomite	\$/tonne
c^{lime}	Cost of lime	\$/tonne
c^{air}	Cost of heating blast air supply at 1000°C	\$/Km^3
c^{steam}	Cost of steam inection	\$/tonne
c^{oil}	Cost of oil	\$/tonne
$c^{De.}$	Cost of removing sulphur in Desulph. Facility	\$/tonne
c_c^{coal}	Cost of coal type c	\$/tonne
c_p^{pell}	Cost of pellet type p	\$/tonne
c^{scrap}	Cost of scrap	\$/tonne
c_{coke}^{inv}	Inventory cost for coke	\$/tonne
$c_{coal,c}^{inv}$	Inventory cost for coal c	\$/tonne
c_{scrap}^{inv}	Inventory cost for scrap	\$/tonne
$c_{pell,p}^{inv}$	Inventory cost for pellet p	\$/tonne
ϵ_{CSR}	Max prediction error allowable for CSR	None
$\epsilon_{Stab.}$	Max prediction error allowable for Stability	None
$\epsilon_{W.P.}$	Max prediction error allowable for W.P.	None
p^*	Market price of volatile matter	\$/tonne
p^{up}	Upper mass fraction of pellet types	None
$D_{BOF,g}$	Demand of steel grade g	batches
m_{min}^{coal}	Minimum allowable coal addition to coke oven	tonne
m_{max}^{coal}	Maximum allowable coal addition to coke oven	tonne

Table A.7: Constant parameter definition listing part II.

Parameter	Parameter Definition	Units
$M_{coal,in}$	Total initial coal mass charge to the coke oven	tonne
M_{steel}^{BOF}	Final mass of steel obtained at the end of a single BOF batch production	tonne/batch
$M_{dol}^{BOF,max}$	Maximum allowable dolomite addition to BOF	tonne/batch
$M_{lime}^{BOF,max}$	Maximum allowable limestone addition to BOF	tonne/batch
N^{coal}	Number of coal types that can be stored on-site during production (integer)	None
r_S^{slag}	Ratio of sulphur in hot metal to slag	None
r_{Mn}^{slag}	Ratio of manganese in hot metal to slag	None
r_{CSR}^{μ}	Vector of mean k_{CSR} input values to CSR model	None
$r_{Stab.}^{\mu}$	Vector of mean $k_{Stab.}$ input values to CSR model	None
$r_{W.P.}^{\mu}$	Vector of mean $k_{W.P.}$ input values to CSR model	None
r_{CSR}^{σ}	Vector of mean k_{CSR} input values to CSR model	None
$r_{Stab.}^{\sigma}$	Vector of mean $k_{Stab.}$ input values to CSR model	None
$r_{W.P.}^{\sigma}$	Vector of mean $k_{W.P.}$ input values to CSR model	None
r^{oil}	Maximum allowable ratio of oil to hot metal	None
s^{up}	Maximum mass fraction of sulphur allowed in hot metal	None
$T_{max,CSR}^2$	Hotelling T^2 maximum value for CSR model	None
$T_{max,Stab}^2$	Hotelling T^2 maximum value for Stability model	None
$T_{max,W.P.}^2$	Hotelling T^2 maximum value for Wall Pressure model	None
T_{length}	Length of optimization time period	hr
$V_{inert\ gas}$	Volume of gas fed to the coke oven during processing	Km^3

Table A.8: Constant parameter definition listing part III.

Parameter	**Parameter Definition**	**Units**
$\dot{V}_{max}$	Maximum volumetric flow rate of blast air to furnace	Km^3
w^{scrap}	Working capital value for scrap	\$/tonne
w_c^{coal}	Working capital value for coal c	\$/tonne
$x_{c,q}^{coal}$	Mass fraction of component q in coal c	None
$x_{p,b}^{pell}$	Mass fraction of component b in pellet p	None
x_i^{max}	Upper limit of component i in hot metal	None
x_i^{min}	Lower limit of component i in hot metal	None
$X_{c,j}^{prop}$	Value of coal property j in coal c	None
$X_{min,Mn,g}^{steel}$	Lower limit of manganese allowed in steel grade g	None
$X_{min,P,g}^{steel}$	Lower limit of phosphorous allowed in steel grade g	None
$X_{min,Si,g}^{steel}$	Lower limit of silicon allowed in steel grade g	None
$X_{max,Mn,g}^{steel}$	Upper limit of manganese allowed in steel grade g	None
$X_{max,P,g}^{steel}$	Upper limit of phosphorous allowed in steel grade g	None
$X_{max,Si,g}^{steel}$	Upper limit of silicon allowed in steel grade g	None
y_{min}^{CSR}	Minimum CSR value allowable for coke produced	%
$y_{min}^{Stability}$	Minimum stability value allowable for coke produced	lb/in^2
$y_{max}^{Pressure}$	Maximum coke oven wall pressure allowable during coke production	%
z_v^{oven}	Value of oven operating condition v for cokemaking	Various
$\rho_{feed\ gas}$	Density of coke oven feed gas	$tonne/Km^3$
ρ_{air}	Density of inlet blast furnace air	$tonne/Km^3$

Table A.9: Formulation sets and definitions.

Set	**Set Definition**
b	Set of components in iron ore pellets: Al_2O_3, CaO, Fe, MgO, Mn, P, S, SiO_2
c	Set of coal types: Coal A, Coal B, Coal C, Coal D, Coal E, Coal F, Coal G
d	Set of sub groups used in calculating PRESS statistic
e	Set of experimental observations used in PLS modeling
f	Set of hot metal components required by BOF regression model: C, Mn, P, Si
g	Set of steel grade types: G_A, G_B, G_C
h	Set of coke prediction models: CSR, Stability, Wall Pressure
i	Set of hot metal and hot steel components: C, Fe, Mn, P, S, Si
j	Set of rheological, petrographical, and chemical coal properties: Ash, H_2O, FSI, Inerts, Ro, Volatile Matter
k_{CSR}	Set of input variables to CSR prediction model
$k_{Stab.}$	Set of input variables to Stability prediction model
$k_{W.P.}$	Set of input variables to Wall Pressure prediction model
l	Set of pricing tiers: 1,2
p	Set of pellet types: Pellet A, Pellet B, Pellet C
p_a	Set of acid pellet types, a subset of p:Pellet C
p_f	Set of flux pellet types, a subset of p: Pellet A, Pellet B
q	Set of components in coal and product coke: Al_2O_3, C, P_2O_5, S, SiO_2, Volatile Matter
s	Set of uncertain scenarios
v	Set of coke oven operating conditions: 900, BD, Grind, Oil, Soak
w	Set of components in slag exiting blast furnace: Al_2O_3, CaO, MgO, MnO, S, SiO_2

Appendix B

Case Study Results

Table B.1: Optimization results for various case studies.

Variable	Units	Problem 1a	Problem 1b	Problem 1c	Problem 3a
m_A^{coal}	tonnes	0	0	0	0
m_B^{coal}	tonnes	19.1	13.5	0	0
m_C^{coal}	tonnes	38.5	0	0	0
m_D^{coal}	tonnes	42.4	28.4	0	0
m_E^{coal}	tonnes	0	58.1	61.8	61.8
m_F^{coal}	tonnes	0	0	23.2	23.2
m_G^{coal}	tonnes	0	0	15.0	15.0
$\dot{m}_A^{pell}$	kg/thm	0	300.8	91.3	0
$\dot{m}_B^{pell}$	kg/thm	571.5	0	210.4	309.4
$\dot{m}_C^{pell}$	kg/thm	948.5	1203.3	1206.7	1200.1
$x_{Al_2O_3}^{coke}$	wt%	2.54	2.36	2.54	2.54
x_C^{coke}	wt%	90.50	91.22	90.32	90.32
$x_{P_2O_5}^{coke}$	wt%	0.0503	0.0388	0.0432	0.0432
x_S^{coke}	wt%	0.0415	0.0523	0.0591	0.0591
$x_{SiO_2}^{coke}$	wt%	4.99	4.44	4.99	4.99
$x_{V.M.}^{coke}$	wt%	0.50	0.64	0.68	0.68
M_{out}^{coke}	tonnes	72.2	67.5	66.3	66.3
$M_{H_2O,removed}$	tonnes	6.5	7.1	7.3	7.3
$M_{S,removed}$	kg	1.0	11.8	13.1	13.1
$M_{V.M.,removed}$	tonnes	21.3	25.4	26.4	26.4
$\dot{M}_S^{De.}$	kg/thm	28.0	34.0	38.0	41.0
$\dot{M}^{slag}$	kg/thm	195.6	198.3	203.0	194.3
$\dot{M}^{coke}$	kg/thm	521.9	516.7	515.8	520.4
$\dot{M}^{dol}$	kg/thm	85.9	91.6	99.4	92.4
$\dot{M}^{lime}$	kg/thm	0	0	0	0
$\dot{M}^{oil}$	kg/thm	0	0	0	2.3
$\dot{M}^{steam}$	kg/thm	0	0	0	0
$\dot{V}^{air}$	km^3/thm	919.9	911.9	911.7	927.0

Table B.2: Continued optimization results for various case studies.

Variable	Units	Problem 1a	Problem 1b	Problem 1c	Problem 3a
M^{BOF}_{scrap,G_A}	kg/thm	278.4	271.3	267.9	297.7
M^{BOF}_{scrap,G_B}	kg/thm	354.4	343.8	339.8	377.8
M^{BOF}_{scrap,G_C}	kg/thm	348.2	339.6	335.4	369.4
M^{BOF}_{dol,G_A}	kg/thm	18.6	16.8	16.0	42.5
M^{BOF}_{dol,G_B}	kg/thm	6.5	5.0	4.5	19.4
M^{BOF}_{dol,G_C}	kg/thm	4.4	3.5	3.0	15.7
M^{BOF}_{lime,G_A}	kg/thm	20.6	20.5	20.5	33.6
M^{BOF}_{lime,G_B}	kg/thm	17.4	16.3	16.3	33.7
M^{BOF}_{lime,G_C}	kg/thm	17.5	17.4	17.4	33.7
$V^{BOF}_{O_2,G_A}$	m^3/thm	63.1	62.4	62.0	63.5
$V^{BOF}_{O_2,G_B}$	m^3/thm	62.0	61.2	60.9	62.1
$V^{BOF}_{O_2,G_C}$	m^3/thm	62.2	61.6	61.3	61.9

Table B.3: Inequality constraint status for Problem 1a.

Description	Slack Value	Equation Number	Constraint Type	Marginal Scaled Cost (per tonne steel made)
Coke CSR	8.3%	3.19	Min	-
Coke Stability	7.2%	3.20	Min	-
Oven wall pressure	0 lb/in^2	3.21	Max	-\$0.33/lb/in^2
CSR T^2	11.4	3.35	Max	-
Stability T^2	8.1	3.36	Max	-
Wall Pressure T^2	5.3	3.37	Max	-
CSR SPE-X	0	3.39	Max	-\$0.47
Stability SPE-X	6.13	3.40	Max	-
Wall Pressure SPE-X	10.744	3.41	Max	-
Slag basicity	0 tph	3.74	Min	\$0.013/tph MgO + CaO
Acid pellet rate	43.2 tph	3.75	Max	-
Flux pellet rate	43.2 tph	3.76	Min	-
Hot metal exit S	0 tph	3.77	Max	-\$2.3/tph S
Hot metal exit C	0%	3.78	Max	-\$0.019/% C
Hot metal exit Mn	0.8%	3.78	Max	-
Hot metal exit P	0%	3.78	Max	-\$1.69/0.01% P
Hot metal exit Si	0%	3.78	Min	\$0.015/0.1% Si
Steel G_A exit Mn	0%	3.88	Max	-\$4.3$\times 10^{-3}$/0.1% Mn
Steel G_A exit P	0%	3.89	Max	-\$2.1$\times 10^{-4}$/0.01% P
Steel G_A exit Si	0%	3.90	Max	-\$1.4$\times 10^{-3}$/0.01% Si
Steel G_B exit Mn	0%	3.88	Max	-\$5.0$\times 10^{-3}$/0.1% Mn
Steel G_B exit P	0.01%	3.89	Max	-
Steel G_B exit Si	0%	3.90	Max	-\$8.4$\times 10^{-4}$/0.01% Si
Steel G_C exit Mn	0%	3.88	Max	-\$4.8$\times 10^{-3}$/0.1% Mn
Steel G_C exit P	0.01%	3.89	Max	-
Steel G_C exit Si	0%	3.90	Max	-\$8.4$\times 10^{-4}$/0.01% Si

Table B.4: Inequality constraint status for Problem 1b.

Description	Slack Value	Equation Number	Constraint Type	Marginal Scaled Cost (per tonne steel made)
Coke CSR	0%	3.19	Min	\$0.028/%
Coke Stability	2.4%	3.20	Min	-
Oven wall pressure	0.77 lb/in^2	3.21	Max	-
CSR T^2	14.9	3.35	Max	-
Stability T^2	12.5	3.36	Max	-
Wall Pressure T^2	10.1	3.37	Max	-
CSR SPE-X	4.5	3.39	Max	-
Stability SPE-X	7.0	3.40	Max	-
Wall Pressure SPE-X	9.9	3.41	Max	-
Slag basicity	0 tph	3.74	Min	-\$0.012/tph MgO + CaO
Acid pellet rate	0 tph	3.75	Max	-
Flux pellet rate	0 tph	3.76	Min	\$3.4$\times 10^{-3}$/tph
Hot metal exit S	0 tph	3.77	Max	-\$2.3/tph S
Hot metal exit C	0%	3.78	Max	-\$0.026/% C
Hot metal exit Mn	0.9%	3.78	Max	-
Hot metal exit P	0%	3.78	Max	-\$0.034/0.01% P
Hot metal exit Si	0%	3.78	Min	\$0.017/0.1% Si
Steel G_A exit Mn	0%	3.88	Max	-\$5.0$\times 10^{-3}$/0.1% Mn
Steel G_A exit P	0%	3.89	Max	-\$5.0$\times 10^{-4}$/0.01% P
Steel G_A exit Si	0%	3.90	Max	-\$1.6$\times 10^{-3}$/0.01% Si
Steel G_B exit Mn	0%	3.88	Max	-\$9.7$\times 10^{-4}$/0.1% Mn
Steel G_B exit P	0%	3.89	Max	-\$6.8$\times 10^{-5}$/0.01% P
Steel G_B exit Si	0%	3.90	Max	-\$1.1$\times 10^{-3}$/0.01% Si
Steel G_C exit Mn	0%	3.88	Max	-\$9.7$\times 10^{-3}$/0.1% Mn
Steel G_C exit P	0.01%	3.89	Max	-
Steel G_C exit Si	0%	3.90	Max	-\$9.7$\times 10^{-4}$/0.01% Si

Table B.5: Inequality constraint status for Problem 1c.

Description	Slack Value	Equation Number	Constraint Type	Marginal Scaled Cost (per tonne steel made)
Coke CSR	0%	3.19	Min	\$0.014/%
Coke Stability	0%	3.20	Min	$\$2.8\times10^{-4}$/%
Oven wall pressure	0.99 lb/in^2	3.21	Max	-
CSR T^2	14.3	3.35	Max	-
Stability T^2	10.9	3.36	Max	-
Wall Pressure T^2	9.1	3.37	Max	-
CSR SPE-X	2.14	3.39	Max	-
Stability SPE-X	6.36	3.40	Max	-
Wall Pressure SPE-X	9.4	3.41	Max	-
Slag basicity	0 tph	3.74	Min	\$0.012/tph MgO + CaO
Acid pellet rate	0 tph	3.75	Max	-
Flux pellet rate	0 tph	3.76	Min	$\$3.5\times10^{-3}$/tph
Hot metal exit S	0 tph	3.77	Max	-\$2.3/tph S
Hot metal exit C	0%	3.78	Max	-\$0.023/% C
Hot metal exit Mn	1.0%	3.78	Max	-
Hot metal exit P	0%	3.78	Max	-\$0.32/0.01% P
Hot metal exit Si	0%	3.78	Min	\$0.017/0.1% Si
Steel G_A exit Mn	0%	3.88	Max	$-\$5.1\times10^{-3}$/0.1% Mn
Steel G_A exit P	0%	3.89	Max	$-\$5.5\times10^{-4}$/0.01% P
Steel G_A exit Si	0%	3.90	Max	$-\$1.6\times10^{-3}$/0.01% Si
Steel G_B exit Mn	0%	3.88	Max	$-\$5.9\times10^{-3}$/0.1% Mn
Steel G_B exit P	0%	3.89	Max	$-\$1.1\times10^{-4}$/0.01% P
Steel G_B exit Si	0%	3.90	Max	$-\$1.1\times10^{-3}$/0.01% Si
Steel G_C exit Mn	0%	3.88	Max	$-\$5.8\times10^{-3}$/0.1% Mn
Steel G_C exit P	0.01%	3.89	Max	-
Steel G_C exit Si	0%	3.90	Max	$-\$1.0\times10^{-3}$/0.01% Si

Table B.6: Inequality constraint status for Problem 3a.

Description	Slack Value	Equation Number	Constraint Type	Marginal Scaled Cost (per tonne steel made)
Coke CSR	0%	3.19	Min	-
Coke Stability	0%	3.20	Min	-
Oven wall pressure	0.99 lb/in^2	3.21	Max	-
CSR T^2	14.3	3.35	Max	-
Stability T^2	10.9	3.36	Max	-
Wall Pressure T^2	9.1	3.37	Max	-
CSR SPE-X	2.14	3.39	Max	-
Stability SPE-X	6.36	3.40	Max	-
Wall Pressure SPE-X	9.4	3.41	Max	-
Slag basicity	0 tph	3.74	Min	\$0.017/tph MgO + CaO
Acid pellet rate	1.3 tph	3.75	Max	-
Flux pellet rate	1.3 tph	3.76	Min	-
Hot metal exit S	0 tph	3.77	Max	-\$2.1/tph S
Hot metal exit C	0%	3.78	Max	-\$0.014/% C
Hot metal exit Mn	1.0%	3.78	Max	-
Hot metal exit P	0.005%	3.78	Max	-
Hot metal exit Si	0.2%	3.78	Min	-
Steel G_A exit Mn	0%	3.88	Max	-\$2.0$\times 10^{-3}$/0.1% Mn
Steel G_A exit P	0.01%	3.89	Max	-
Steel G_A exit Si	0.01%	3.90	Max	-
Steel G_B exit Mn	0%	3.88	Max	-\$2.3$\times 10^{-3}$/0.1% Mn
Steel G_B exit P	0.01%	3.89	Max	-
Steel G_B exit Si	0.01%	3.90	Max	-
Steel G_C exit Mn	0%	3.88	Max	-\$2.2$\times 10^{-3}$/0.1% Mn
Steel G_C exit P	0.01%	3.89	Max	-
Steel G_C exit Si	0.01%	3.90	Max	-